DISCLAIMER: More detailed information on the results and/or performance obtained and their use is available in the Subproject's subsequent Deliverable (D3.7.4) and/or Periodic Report.

Project Number:	604102	Project Title:	Human Brain Project

Document Title:	Functional Mapping Data, Cognitive Architectures and Models for the HBP Human Brain Atlas: Package 1
Document Filename:	SP3 D3.7.3 FINAL.docx
Deliverable Number:	D3.7.3
Deliverable Type:	Data and models
Work Package(s):	WP3.1, WP3.2, WP3.3, WP3.4, WP3.5, WP3.6, WP3.7
Dissemination Level:	PU=Public
Planned Delivery Date:	M19 / 30 April 2015
Actual Delivery Date:	M23 / 11 August 2015

Authors:	Stanislas DEHAENE, CEA (P9) and SP3 Task leaders
Compiling Editors:	Thien-Ly PHAM, CEA (P9)
Contributors:	Stanislas DEHAENE, CEA (P9), Rafael MALACH, WIS (P78) Pascal FRIES, ESI (P14), Chris LEWIS, ESI (P14), Clément MOUTARD, CEA (P9), Martin GIESE, EKUT (P12), Olaf BLANKE, EPFL (P1), Nathan FAIVRE, EPFL (P1), Mel SLATER, UB (P64), Peter DE WEERD, UM (P108), Avgis HADJIPAPAS, UNIC (P84), Matias PALVA, UH (P86), Viktor JIRSA, AMU (P104), Mariano SIGMAN, CEA (P9), Rui COSTA, FCHAMP (P19), Rodrigo FREIRE OLIVEIRA, FCHAMP (P19), Tobias DONNER, UVA (P109), Andreas Karl ENGEL, UKE (P103), Talma HENDLER, TASMC (P98), Tomer GAZIT, TASMC (P98), Avi KARNI, UHAIFA (P72), Yadin DUDAI, WIS (P78), Rony PAZ, WIS (P78), Jan BORN, EKUT (P12), Lars NYBERG, UMU (P56), Johan ERIKSSON, UMU (P56), Neil BURGESS, UCL (P71), Fabian CHERSI, UCL (P71), Yves FREGNAC, CNRS (P7), Brice BATHELLIER, CNRS (P7), Christophe PALLIER, CEA (P9), Florent MEYNIEL, CEA (P9), Riitta HARI, AALTO (P2), Lauri PARKKONEN, AALTO (P2), Linda HENRIKSSON, AALTO (P2)
STO Review:	UHEI (P45): Björn KINDLER, Sabine SCHNEIDER, Martina SCHMALHOLZ
Editorial Review:	EPFL (P1): Richard WALKER, Guy WILLIS, Lauren ORWIN

Abstract:	This report describes the Month 18 Deliverable for the HBP Subproject 3, Cognitive Architectures. The Deliverable, entitled "Functional mapping data, cognitive architectures and models for the HBP Human brain Atlas: package 1" aims at identifying and inventorying the data sets that SP3 is delivering in phase I of the Ramp-Up Phase of the Human Brain Project. Based on this report, SP3 will make key contributions to a successful Operational Phase of the HBP.

Keywords:	Cognitive architectures; data; models

Table of Contents

List of Figures and Tables

1. Introduction

This Deliverable identifies and inventories the data sets that Subproject (SP) 3 is delivering in phase I of the Ramp-Up Phase of the Human Brain Project. The goal of SP3 is to select well defined, challenging cognitive domains already partially studied by cognitive neuroscience, and to refine the understanding of their "cognitive architecture" (areas, circuits, internal codes, dynamics).

To this end, the scientists in SP3 review the existing literature on specified cognitive functions, and generate data from innovative strategic experimental protocols aimed at dissecting the associated patterns of brain activation and response dynamics. The generated data provide fundamental constraints on any attempt at modelling the corresponding function. By providing top-down constraints that arise from our knowledge of behaviour and brain circuits, cognitive neuroscientists in the HBP help create and constrain theoretical models, possibly framed in the form of computer simulations that capture and reproduce the main facts about a cognitive architecture.

As detailed further below, in the first 18 months of the HBP Ramp-Up Phase, SP3 has delivered or is planning to deliver the following data and models:

DATA

2.1.1.2 Dynamics of the internal model of objects and faces (human behaviour and MEG)

2.1.1.3 Localization and dynamics of spontaneous activity in visual areas (human fMRI)

2.1.2 Dynamics of attention (non-human primate local-field potentials)

2.3 Cortical representation of the body (human behaviour, ERPs and fMRI)

2.3.3 Genetic programming approach to EEG agency related data

2.5 Map of human inter-areal connectivity and phase lags (human SEEG)

3.1.2 Human networks involved in computing confidence (human behaviour and fMRI)

3.1.3 Mouse computation of confidence in action (mice behaviour)

3.2 Human networks involved in motivation and effort (human behaviour and fMRI)

3.3 Brainstem modulation of decision processes (human behaviour and fMRI)

3.4 Human networks for motivation, decision and valuation (intracranial recordings)

4.1 Brain signatures of procedural memory consolidation (human behaviour and fMRI)

4.2 Human networks for episodic memory consolidation (human behaviour and fMRI)

4.3 Human network for conscious and unconscious working memory (human fMRI)

5.1.2 Perfomance of lesioned and control rats

6.1 Database of neuronal recordings in primary visual cortex (cat intracellular data)

6.2 Neural responses to unimodal and multi-modal stimuli (mice two-photon data)

7.2.2 Human networks encoding syntactic structures (human fMRI)

7.2.3 Cortical encoding of probabilistic sequences (human behaviour and MEG)

7.2.4 Brain networks encoding geometrical sequences (human and monkey fMRI)

7.3 Human networks for social cognition (human fMRI)

MODELS

2.4 Model of gamma oscillations in visual cortex

2.2.2 Model of visual action recognition (+ stimuli + human behavioural data)

4.2.3 Neural mass model of the sleeping brain

5.1 Model of spatial navigation and spatial memory

7.1 Model of the emergence of human areas responsive to letter and number symbols

Actual delivery of the data will have to await the opening of the beta version of the Neuroinformatics Platform to its users. SP3 users were first contacted by SP5 in late March and in early April 2015 to start discussing the practical details of how these data will be transferred to the platforms. A specific pipeline to transfer the data still needs to be worked out. In agreement with Martin TELEFONT from the Neuroinformatics Platform (SP5), SP3 researchers agreed that the next practical steps should be to focus on a few selected examples to set up a pipeline that is efficient for the data provider, the platform, and most importantly the user. On the SP3 side, we will use the current M18 deliverable document to identify these best examples. We also agreed to start by focusing first on providing key results of data analysis, instead of the raw data, as the former may be most beneficial to a broad community of users.

Given that the practical details about the delivery of data are still being defined, the Data Set Identification Card requested by the Science and Technology Office will be provided later, together with the data, after its exact content is defined in coordination with SP5.

2. Perception-Action (WP3.1)

2.1 Study of the Circuits Involved in Non-Conscious and Conscious Mechanisms of Visual Recognition (T3.1.1)

This Task involves the following two sub-Tasks, each of which is reported on separately:

- Visual Perception
- Visual attention and the mechanisms of inter-areal communication

2.1.1 Visual Perception

2.1.1.1 Overview

The overall research goal of this task is to achieve a detailed map of both long- and short-term predictions in visual recognition. While many models of visual recognition operate solely in a fast feedforward manner, it is becoming evident that a critical aspect of visual perception is the implementation, in a top-down manner, of *a priori*, predictive information in neuronal circuits. Such prior information, which is assumed to be implemented in the form of "internal models" of objects, and is likely to be operating below the threshold of awareness, allows the visual perceptual system to operate at high efficiency and adaptively, behaving close to an optimal Bayesian inference device. This is particularly critical when faced with ambiguous or noisy information. However, the specific details and neuronal implementation of such predictive information processing remains to be clarified.

In Stanislas DEHAENE's group at the *Commissariat àommissaria atomique et aux énergies alternatives (*CEA – P9), a new paradigm has been designed to investigate the temporal dynamics of view-specific and view-invariant object recognition, and the manipulation of predictive mental models of objects in the human brain. The associated behavioural and magneto- and electro-encephalography (MEEG) were acquired by Clement MOUTARD (CEA), and will be made available by the end of the Ramp-Up Phase. This data set is described in more detail in Subsection 2.1.1.2.

Rafael MALACH's group (Weizmann Institute of Science WIS – P78]) has developed new approaches to study the architecture of visual perceptual networks and other cortical networks. These are based on their hypothesis (formulated in HARMELECH and MALACH, TICS 2013[1]) that coherent patterns which spontaneously emerge when the visual system is at rest, i.e. not processing any visual stimulation, reflect the "imprinting" of habitual network activations of the visual system and other cortical networks during natural activations[2,3]. We have now completed three studies that are compatible with this hypothesis. In the first study, published in *Nature Neuroscience*, we demonstrated that high functioning autistic individuals show unique "idiosyncratic" spontaneous patterns[4]. In a second study, we have shown that the cross hemispheric correlation patterns reflect bi-manual hand use in amputees[5]. Both these results show the significant information contained in the correlation patterns of spontaneous brain fluctuations. In the third study, which has not yet been published, and is therefore described in further detail below, we have obtained a detailed description of coherent patterns of activity in the human visual system, reaching a detailed intra-areal level of accuracy. We have shown that the spontaneously emerging patterns recapitulate the nature of cortical co-activations that occur during naturalistic vision in a remarkably significant manner. This information is of extreme importance, because a serious shortcoming of controlled laboratory approaches to study cognitive architecture is that they typically use highly artificial means to generate the experimental data. Here, we demonstrate a promising new approach that could

potentially uncover activation patterns as they occur in "real life", i.e. during habitual naturalistic performance.

2.1.1.2 Data Set One: MEEG Recordings of the Time Course and the Manipulation of View-specific and View-independent Content in Object Recognition

2.1.1.2.1 Description of Data and Models

Participants examined an item in slow rotation on screen (either a face or an object, rotating clockwise or counter clockwise at 12 rpm). Two time scales of prediction are of interest: long time scales reflecting the internalisation of natural world statistics of objects such as faces, and short time scales reflecting the "on-line" acquisition of new expectations about a specific object.

The stimuli were specially designed to cross these two scales. To study long-term predictions, we employ natural dynamic changes of an object, such as a rotating head, whose geometry is familiar to the viewer. To study short-term predictions, the paradigm also requires learning one new view of the object (the front and profile views of the object conform to everyday life, but subjects also learn that the back view is a specific texture, either a checkerboard or colourful flowers). This latter configuration enables us to test theories according to which invariant object recognition is achieved by an association of multiple, possibly arbitrary views [6-8].

The protocol includes two parts. In the first part, four cardinal views of two objects (a face and a coffee machine) were learned during an initial exposure period, based on a Rapid-Serial Visual Presentation (RSVP) protocol. The textures of the back faces were displayed on a disc rather than on the shape of the objects, to prevent the participants from associating textures and objects at this stage (cf. Figure 1). This sequence was repeated at the end of the experiment to check whether learning the whole object representation (see second part below) made an association between textures and objects. Furthermore, these RSVP data allowed us to train multivariate decoders for each object and each orientation, using generalisation of decoding, to test whether an invariant representation of the object was present, regardless of which view was presented (familiar or recently acquired), and to investigate the time-course of view-specific and view-invariant representations.

In the second part, the participants first viewed the whole spinning objects for several minutes. Then, while the object was rotating, an occluder hid the object for a variable duration (¼, ½, ¾, or a full turn). Using multivariate decoding, this period allows us to probe the presence of an internal model of the rotating object: can we continuously decode what object is occluded and its orientation? Additionally, when the screen dropped, it revealed either the right object or the wrong object, in either the correct rotation or the counter-rotation, and with either the appropriate angle or a different angle. The subjects' task was to report whether the post-occluder situation matched what was expected. If the predictive coding hypothesis is correct, each of those mismatches should elicit error signals in MEEG, and the classifiers should present an update in the representational model of the object, either in terms of object identity or object orientation.

A behavioural version of the paradigm was performed to clarify the latent variables explaining the psychophysical results (n=3 participants). MEEG and eye tracker data (102 magnetometers, 204 gradiometers, 60 EEG electrodes, sampling rate = 1000 Hz) were collected from 20 healthy human adults for part two of the protocol. We are currently analysing the data.

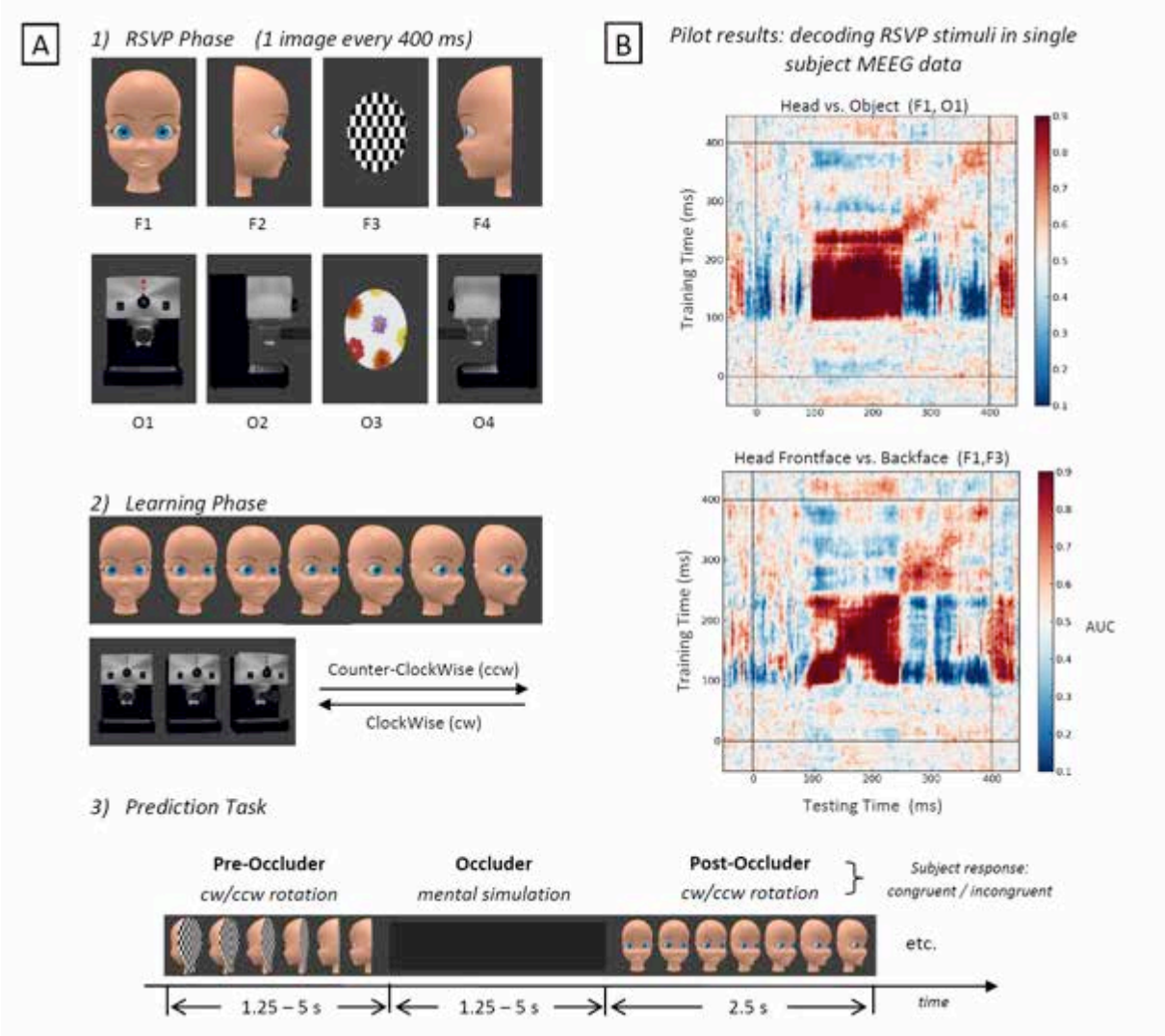

Figure 1: Paradigm Design and Decoding Results – From Static to Dynamic Depresentations, and Manipulation of Objects

A) Experiment design. *1)* RSVP Phase. RSVP enables the acquisition of 60 event-related fields/potentials for the four cardinal views of each object (F1, F2, F3 and F4 for the head; O1, O2, O3, O4 for the coffee machine), one image presented every 400 ms. These data will be used as spatio-temporal localisers. *2)* Learning Phase. The participant is introduced to the continuous stimuli within four sequences: one for each object and rotation direction (clockwise [cw] and counterclockwise [ccw]). 3) Predictive Task. While the rotating stimuli are occluded, the participant is asked to mentally simulate the continuation of the rotation. When the stimuli reappear, the subject has to say whether the stimulus viewpoint is what they expected. The numerous independent variables are balanced and crossed. B) Analysis tool. The stimuli are classified with Support Vectors Machine decoders for each trial time and also applied to all the other time slots (called generalisation across time). The classification of the objects, and of the views of a same object, is tested. The high efficiency of the decoders (Area Under the Curve - AUC - > 0.95) in the two conditions and its stability across time suggest that decoding the objects and their views during both visible and mental simulation rotations is possible as a first step of additional analysis.

2.1.1.2.2 How Data are Related to Specific Platform Requirements

Different kinds of data could be provided:

- Event-Related Potentials/Fields associated with the RSVP images
- Time-generalisation matrices (see Figure 1.B)

- Reconstructed sources of the electromagnetic fields measured. These data will clarify the time course of visual processing regarding view-specific and view-independent information.

2.1.1.2.3 Quantitative Indicators of Data Completeness

The behavioural (three subjects) and the MEEG (20 subjects) datasets have been fully acquired. The behavioural data set has been fully analysed. The MEEG data analysis is on-going.

2.1.1.2.4 Status of Data Delivery

Raw data are available. Fully processed data will be delivered during data delivery phase II (end of the Ramp-Up Phase, March 2016).

2.1.1.2.5 List of SP4 Collaboration Partners

Our data are optimally suited to all SP4 partners interested in theorising and modelling the internal models of visual objects, and their role in sending top-down statistical signals in anticipation of incoming visual inputs.

2.1.1.2.6 Data Provenance

The MEEG and behavioural data were collected by Clément MOUTARD, working as part of Stanislas DEHAENE's team at NeuroSpin, CEA.

2.1.1.2.7 Plan Until the End of the Ramp-Up Phase

We aim to finalise the data analysis and to publish the results of this project in two articles. One will report the first part of the experiment based on the RSVP paradigm. The other will report the results of the second part of the experiment, corresponding to the occluded object rotation paradigm.

2.1.1.3 Data Set Two: The Patterns of Co-activation During Natural Sensory Processing Uncovered Through Resting State and Naturalistic Stimulation Paradigms

2.1.1.3.1 Description of Data and Models

The MALACH group has now collected data from a novel localiser paradigm including three major elements:

- A "conventional" resting state fMRI scan, in which participants rest with their eyes closed.
- A controlled visually-specific resting state scan, in which the participants complete a non-visual cognitive task (beep detection). We have demonstrated that this approach uncovers the same coherent patterns as found during more conventional resting state-albeit under highly controlled cognitive states.
- Two repeat presentations (separated by at least one hour) of an audio-visual movie aimed at capturing the statistics of natural sensory stimulation. Using this approach, we have succeeded, using fMRI in mapping the details of natural network co-activation reaching the level of intra-areal functional connectivity patterns.

The Figure 2 below depicts the experimental structure of the experiments.

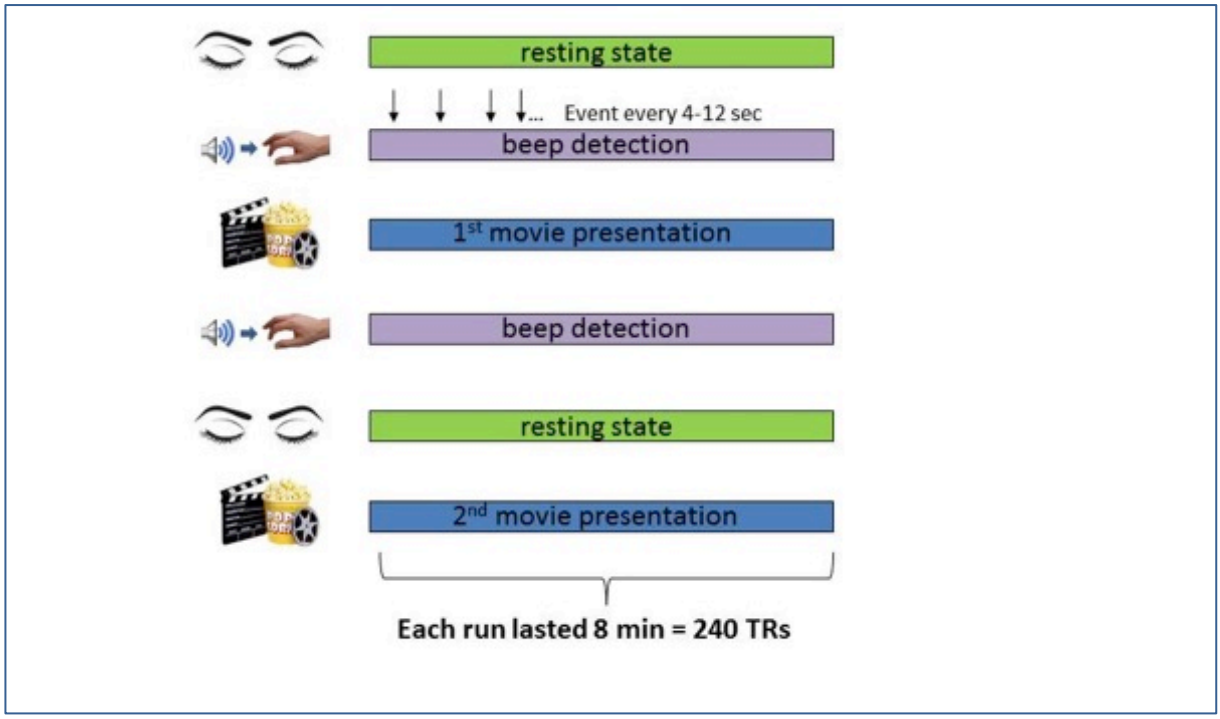

Figure 2: Uncovering Long-term Visual Biases and Predictions in the Human Brain

The different experimental conditions used in revealing intra-areal patterns of co-activations that are generated in the human cortex under natural viewing conditions.

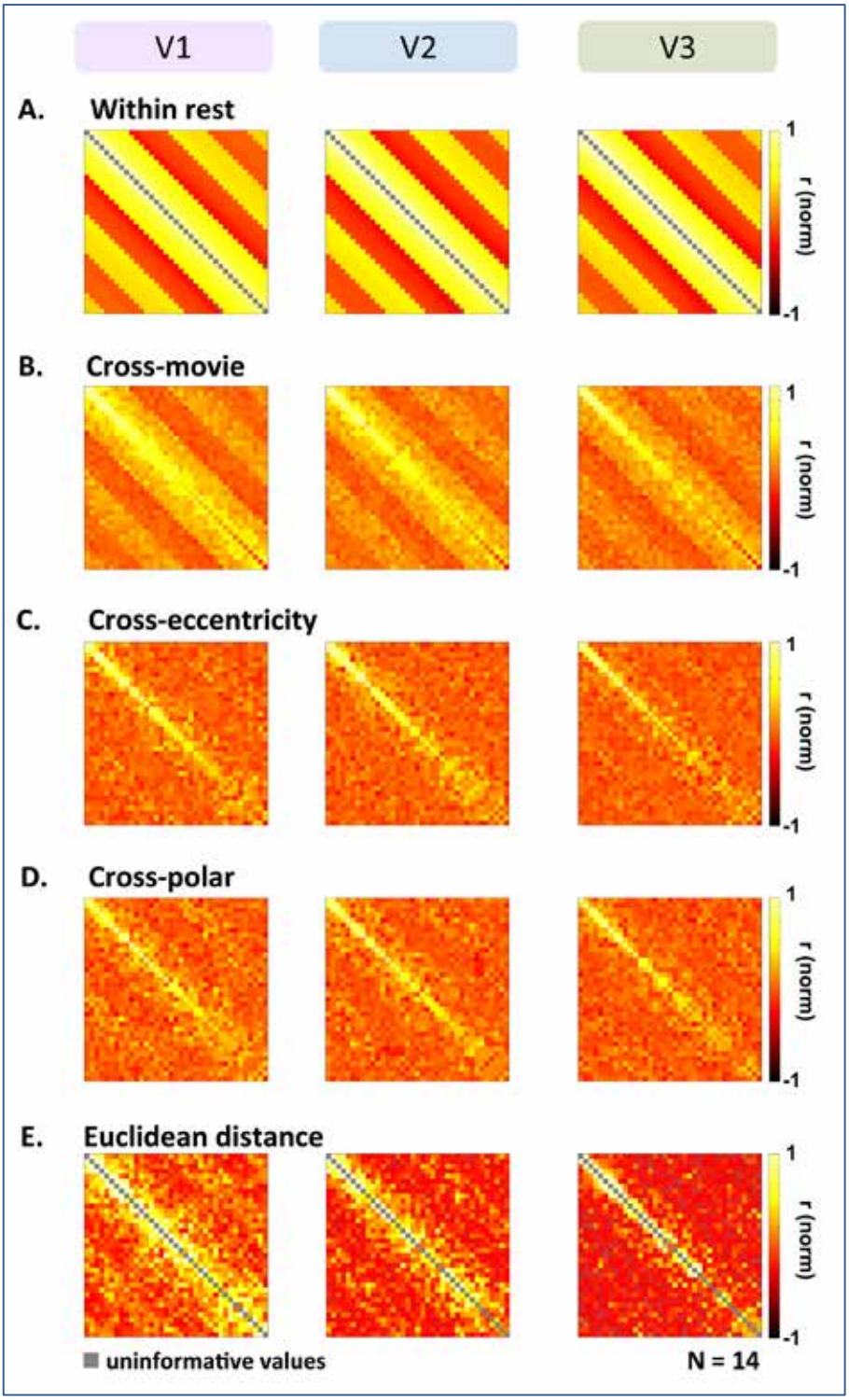

Figure 3

Patterns of correlations between cortical voxels in three visual areas (arranged in arbitrary diagonals for visualisation purposes during the resting state) during rest, and compared to conventional, laboratory-controlled visual mapping approaches using polar angle and eccentricity, and more naturalistic stimulation using an audio-visual movie under natural viewing conditions. The figure shows that the resting state patterns are closer to the organisation of activity produced by naturalistic conditions, than those produced by highly effective but artificial controlled stimuli.

2.1.1.3.2 How Data are Related to Specific Platform Requirements

The data collected by the MALACH group offer a resolution to a fundamental problem in brain research; the fact that data generated under laboratory conditions may not be relevant or informative as to the natural cognition of the organism. Here, we have demonstrated that by using controlled resting state conditions, we could potentially uncover detailed information about the human visual system that captures such naturalistic principles. Therefore the data are highly relevant to models attempting to capture the meso-scale, i.e. intra-areal, functional connectivity patterns under natural vision.

The MALACH group data will include raw magnetic resonance imaging (MRI) image sequences; both structural T1 brain sections, and EPI (Echo_Planar Imaging) BOLD (Blood Oxygenation Level Dependent) fMRI series obtained using our 3T Siemens system. Processed data will include various parameters (contrast, power, Fourier phase and correlation levels) processed using Brain Voyager software and FMRIB Software Library (FSL).
Processed data will include individual subjects' contrast maps in localiser scans, Fourier phase maps in the case of periodic stimuli (polar and eccentricity mapping) and correlation matrices between voxel pairs' time courses, both across movie presentations and during various spontaneous paradigms. Importantly, the correlation matrices are available both at whole brain level, and separately for each retinotopic area.

2.1.1.3.3 Quantitative Indicators of Data Completeness

We have completed fMRI scans on 12 participants, and have analysed all BOLD fMRI patterns under the different experimental conditions. We have generated correlation maps proving our central thesis that the spontaneous, resting state patterns capture essential features of natural vision, and are superior to more controlled laboratory approaches such as polar and eccentricity mapping.

2.1.1.3.4 Status of Data Delivery

We have published a number of papers relating to our approach; some specifically related to natural perception[1-3], and others reporting general findings related to our hypothesis[4,5].

Available data include raw MRI images (structural and EPI), experimental protocols, behavioural responses, processed data (contract, Fourier phase, correlation matrices).

2.1.1.3.5 List of SP4 Collaboration Partners

Our data are suited to all SP4 partners interested in modelling the functional organisation principles of the human visual cortex at resolution level.

2.1.1.3.6 Data Provenance

Our data were collected at the WIS Norman and Helen Asher Center for Brain Imaging. They are available both as raw functional imaging data, and as processed data at various stages, such as connectivity matrices, power spectra and global signal measures.

2.1.1.3.7 Plan Until the End of the Ramp-Up Phase

We now plan to integrate the data into a coherent set of architectures and principles. We aim in particular to plan visualisation on strategies and statistical approaches, to reveal the central principles and patterns that emerge from our experiments.

2.1.2 Visual Attention and the Mechanisms of Inter-areal Communication

2.1.2.1 Overview

In Pascal FRIES' group (Ernst Strüngmann Institute for Neuroscience [ESI – P14]), large-scale (~256 sites) electrophysiological measurements were acquired from both whole-brain and local networks of visual areas. These data allow information transfer within and between distributed populations to be analysed. The "benchmarking" data were acquired by Conrado BOSMAN and Christopher LEWIS, and will be made available by the end of the Ramp-Up Phase. This data set is described further in Subsection 2.1.2.2.

2.1.2.2 Data Set One: Large-scale Recordings from Distributed and Local Visual Networks During Rest

2.1.2.2.1 Description of Data and Models

Recordings were made from conscious macaque monkeys, while they passively viewed a white screen, or sat in a dark recording booth. Recordings were made from 252 sites covering large portions of one cerebral hemisphere. Visuotopic mapping was performed by visual stimulation to quantify the selectivity of recording sites. Local field potentials were recorded from many distributed sensory and higher-order areas. Retinotopic mapping was performed to assess the specificity of sensory responses in early and intermediate visual areas.

Data were acquired during both passive and active states to assess the specific patterns of inter-areal interaction present in these two distinct states.

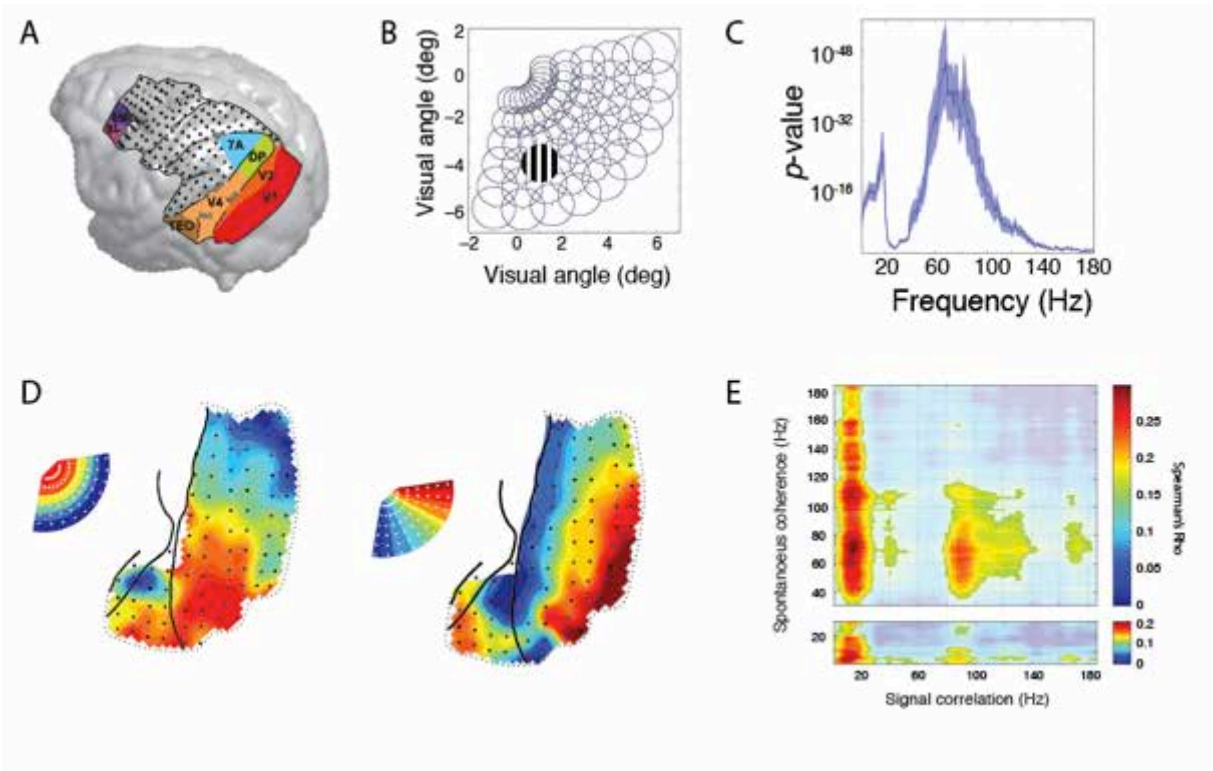

Figure 4: Paradigm Design and Decoding Results - From Static to Dynamic Representations, and Manipulation of Objects

A) Location of multi-electrode array on the reconstructed cortex of one monkey. Black dots indicate recording sites. Coloured regions indicate putative anatomical landmarks of particular interest for visual analysis. B) Visuotopic mapping. Visual selectivity of recording sites were computed based on retinotopic mapping at 60 locations. C) Visual selectivity of visual recording sites as a function of spectral power induced in the local field potential by stimuli. D) Retinotopic organisation of early (V1/V2) and intermediate (V4/TEO) visual areas showing well structured topography. E) The correspondence of spontaneous inter-areal synchronisation to regional topography is limited in a spectrally-specific manner.

2.1.2.2.2 How Data are Related to Specific Platform Requirements

Different kinds of data could be provided, such as:

- Raw field potentials recorded from distributed brain networks.
- Spectrally-resolved tuning, selectivity and topographies (see Figure 4C and D).
- Spectrally-resolved inter-areal interaction matrices, characterising inter-areal coupling by phase-synchronisation or power-covariation, under both visual stimulation and spontaneous activity.

2.1.2.2.3 Quantitative Indicators of Data Completeness

The datasets have been fully acquired. The data analysis is on-going.

2.1.2.2.4 Status of Data Delivery

Raw data are available. Fully processed data will be delivered during data-delivery phase II.

2.1.2.2.5 List of SP4 Collaboration Partners

Gustavo DECO's group (*Universitat Pompeu Fabra* [UPF – P65]) is currently analysing these data and using them to validate dynamical models.

2.1.2.2.6 Data Provenance

The data were collected by Conrado BOSMAN and Christopher LEWIS at The Donders Institute for Brain, Cognition, and Behaviour, at Radboud University, the Netherlands, and the ESI.

2.1.2.2.7 Plan Until the End of the Ramp-Up Phase

We aim to finalise the data analysis and publish the results of this project in two articles. The first will report on the large-scale interaction of visual areas during rest. The second article will address the micro-organisation of areas underlying large-scale inter-areal interactions.

2.2 Understanding the Circuits Linking Perceptions to Actions (T3.1.2)

2.2.1 Overview

The goal of T3.1.2 is primarily to develop new models, and to explore how existing models for action recognition might be linked to simulation tools in other SPs.

As basis for developing models, selected stimulus sets have been developed. These constrain specific computational functions in the recognition of actions. A critical part of this data set can be made available as part of the data sharing initiative within the HBP. In addition, psychophysical results concerning the judgement of agency from abstract stimuli vs. hand actions, which have been obtained with this data set, can be provided. The goal of this is to support the development of alternative models, with the aim of providing a benchmark data set on which the performance of multiple models can be compared.

Due to the lack of available staff within the HBP (equivalent to 0.3 PhD students), we will not be able to develop extensive new data sets. This is compounded by the fact that the available staff will focus on creating links between the existing models, the simulation frameworks in SP4, and the simulator pillars of the HBP. However, the same stimuli might also be useful for the development of new fMRI and electrophysiology experiments, as they have been in the past.

We plan to provide a simplified version of an action recognition model, as context of the data sharing initiative, at the end of the Ramp-Up Phase, a contribution that makes good use of the skills available at our institution.

The available data set consists of image sequences that were recorded, reproducing established paradigms from relevant literature, to provide coherent stimulus data sets for developing models that show the visual processing of goal-directed actions. The stimuli were optimised to minimise computer vision problems, such as segmentation from cluttered scenes, as the work focused on principles of neural circuits in action recognition, rather than on lower-level image processing. This makes the data set suitable for deriving highly controlled stimuli via video editing techniques, achieving exact and independent control of the timing and spatial structure of objects and effectors in visual scenes. In addition, the data set contains versions of stimuli that allow us to study abstract forms of action encoding, e.g. replacing the moving stimulus elements with simple geometrical figures, as used in studies on the perception of causality[9]. Stimuli derived from this stimulus set have been used in a variety of psychophysical and electrophysiological experiments on the neural basis of the visual processing of goal-directed actions, the processing of visual causality[10-14], and for the development of associated models[15,16]. Further studies using these stimuli are in progress. The same type of stimuli will be of high relevance for an on-going collaboration with Markus DIESMANN and Sonja GRÜN at *Forschungszentrum Jülich* (JUELICH – P17). A joint project is planned to study the neural encoding of visually perceived and executed actions in monkeys, exploiting multi-unit recordings with Utah arrays. Data obtained with the same stimuli is also central to a collaboration with Wolfgang MAASS (SP4), which addresses the link between computational and neural representations of temporal sequences in the premotor cortex. In addition, related stimuli will play a central role in new experiments studying the representations of causality and action semantics in populations of mirror neurons in area F5 of the macaque brain.

2.2.2 Data Set One: Benchmark Data set Constraining Computational Mechanisms for the Recognition of Goal-directed Hand Actions

2.2.2.1 Description of Data and Models

The data set aims to identify the key computational properties of the visual processing of goal-directed actions. It reproduces critical stimuli derived from a wide spectrum of experiments within a homogeneous environment (see Fleischer et al. 2012, 2013[10,15] for a more detailed description and cross references to the original experiments).

To evaluate the model in FLEISCHER *et al.*,[15] we recorded sets of video stimuli showing a hand grasping objects. Videos were recorded using a CANON XL1-S camera with a frame rate of 25 Hz. A subset of these stimuli was also used in physiological experiments with monkeys, partially testing hypotheses derived from the proposed model[11]. All video frames were converted to gray-scale, and preprocessed by using intensity thresholds to remove low-intensity background noise. Typical example frames are shown in Figure 5.

The first data set (dataset A) consisted of 270 videos (resolution of 360 × 176 pixels), depicting side views of grasps (view direction 90° relative to the direction the actor was facing. All actions were performed by the same actor). Videos showed a hand grasping

balls with different diameters (4, 8, and 12 cm), with either a power or a precision grip. The stimulus set was derived from 50 original movies via video manipulation, where the original videos included power grips of large and medium-sized balls, and precision grips of all tested ball sizes. In the original movies, the hand started in a resting position, 30 cm in front of the object on the table, and moved naturally, grasping the object. The manipulated videos were generated by colour segmentation of the hand, the object and the background. The manipulated set included movies showing only the hand, or only the object. Another set of movies showed spatially shifted versions of the action scenes (9 different positions displaced by maximum ± 4°, again for precision and power grip).

The second set (dataset B) contained 150 videos (resolution 405 × 364 pixels), showing different views of power grips. These were performed either above, or to the side of, a cylindrical goal object (height 10 cm, diameter 4 cm). This action was recorded from 19 different angles, differing by ~10°. The grips were performed by the same actor. This angle set specifically included the first person perspective (0°) and the "third person perspective" (180°). Each grip was repeated three times. An additional data set contained examples of the same action shown with three view angles (0°, 90°, and 180°) by two additional actors, again with three repetitions.

A third dataset (dataset C), created by editing videos, was a subset of the videos from dataset A. These data set contained videos showing grasping and placing actions, similar to the stimuli used in the studies by BARRACLOUGH et al. (2009)[17] and NELISSEN et al. (2005)[18]. In these movies, the hand entered the scene, grasped a small ball with a precision grip, and moved out (grasping). A second set of sequences was generated by reversing the order of the original video frames, so that the hand entered the scene with the ball and left after releasing the ball (placing). Additional control stimuli showed only the hand (pantomimed action) and only the object. Additional views for testing view dependence were generated by mirroring the grasping and placing stimuli along the vertical axis, resulting in movies showing the opposite hand interacting with the object from the opposite side[17]. This data set was based on nine repetitions of each condition, and was cross validated by using the relevant model parameters with the data from eight repetitions, testing the remaining repetition, and averaging all partitions in the training and test sets.

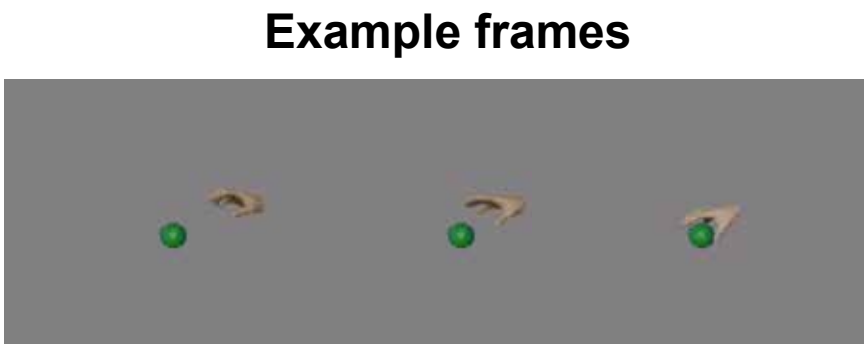

Figure 5: Example Frames from the Benchmark Stimulus Set Used for the Development of Neural Action Recognition Models in T3.1.2

Stimuli were derived from real grasping actions, and were optimised for video manipulation. This allowed for the separation of effector and object, and the introduction of spatio-temporal manipulations that are of interest concerning constraining models for visual action recognition.

2.2.2.2 How Data are Related to Specific Platform Requirements

Critical parts of the stimulus set will be provided for the platform as a basis for the development of models, and potential fMRI experiments testing aspects of the model. We will not be able to provide fMRI data ourselves. Processed psychophysical data from the study of FLEISCHER et al. 2012[10] can be added to the corresponding stimuli if this is of interest to other HBP partners. In the second phase, we will work on providing a simplified version of the recognition model as part of the platform.

2.2.2.3 Quantitative Indicators of Data Completeness

The data are fully recorded and processed, and could be uploaded if access to an appropriate data structure is provided.

2.2.2.4 Status of Data Delivery

Stimulus data are ready and available. Psychophysical data are available. The model will require substantial additional work to make it accessible for sharing purposes. This processing is planned for the rest of the Ramp-Up Phase.

2.2.2.5 List of SP4 Collaboration Partners

Close interactions exist with Markus DIESMANN and Sonja GRÜN, who also develop the simulation platforms. We also collaborate with Wolfgang MAASS on the link between computational and neural representations of temporal sequences in the premotor cortex.

2.2.2.6 Data Provenance

The stimulus data basis is available in Tübingen, and will be made accessible once an appropriate software framework is available.

2.2.2.7 Plan Until the End of the Ramp-Up Phase

A further physiological study using the stimulus set has been submitted. A further collaborative study also using this stimulus set has been submitted by Rufin VOGELS from the *Katholieke Universiteit Leuven* KUL – P89). The few staff available (consistent with the promises made in the work program) will focus on linking the existing model to existing simulation tools for spiking networks, and on transforming of the existing model into something that can be shared as part of the platform.

2.3 Understanding how Body Perception Becomes a Reference Point for the Sense of Self (T3.1.3)

This Task involves the following two groups, each of which is reported on separately:

- That of Olaf BLANKE (*École Polytechnique Fédérale de Lausanne* [EPFL – P1])
- That of Mel SLATER (*Universitat de Barcelona* [UB – P64])

2.3.1 Overview

Conscious percepts are bound to the self, and experienced as unitary entities; any experience is felt in the body and is bound to the self, rather than being detached in the outside world. The sense of self is commonly held to involve self-identification (the experience of owning "my" body), self-location (the experience of where "I" am in space), and first-person perspective (the experience of the position from where "I" perceive the world). Using robotic technology, we achieved specific bodily conflicts, and induced predictable changes in self-location, by altering where healthy subjects experienced themselves to be. Functional magnetic resonance imaging showed that temporo-parietal

junction (TPJ) activity reflected experimental changes in self-location, which also depended on the first-person perspective, due to visuo-tactile and visuo-vestibular conflicts. Our findings reveal that multisensory integration at the TPJ reflects one of the most fundamental subjective feelings in humans: that of being an entity localised at a position in space and perceiving the world from this position and perspective.

2.3.2 Data Set One: Multisensory Mechanisms in Temporo-parietal Cortex Support Self-location and First-person Perspective

2.3.2.1 Description of Data and Models

In the present fMRI study[19,20], Olaf BLANKE's group adapted the ''mental ball dropping'' (MBD) task[21] to the Magnetic Resonance environment. To induce changes in self-location, we manipulated the synchrony between the stroking of the participant's back, and the back of a visually presented virtual human body. In the MBD task, participants were asked to estimate how long the ball they were holding in their hands would take to hit the ground if they were to release it. This provided repeated quantifiable measurements of self-location (height above the ground) during scanning. We expected longer response times (RTs) for higher self-location and shorter RTs for lower self-location[21]. The visual stimuli in the experimental conditions were presented through video goggles. It consisted of short movies showing the back view of the virtual body, filmed from an elevated position[21]. The virtual body was being stroked by a sphere positioned at the end of a rod, moving vertically along the midline of the virtual person's back (body conditions). The video during the control conditions showed only the moving rod and stimulator, without the person's body (no-body conditions). A custom-built robotic device allowed us to control the trajectory of the tactile stimulation of the participant's back in both body and control conditions (using the same movement profile). This trajectory either matched (synchronous) or did not match (asynchronous) the applied tactile stimuli to the visually displayed position of the virtual rod (supplemental information). Thus, we precisely controlled the spatial and temporal aspects of the stimulation sphere's movement during scanning (supplemental information). Participants performed the MBD task under four different conditions according to a 2 x 2 factorial design with Object (body; no-body) and Stroking (synchronous; asynchronous) as main factors.

All MR images were collected using a Siemens Trio 3T scanner. Functional images were preprocessed with SP8 (Wellcome Department of Cognitive Neurology, Institute of Neurology, University College London, - P71), and subsequently analysed at a single subject level using a first-level fixed effects analysis. According to a 2-3-2 design with Object and Stroking as main factors, four contrast images were computed for each participant. These represented the estimated amplitude of the hemodynamic response in the synchronous and asynchronous stroking for the body and no-body conditions, relative to the baseline condition. Contrast images were then entered into a second-level random-effect analysis.

2.3.2.2 How Data are Related to Specific Platform Requirements

We plan to deliver the key statistical results of the fMRI analysis in the form of contrasts at the group level. As the data is being analysed with the Statistical Parametric Mapping software (SPM toolbox, Matlab), the statistical results will be provided as a SPM.mat file; a common practice in the field. The raw data could be made available in a second phase.

2.3.2.3 Quantitative Indicators of Data Completeness

The behavioural and brain imaging datasets (22 subjects) are now fully acquired and analysed. The results have been published[19,20].

2.3.2.4 Status of Data Delivery

All data is now available.

2.3.2.5 List of SP4 Collaboration Partners

We plan on renewing a previous collaboration with Wulfram GERSTNER (SP4, EPFL), with whom we previously developed a model of the rubber hand illusion.

2.3.2.6 Data Provenance

All data were acquired by Silvio IONTA at the *Centre Hospitalier Universitaire Vaudois*, (CHUV – P23) in collaboration with the *Centre d'Imagerie BioMedicale* at EPFL.

2.3.2.7 Plan Until the End of the Ramp-Up Phase

In parallel to the modelling collaboration with Wulfram GERSTNER, we will transfer our experimental setup for strategic human brain data acquisition in collaboration with Bertrand THIRION (SP2, CEA) from September 2015.

2.3.3 Genetic Programming Approach to EEG Agency Related Data

2.3.3.1 Description of Data and Models

Mel SLATER's group has carried out an experiment using virtual reality (VR). It aims to enhance previous results by exploiting perspective as a modulator of the effects of the mirror neuron system. Prior research has found that VR can be used to create an illusion of ownership over a virtual body. We are particularly interested in what happens in conditions of strong body ownership, when the virtual body acts independently of the movement of the person's real body; such as moving a limb. We are also interested as to whether there is a corresponding illusion of agency over the virtual body movements, and whether this is reflected in associated detectable brain activity. The objective is to understand the relationship between real and embodied virtual arm movements. The experiment has three conditions: movement execution in a first person perspective view (1PP) over a virtual collocated body, movement observation in 1PP, and movement observation in third person perspective (3PP).

A major part of this is to explore methods of "big data analysis". This involves automatically analysing significant amounts of EEG data, to discover equations that may shed light on the relationships between real and virtual body activity under different conditions. For this we use the Nutonian/Eureqa technology for genetic programming[1].

Data was collected on 18 male subjects. The setup of the experiment is shown in Figure 6. The study was approved by the UB ethics committee. In the laboratory, participants were first placed in the same position as the avatar that they saw through the head-mounted display (HMD) co-located with their own body. The experiment consisted of 80 trials where either the avatar moved the hand or the participant moved the hand, i.e. where the participant was asked either to observe or to execute a movement. Movements lasted only two seconds, and within this time participants should have moved the arm towards the chin and back to the original position. The avatar movements for the observation condition were recorded with motion capture and also lasted two seconds. Each block of 80 trials targeted the same hand, There was then a short pause, after which the other hand was targeted for 80 trials. This was done to avoid error monitoring systems, due to hand decision making, such as Error Related Negativity.

[1] http://www.nutonian.com

Participants went through three different conditions that were counterbalanced to avoid order effects.

1) Motor execution in Virtual Reality (VRME): participants entered the virtual environment and saw an avatar from 1PP. Their task was to perform the motor action 80 times with one arm, and then with the other arm.
2) Motor observation in 1PP (MO1PP): participants entered the virtual environment and saw an avatar from 1PP. Their task was to observe the motor action that was performed by the avatar, while not moving themselves.
3) Motor observation in 3PP (MO3PP): participants entered the virtual environment and saw an avatar from 3PP. Their task was to observe the motor action that was performed by the avatar 80 times, while not moving themselves.

Finally, an extra condition was run for a consistency check; in this condition the participant performed the motor execution in the real scenario without VR or HMD. For that condition, a real screen was used to indicate the trial flow to the participants (see Figure 6). We will refer to this condition as real motor execution (RME). The whole experiment lasted for a total of two, and the participants had the HMD removed between the conditions. One block of 80 trials lasted for approximately 13 minutes. Lateralised readiness potentials (LRP) were first studied, as they have been shown to elicit activations as a result of the mirror neuron system. A significant LRP was found for both motor execution conditions (RME and VRME) from 300 ms to 600 ms (t-test >0.05). No differences were found between the two conditions in the time course. This indicates that, when the participant was executing the actions, the LRP was equivalent in the real environment and in the virtual environment. Furthermore, both the MO1PP and MO3PP elicit significant LRP at different timings. The voltage of the LRP during the observation of movements' conditions (MO1PP and MO3PP) is reduced when compared to the real execution conditions (RME and VRME). However, it is of note that the first person perspective MO1PP has an earlier activation than third person observation MO3PP, and it is more in line with the temporal dynamics observed in the case of the real motor execution. This alone is a promising result for the idea that virtual embodiment may be a significant factor describing the motor resonance mechanisms.

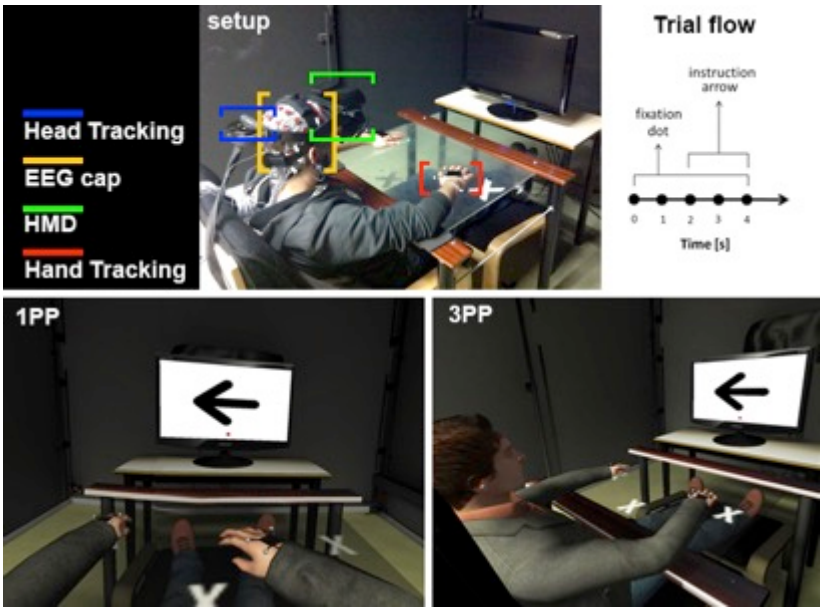

Figure 6

The top of the figure shows a participant fitted with the equipment. The participant was sat in the same position as the avatar (bottom). 1PP and the 3PP were used. The top right shows a small schema of the trial flow; participants fixated on a dot and performed the on-screen instruction. Every 10 trials, they had a specific time for blinking.

For one individual the data consists of an 11,480 x 64 data matrix of event-related potentials (ERP) values (64 electrodes). The time sequence is partitioned into eight segments:

1) The participant moved their real right hand (outside of VR)
2) The participant moved their real left hand (outside of VR)
3) VR moves right hand
4) VR moves left hand
5) VR 1PP observed virtual right hand moved (real stationary)
6) VR 1PP observe left (real stationary)
7) VR 3PP observe right (real stationary)
8) VR 3PP observe left (real stationary).

In our preliminary analysis, we considered only segments 1, 5 and 7. Therefore, we compared:

- The real hand moving.
- The real hand stationary, with the virtual hand seen to move by itself from a first person perspective over the virtual body (with an illusion of body ownership).
- The virtual hand moving by itself but where the body is seen from a third person perspective (i.e. there is no illusion of body ownership).

Three genetic programming exercises were therefore executed. A minimum of 500,000 equations were generated in each case, run on a four-processor machine. We wanted to see whether this approach worked at all, and if so, much larger scale multiprocessor machines would be used for further research. In each case, the genetic programming generated almost perfect fits to the data, based on results from a very small number of electrodes: for 1) P07, O9 and Oz, for 5) Cz and C6 and 7) PO3, P7, C3, P5.

Although the genetic programming (GP) programme was fed with many electrodes and ERPs for the different conditions, some of the results reflect previous studies on motor action observation. These have found that visual and kinaesthetic information may converge in parietal areas of the brain, and in our current GP analysis we find parietal electrodes to be significant descriptors of the mathematical equations, this is the case of PO7, P5, PO3 and P7. The motor cortex also seems to be contributing significantly to the equations in the observation conditions, as suggested by the role of electrodes Cz, C6 and C3.

Overall, the method appears to be a promising way of exploring these very large data sets, though at the time of writing we cannot draw conclusions on its long-term viability. We will next study the combined data of all 18 participants, and design further studies in collaboration with our HBP Partners.

2.3.3.2 How Data are Related to Specific Platform Requirements

These data will help us to understand the brain activity related to illusory agency. If we understand how agency can be artificially induced, we can gain a better understanding of

the mechanisms involved. This would allow us to move towards testing whether this can be achieved with an artificial brain.

2.3.3.3 Quantitative Indicators of Data Completeness

The data is complete and no more will be collected.

2.3.3.4 Status of Data Delivery

The data is not available at this time, as the authors are still in the process of analysing it and submitting it for publication.

2.4 Multiscale Data Analysis and Multiscale Transfer Modelling (T3.1.4)

2.4.1 Overview

Task T3.1.4 is led by Peter DE WEERD's group at *Universiteit Maastricht* (UM – P108) and Avgis HADJIPAPAS' group at the University of Nicosia (UNIC – P84). The overall aim is to construct empirically-validated network models of gamma oscillations in the visual cortex. These will have increasing levels of complexity: beginning with spatially undifferentiated Pyramidal Interneuron Gamma Network (PING) models (single-layer), to multi-layer models (single-column), and finally laterally expanded multi-column models. Even the simplest of these models requires a large number of parameters to be specified, which are at present largely unknown (for instance the strength of neuronal class connectivity, neuronal phase response curves, cross-layer connectivity, etc.). Our approach is to specify these crucial network parameters by using constraints derived from previously acquired empirical data at many different spatial scales (spikes, local field potential (LFP), electrocorticography (ECoG), magnetoencephalography (MEG)), from laminar recordings with a spatial resolution of 0.15 mm, from ECoG Non-Human Primate (NHP) recordings covering several cm, and from human MEG recordings under the same task (perception of grating stimuli of varying contrast). Using multiple constraints derived from the data to specify the unknown model parameters is at the heart of the approach. For instance, the free unknown model parameters are set such that the model produces input-dependent modulations of single unit firing rates, LFP oscillation frequency, and LFP oscillation power, that are similar to what is observed in the empirical data. The physiologically-constrained models derived will then represent the best possible model for V1, and will yield predictions that can be tested in experiments.

2.4.2 Data Set One: Establishing the Key Parameters for an Empirically-validated Spatially-unstructured PING Network Model of Gamma Oscillation in the Visual Cortex

In previous and on-going projects, we have collected a unique data set comprising highly comparable recordings at multiple spatial scales in the NHP and Human primary visual cortex (V1). This data shows the response properties of single units (NHP only) and neuronal populations (NHP and Human) during parametric variation of stimulus contrast, which is a fundamental feature of visual stimuli and directly related to input strength. In order to build a model which best represents the population activity, we must quantify several features of single unit activity, which are currently poorly understood. We have so far shown that broad spiking neurons, putatively excitatory, fire at an earlier phase in the gamma cycle than narrow spiking neurons, putatively inhibitory. We have so far quantified how the preferred phase and phase consistency varies as a function of contrast. We are, however, cautious of verifying the classification of neurons as inhibitory and excitatory cell types, as the primary visual cortex has particularly diverse anatomical cell classes. In line

with this, we find that the distribution of spike widths varies between layers, despite expecting the ratio of excitatory to inhibitory cells to remain constant. We are now repeating our analysis of preferred phase, phase difference and phase consistency in a laminar-specific manner. Moreover, we are exploring alternative methods for determining excitatory and inhibitory neuron classes.

We will be able to provide layer-specific quantitative assessments of putative inhibitory and excitatory neurons' average response properties in V1. These response properties will include the firing rate, gamma preferred phase, and phase consistency as a function of visual contrast. These values are crucial for modelling, yet are currently poorly reported in literature.

2.4.2.1 Description of Data and Models

In the first part of the project, we aim to establish the key parameters for a model of a spatially-unstructured PING network. The goal is to make the key findings of the data-analysis and models available by the end of the Ramp-Up Phase. The raw empirical (NHP and human) data will not be made available, as these were not acquired during the HBP, and are part of an on-going project.

The spatially-unstructured PING model can be thought of as a single layer network of randomly coupled regular-spiking excitatory and fast-spiking inhibitory neurons. Model neurons are described by coupled Hodgkin-Huxley-style single compartment neuron models. The intrinsic frequency of excitatory neurons in response to input is relatively lower than in inhibitory cells. As in the empirical data, model neurons fire sparsely, with model inhibitory neurons firing more frequently than model excitatory neurons. Coupling within and between populations is random (through voltage-dependent synapses) and occurs within a certain probability of connection. Input representing the LGN afferent inputs is provided in the form of Poissonian spike trains. The strength of input to the excitatory cells is varied, to represent stimulus contrast-dependent input.

The model is constrained such that it reproduces the following empirically-observed phenomena:

1) Realistic firing rates for E and I neurons
2) Oscillations within a certain frequency range and frequency shift with input
3) Power decay with increasing input.

Once the unknown parameters are obtained, predictions of the models (e.g. phase locking of units to population as a function of input) can be tested in empirical data.

Some of the empirical data constraints can be readily extracted from population signals (LFP, MEG) or from entire of neuron populations (unit phase locking to LFP, average firing rate). However, some key constraints rely on successfully classifying neurons as either excitatory or inhibitory, which has so far not been done for the NHP V1. Placing neurons in the NHP V1 into the main inhibitory and excitatory classes may be difficult due to the marked neuronal variability in NHP visual cortex. We have, however, made considerable progress. We are now focusing on classification per cortical layer and performing comparisons between layers. If successful, the outcome of this analysis will provide a significant level of validation for our models.

2.4.2.2 How Data are Related to Specific Platform Requirements

We plan to deliver the developed models and the key results obtained from their simulation and analysis. So far, the models were simulated with the BRAIN simulator, a Python package (all models and are written in the Python programming language). Simulation results are analysed in MATLAB. Upon publication, the spatially-

undifferentiated PING model will be made available for public download from the ModelDB model repository of the SenseLab database (senselab.med.yale.edu/SenseLab/ModelDB). The models will be delivered as .py files and the results will be provided as .mat files, a practice that is common in the field.

2.4.2.3 Quantitative Indicators of Data Completeness

We are currently finalising our spatially-undifferentiated PING model (first Milestone). We have also started studying the interaction among coupled PING networks as a step towards modelling columns (second Milestone). This effort will take place rapidly once we have optimised the undifferentiated model. Upon publication, the spatially-undifferentiated PING model will be made available.

2.4.2.4 Status of Data Delivery

We currently have no published data that we can deliver immediately. This is because work on the spatially-undifferentiated PING model started less than a year ago, and has not yet been published. All models and the generated results will be delivered after publication.

2.4.2.5 List of SP4 Collaboration Partners

At the moment we do not have an on-going collaboration with any SP4 Partners.

2.4.2.6 Data Provenance

The models were developed by Margarita ZACHARIOU and Avgis HAJDIPAPAS. The previously acquired experimental data came from on-going projects at UM funded by the Dutch National Science Foundation (NWO). The data were acquired by Peter DE WEERD and Mark ROBERTS, and were analysed by Mark ROBERTS and Ali BAHRAMISHARIF.

2.4.2.7 Plan Until the End of the Ramp-Up Phase

We have published a first paper with multi-scale analysis among NHP and human V1 data, which forms the basis for current modelling[22]. Beyond this, we anticipate the following steps:

1) Present results of modelling at a conference[23].
2) Publish the results of the empirically validated, spatially-undifferentiated PING model.
3) Finish analysis of NHP data, and publish on the classification of V1 NHP neurons in inhibitory and excitatory classes. We aim to submit these manuscripts before the end of the Ramp-Up Phase.
4) Build empirically informed columnar.
5) Create laterally expanded, empirically-constrained models.

In this process, where computing power is essential, we aim to make use of the HBP computing Platform. All published models and the modelling results generated will be delivered during data-delivery phase II.

2.5 Development and Validation of Brain Network Models Constrained by Realistic Physiological Phase Lags and Interaction Time Delays (T3.1.5)

2.5.1 Overview

The objective of this task (led by Matias PALVA, *Helsingin yliopisto* [UH – P86] and Viktor JIRSA, *Université d'Aix-Marseille* [AMU – P104]) is to understand the dynamic nature of

spontaneous brain activity through both electrophysiological recordings and biologically realistic brain network models with concurrent oscillations in multiple frequency bands.

Using a large amount of intra-cranial stereo-electroencephalography (SEEG) data, we aim to rigorously characterise the spontaneous spatio-temporal patterns in resting- and task-state data. We aim to achieve a comprehensive map of 1-500 Hz dynamics, inter-areal connectivity, and phase/time lags among cortical areas. The two key advantages of these SEEG data are the localisation of the electrode contacts in cerebral tissue accurate to less than a millimetre, and the consequent ability to use local white-matter contacts as "silent" references for nearby grey matter contacts. This, for the first time, will yield top-quality measurements of not only inter-areal interactions, but also of the associated phase and time lags that cannot be measured accurately, either non-invasively or with bipolar SEEG.

Knowledge of neuronal communication delays is fundamental for any biologically-realistic modelling of brain network activity. We will clarify the structural and anatomical constraints (connectivity, time delays) imposed upon a network, which will then lead to the emergence of self-organised brain pattern dynamics. The ultimate goal is to understand how distributed information is integrated in the structure of human cognition. Using the lag estimates from SEEG, and MRI-based structural connectivity maps for biologically realistic large-scale brain network simulations, we will account for how coherent oscillations emerge, and how they integrate robustly distributed information. We will then validate the theoretical findings against the SEEG dataset.

2.5.2 Data Set One: Map of Human Inter-areal Connectivity and Phase Lags Based on Resting-state SEEG

We use white-matter referenced local field potential recordings from human cortical and subcortical structures to accurately map the time and phase lags of the interactions among local neuronal oscillations. These lags cannot be estimated non-invasively, or with conventional referencing schemes, because volume conduction and the mixing of signals from multiple sources corrupt the lag estimates.

The initial results show that most electrode pairs have a unimodal phase lag distribution, of which the predominant lag is very similar in time-averaged (static) phase-locking estimates, and in short time windows, to strong coupling. Therefore, even in task-free conditions, there are systematic phase lags between cortical regions, and these lags are robust with respect to the estimation method. A subset of inter-areal couplings exhibited near zero lag coupling, even at long distances (> 3 cm).

2.5.2.1 Description of Data and Models

Uninterrupted recordings of 10 minutes of spontaneous activity, with the eyes closed, were acquired with a 192-channel SEEG amplifier system, at a sampling rate of 1 kHz. In the initial 27-subject cohort, each subject had on average 14 ± 1.9 (mean ± standard deviation, SD) shafts (range 17–10) with a total of 152 ± 20 electrode contacts (range 184-122, left hemisphere: 37 ± 49, right hemisphere: 115 ± 51 contacts). The electrode contacts have been automatically segmented with a novel algorithm[24], and co-localised with neuroanatomically labelled individual cortical surfaces, and volumetric identification of sub-cortical structures. Electrode contacts in or near grey matter are used for local field potential recordings, and are always referenced to the closest contact in underlying white matter[25].

2.5.2.2 How Data are Related to Specific Platform Requirements

Not applicable.

2.5.2.3 Quantitative Indicators of Data Completeness

The SEEG resting- and task-state datasets are being acquired in a project funded by the Academy of Finland. The analyses of inter-areal connectivity and, in particular, phase-lags from these data, are the focus of this HBP project. The total projected size of the resting-state cohort in March 2016 is at least 77 patients, which is by far the largest SEEG cohort ever collected, but is slightly short of the aimed cohort size of 100 patients. Whether a new epilepsy centre will be recruited to support data acquisition is being considered at the moment. Of the 77 patients, 27 have already been fully analysed, and 13 pre-processed. From these data, five subjects were rejected because of macroscopic cortical malformations. Data from 13 patients have already been collected and await transfer from the hospital, while a further 24 patients are expected to be recorded between May 2015 and March 2016.

2.5.2.4 Status of Data Delivery

Raw data will not be made available due to restrictions put in place by the ethical committee. Dynamic and static connectome matrices of phase locking and phase lags will be made available when the first half (40 subjects) of the cohort has been analysed. The algorithm for SEEG electrode contact localisation has been made freely available.

2.5.2.5 List of SP4 Collaboration Partners

Gustavo DECO, *Universitat Pompeu Fabra* (UPF – P65).

2.5.2.6 Data Provenance

The raw data is being acquired in a collaboration project comprising Matias PALVA, UH, and Lino NOBILI, Claudio Munari Epilepsy Surgery Centre, Niguarda Hospital, Italy.

2.5.2.7 Plan Until the End of the Ramp-Up Phase

New subjects will continue to be acquired until the end of March 2016. Full cohort data will be deposited after April 2016.

2.5.3 Data Set 2: Effects of Multimodal Distribution of Delays in Brain Network Dynamics

Large-scale modelling of the brain is defined by the local oscillatory dynamics that are superimposed on an architecture. This architecture is based on a comprehensive map of neural connections in the brain-connectome[26]. Coupling strengths, and time-delays due to transmissions via tracts, are crucial features of a connectome. They represent a proxy of the spatial structure to the temporal dynamics. Thus, the most straightforward approach to model brain dynamics in space and time is to link oscillatory nodes to a connectome-based network. The analysis that we performed on the experimentally derived connectome suggests that the tract lengths, i.e. distances between different brain nodes, and thus the time delays, follow a multimodal distribution.

2.5.3.1 Description of Data and Models

We investigated the implementation of multimodal distributions of discrete time delays, and its effects on the mean-field dynamics. Because of analytical tractability, the Kuramoto oscillator describes the temporal dynamics of each node, and the links between the nodes are symmetric but heterogeneous. Therefore, we analysed synchronisation in populations of phase oscillators[27], which have the same distribution of natural frequencies and coupling strengths, but whose structure is defined solely by their different intra- and inter-population delays.

2.5.3.2 How Data are Related to Specific Platform Requirements

The results are relevant to understanding the synchronisation that underlies cognitive processes. They describe the conditions necessary for achieving synchronisation in large-scale networks in the Simulation and Neuroinformatics Platforms.

2.5.3.3 Quantitative Indicators of Data Completeness

Assuming a same overall distribution of time delays, several cases were investigated. These ranged from fully random distributions, to two delay-imposed structures of subpopulations (Figure 7). For all scenarios, mean-field dynamics were analytically obtained[28] and numerically confirmed (Figure 8). In addition, boundaries and stabilities of different low-dimensional solutions were investigated. These revealed a split of phase dynamics in different clusters, which can be phase shifted, or even non-stationary, with different time-varying order parameters for the clusters.

The large-scale spatial organisation of the brain was integrated in a network model. Using this model, we presented the effects of the multimodal distribution of time delays, and the structure they impose on the network dynamics, such as synchronisation. Therefore, we stress the role of the spatial organisation of the brain, which is reflected in the different time-delays between different parts of the brain in the formation of spatiotemporal dynamics.

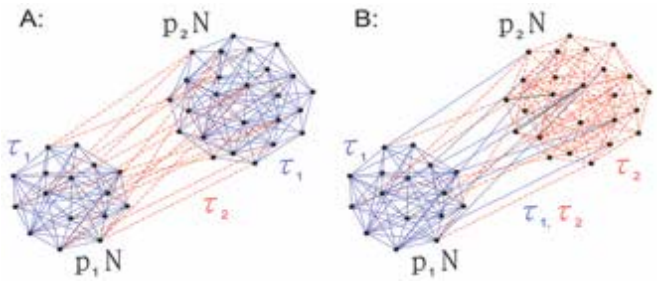

Figure 7: Sketch of Delay-imposed Structure of Population of Oscillators

A) Different inter and same intra delays, B) same inter and intra delays.

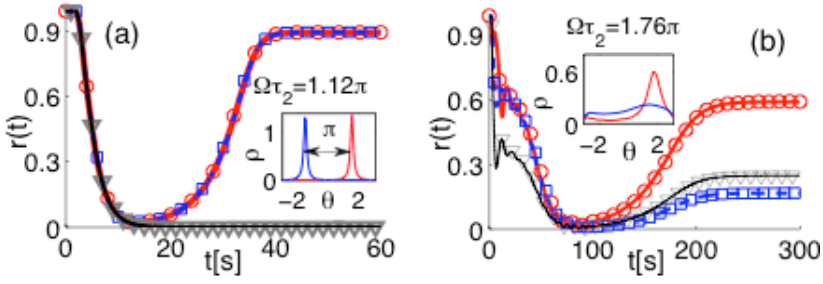

Figure 8: Order Parameters for Model A. Inset: PDF of the Phases

Theoretical predictions (lines) are compared with numerical simulations (lozenges). Blue and red correspond to the first and second populations respectively, and black and grey lines are from the overall population.

2.5.3.4 Status of Data Delivery

Not applicable.

2.5.3.5 List of SP4 Collaboration Partners

Gustavo DECO, UPF.

2.5.3.6 Data Provenance

Not applicable.

2.5.3.7 Plan Until the End of the Ramp-Up Phase

The same analysis will be performed for more realistic, amplitude oscillators (Stuart-Landau). In addition, the connectivity matrix of the connectome will be implemented, and the influence of the spread of peaks in the delay distribution will be also studied.

3. Motivation, Decision and Reward (WP3.2)

3.1 Mapping and Understanding the Neuronal Circuits Involved in Decision Making, Confidence and Error Correction (T3.2.1)

3.1.1 Overview

T3.2.1 addresses how confidence is computed in the brain. Data from human participants were generated at NeuroSpin by Florent MEYNIEL during abstract probabilistic reasoning. Data from mice was generated by Rui COSTA at *Fundação Champalimaud* (FCHAMP – P19), in a much simplified task also involving a form of confidence computation.

The NeuroSpin group is also working on a data set to characterise confidence in perceptual decisions. The same experiment will be used to acquire behavioural, fMRI and MEG data. The MEG part is a new collaboration with Tobias DONNER from T3.2.3 (*Universiteit van Amsterdam*, [UVA – P109]), and the behavioural part is in collaboration with Mariano SIGMAN. However these acquisitions are not funded by the HBP and may not be included eventually as a Deliverable. In a nutshell, this experiment is designed to compare different models of perceptual decision-making. The two predominant models currently differ in how confidence is computed. One proposes that the decision is made when one possible answer, out of several, has received substantial evidence (the race model); the other proposes that the decision is made when there is a substantial difference between the evidence supporting the first and second best options (the diffusion model)[29-33]. We will benefit from behavioural data and the complementary temporal and spatial resolutions of MEG and fMRI to compare these two decision models.

The mouse data on action performance monitoring were collected at the Champalimaud Centre for the Unknown in Lisbon, Portugal by Rodrigo FREIRE OLIVEIRA (post-doc at the Neurobiology of Action under the supervision of Rui COSTA).

At this stage, we are making available the raw behavioural data set of the confidence estimation task in mice. The data set is composed of behavioural sessions including different phases of training, and a final asymptote performance, where the confidence estimation was calculated. These data were collected during 2012 and 2013 and are described below.

Currently, confidence estimation has been studied in perceptual decision making tasks in primates[34], rodents[35] and humans[36]. The brain circuitry responsible for confidence estimation in humans is also being investigated (see 3.1.2.1). The estimation of confidence after one's own performance has received considerably less attention and has, to our knowledge, not yet been studied in rodents. The development of a robust behavioural rodent assay for confidence estimation in action performance paves the way for the investigation of the brain circuitry required for its computation.

The brain areas implicated in estimating confidence of action performance remain unknown. We are investigating the role of the Anterior Cingulate Cortex (ACC), which has been previously implicated in error detection, and the somatosensory system (particularly S1 and M1) which has been implicated in sensory-motor integration. We predict that the optogenetic inactivation of the ACC would increase the overall fraction of aborted trials without changing the accuracy of the performance monitoring. We predict that inactivation of S1 will lead to a flat distribution of fraction of aborted trials, therefore a degradation of the ability of the animals for confidence estimation in action performance. This will give important convergence data for the human studies.

3.1.2 Data set One: Confidence During Probabilistic Reasoning, Behavioural and fMRI Recordings

3.1.2.1 Description of Data and Models

The data set aims to identify the brain networks involved in computing confidence during probabilistic reasoning, and the algorithms that underlie this computation.

Participants performed a probabilistic learning task, which was to observe binary sequences of stimuli that were generated randomly based on transition probabilities. These transition probabilities were constant only piecewise in time. Participants had to infer the transition probabilities generating the observed sequence online and, from time to time, report their level of confidence in that estimation (see Figure 9). The probabilistic and time-varying nature of the task purposefully induced fluctuations of confidence.

The fluctuations in subjective confidence levels were compared to a normative estimate of confidence using an optimal Bayesian Observer. This model gave a clear formalism of the task, and also quantitative variables to describe the inference process. Subjective confidence ratings were linearly related to the optimal confidence level. This provided a normative account of subjective confidence. It also provided a quantitative model from which key variables of the inference process could be computed on a trial-by-trial basis, such as the estimated confidence, the inferred probability, the likelihood of observing a particular outcome given its inferred probability, and the update of the internal model. In addition, the use of different modality (auditory and visual) in the fMRI task allows modality-specific and generic computations in the brain to be identified.

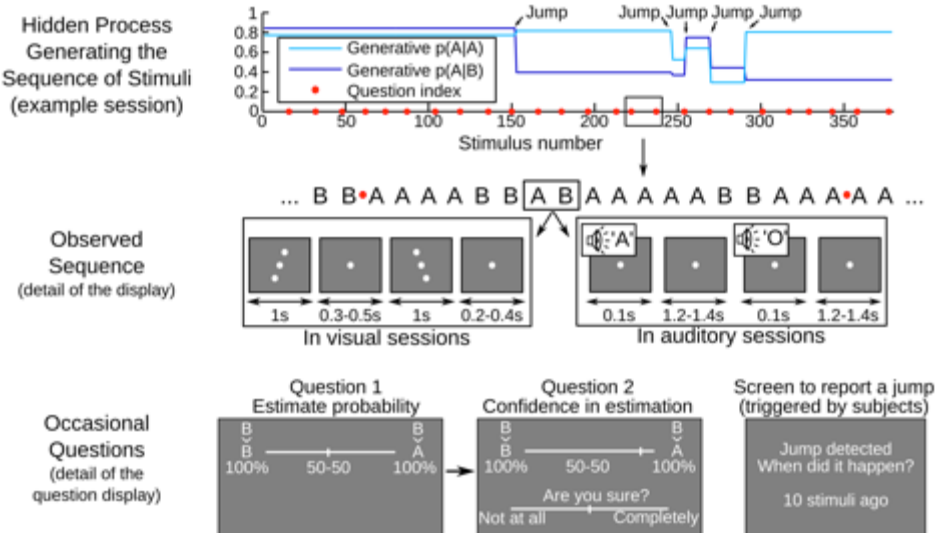

Figure 9: Task Design for T3.2.1 - Mapping and Understanding the Neuronal Circuits Involved in Decision-making, Confidence and Error Correction

Subjects were exposed to sequences of binary stimuli. The sequence depended on the transition probabilities between stimuli A and B. The transition probabilities themselves were stable piecewise: they were constant for only a limited time and changed abruptly and randomly, delineating "chunks" in the sequence separated by "jumps". Subjects had to report the occurrence of jumps, and occasionally they were jointly asked to estimate which stimulus should come next (i.e. guess the transition probabilities in sensory stimuli) and to report their degree of confidence in those estimates.

A first behavioural study (n=18 participants) was performed to investigate the confidence ratings of participants in this task in detail. The results and the Ideal Observer model are described in a submitted publication.

In a second study, we acquired fMRI data using a similar protocol, slightly adapted to the constraints of fMRI. The data set was acquired from 21 human healthy adults, using a whole brain coverage at the 1.5 isotropic resolution, with one scan acquired every 2 seconds. The data were collected while participants performed the estimation task. We are currently analysing the data.

3.1.2.2 How Data are Related to Specific Platform Requirements

We plan to deliver the key statistical results of the fMRI analysis in the form of contrasts at the group level. As the data being analysed with the Statistical Parametric Mapping software (SPM toolbox, Matlab), the statistical results will be provided as SPM.mat file, a practice that is common in the field. The raw data could be made available in a second phase.

3.1.2.3 Quantitative Indicators of Data Completeness

The behavioural (18 subjects) and brain imaging (21 subjects) datasets are now fully acquired. The behavioural data set is fully analysed. The results were submitted for publication. The fMRI data analysis is still on-going.

3.1.2.4 Status of Data Delivery

Raw data is available. Fully processed data will be delivered during data-delivery phase II.

3.1.2.5 List of SP4 Collaboration Partners

Our behavioural and brain imaging results challenge the current models of learning, and of probabilistic learning in particular. SPs 3 and 4 therefore scheduled an international workshop, organised by Stanislas DEHAENE (SP3), Alain DESTEXHE (SP4), Florent MEYNIEL (SP3) and Wolgang MAASS (SP4). This is to be held in Paris in September 2015, and is entitled 'Probabilistic inference and the Brain'. This workshop will gather prominent scientists from theoretical and experimental fields.

3.1.2.6 Data Provenance

The fMRI and behavioural data were collected by Florent MEYNIEL at NeuroSpin.

3.1.2.7 Plan Until the End of the Ramp-Up Phase

We aim to publish the results of the behavioural study (publication submitted). We also aim to fully analyse the results of the brain imaging study and report them in a publication (submitted).

3.1.3 Data set 2: Confidence Estimation on Motor Skill Performance in Mice

3.1.3.1 Description of Data and Models

This behavioural data set aims to determine whether rodents are capable of estimating confidence during motor skill performance. In addition, the data shows that variables with different time scales are integrated in the course of this computation.

Mice were trained daily in an instrumental box with one active lever (extended) and a magazine (with IR break sensor) where reinforcement is delivered. The mouse had to execute an action sequence (of 4 or 5 presses) before visiting the magazine. After arriving at the magazine, the animal had to wait for 8 seconds before the reinforcement was delivered. If an incorrect number of presses were performed, no reinforcement was delivered, and the sequence was reset. If the animal left the magazine before 8 secs had passed, the trial was considered aborted. Sessions finished once 60 reinforcements had been collected, or two hours had passed. In summary, the reinforcement was cached, and the time waited in the magazine added extra cost to the performance, which drove the mice to select the trials to which they should commit.

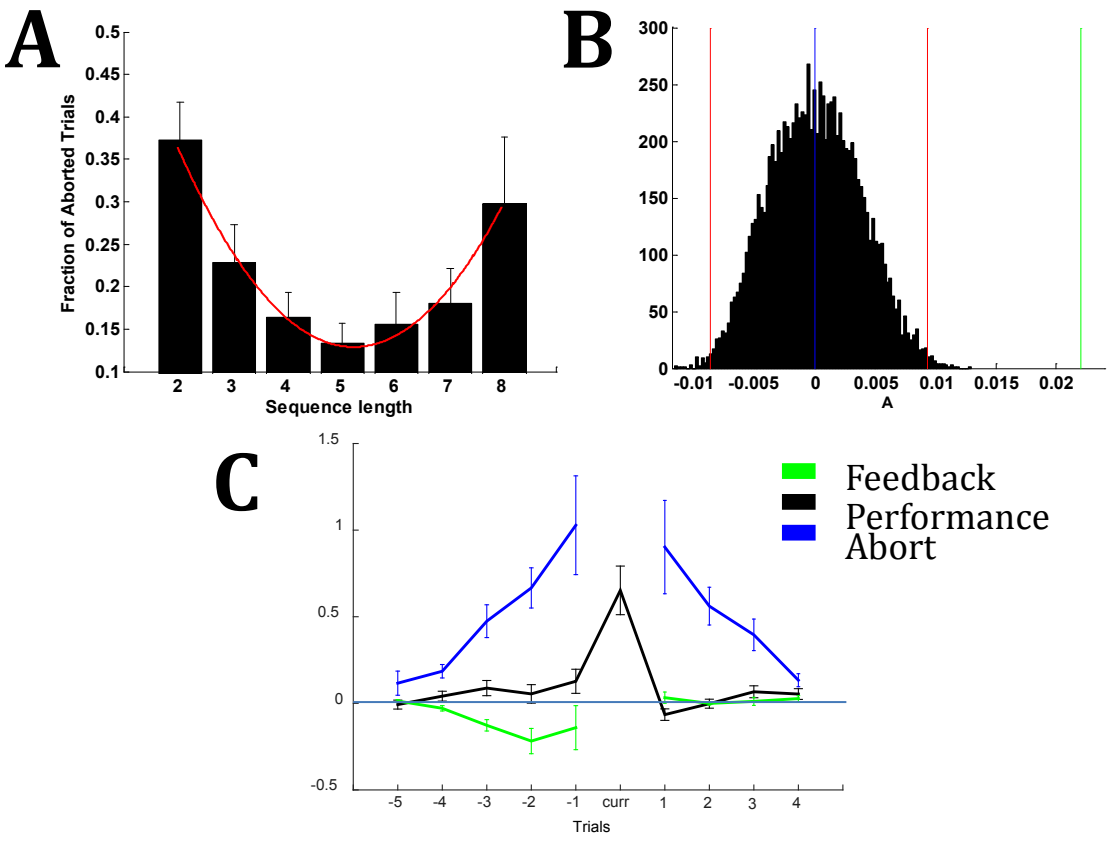

Figure 10: Confidence Estimation in Motor Skill Performance

(A) Fraction of aborted trials as a function of sequence length. Figure shows the distribution of the mean of the fraction of aborted trials (with all sessions grouped together) by animal (error bars correspond to standard error of the mean (SEM) over animals). The red line is the quadratic fit to the data with an R^2 0.98.

(B) Comparison between experimental and permuted data. Figure shows the distribution of the curvature parameter of the quadratic fit derived from 10 000 permutations (dark blue) of the original data. All permutations generated a distribution centred away from the experimental value observed (light green). The chances of the experimental curvature happening by chance are statistically much smaller than 0.01 (red lines).

(C) Logistic regression analysis of trial abortion probability. Logistic regression analysis predicting abortion, using different trial events (abortion, performance and feedback), at different lags (trials relative to predicted trial). The blue trace shows the loading for abortions on prior and future trials, i.e. the extent to which aborting on a given trial predicts aborting in future trials. The symmetric high loadings in previous and future trials suggest that a slow variable (i.e. engagement in task) is a strong determinant of the likelihood of current trial abortion. The black trace shows the loadings for incorrect performance of sequences, i.e. the extent to which incorrect performance on a given trial predicts aborting in future trials. It has a large loading on only the current trial, consistent with performance monitoring. Finally, the light green trace shows the loadings for feedback (which takes values of 0 in aborted trials, -1 in incorrect completed trials and +1 in correct completed trials). This variable aims to capture the effect of reinforcement obtained in correct vs incorrect sequences).

Mice decide on abortion in a fast trial-by-trial basis, depending on their performance. The fractions of aborted trials for the target sequences (Fig. 10, A, lengths 4 and 5) are lower than the flanking incorrect sequences, with either fewer or extra presses. This suggests that mice keep track of their current performance, compare it to a target, and abort sequences based on the difference between the former and the later (Figure 10 A and B). The logistic regression analysis confirms that the performance in the current trial has a higher probability of aborting. Furthermore, it shows that a slower variable linked to the history of abortion also predicts the probability of aborting (Figure 10C).

The data set includes the time stamps of the animals' responses during the sessions, including lever presses, visits to the magazine, and consummatory behaviour (licks). It also includes the timestamps of other relevant events, e.g. sucrose delivery and box light switching on-off. The data was acquired from 12 mice BL6/C57, with a time resolution of 1 msec.

3.1.3.2 How Data are Related to Specific Platform Requirements

Our task will provide a localiser for the brain structures involved in monitoring action performance.

3.1.3.3 Quantitative Indicators of Data Completeness

The behavioural dataset included in this phase illustrates the strategies used by mice in estimating their confidence of action performance, and aborting trials, based on their own performance and other variables (potentially attention and/or motivation). This behavioural data set is fully analysed.

3.1.3.4 Status of Data Delivery

Raw data is being shared at this stage. Data collected with optogenetic manipulations will be delivered during data-delivery phase II.

3.1.3.5 List of SP4 Collaboration Partners

Our data are optimally suited to all SP4 partners interested in theorising brain operations as a form of Bayesian inference, e.g. Wolfgang MAASS.

3.1.3.6 Data Provenance

The mouse data set on confidence estimation and action performance was collected at the Champalimaud Centre for the Unknown by Rodrigo FREIRE OLIVEIRA.

3.1.3.7 Plan Until the End of the Ramp-Up Phase

We are currently writing a manuscript and testing manipulations for optogenetically silencing cortical circuitries that we consider to be the best candidates for computing confidence estimation (ACC and S1). We aim to submit a publication with the behavioural data, analysis and the effects of manipulations by June 2016.

3.2 Mapping and Understanding the Neuronal Circuits Involved in Motivation, Emotion and Reward (T3.2.2)

3.2.1 Overview

The goal of this Task (led by Mathias PESSIGLIONE, *Institut du Cerveau et de la Moelle épinière [ICM - P25])* is to provide datasets from a battery of motivational tests. We will start with two key paradigms that assess effort production and instrumental learning. FMRI data have been previously acquired using these two tests. During this ramp-up period (only six months so far for this task), we have acquired some behavioural data in patients and in healthy volunteers using pharmacological manipulation. Below is a short description of the two tests.

3.2.1.1 Effort Test

Patients have to squeeze a handgrip to win money, knowing that the payoff is proportional to both incentive level and force peak. This task assesses the energisation process, which is the ability to boost behavioural output in proportion to what is at stake. This can be captured with a computational model that weighs the impact of incentives on force independently of sensitivity to effort cost, compliance to instructions, and motor

limitations. It requires efficient connectivity from the valuation system to the motor circuits responsible for movement execution[37-39]. Deficits were found in various clinical populations (auto-activation deficit, Parkinson's disease, major depressive episode) and correlated to apathy scores measured with Starkstein's questionnaire[40-42].

3.2.1.2 Learning Test

Patients make a series of binary choices between novel cues associated through probabilistic contingencies to rewarding, neutral or punishing outcomes. The progression of correct choices across trials can be fitted using a Q-learning algorithm, which combines a Rescorla-Wagner rule to update values, and a softmax function for making decisions[43-45]. This task enables us to assess global learning ability and specific sensitivity to positive versus negative reinforcements. It has been used to show the opposite effects of dopamine enhancers and dopamine blockers on reward versus punishment learning in pathological conditions such as Parkinson's disease and Gilles de la Tourette syndrome[45-48]. Differential sensitivity to reward and punishment was also found in Huntington's disease and patients with low-grade tumoral mass around the anterior insula[42].

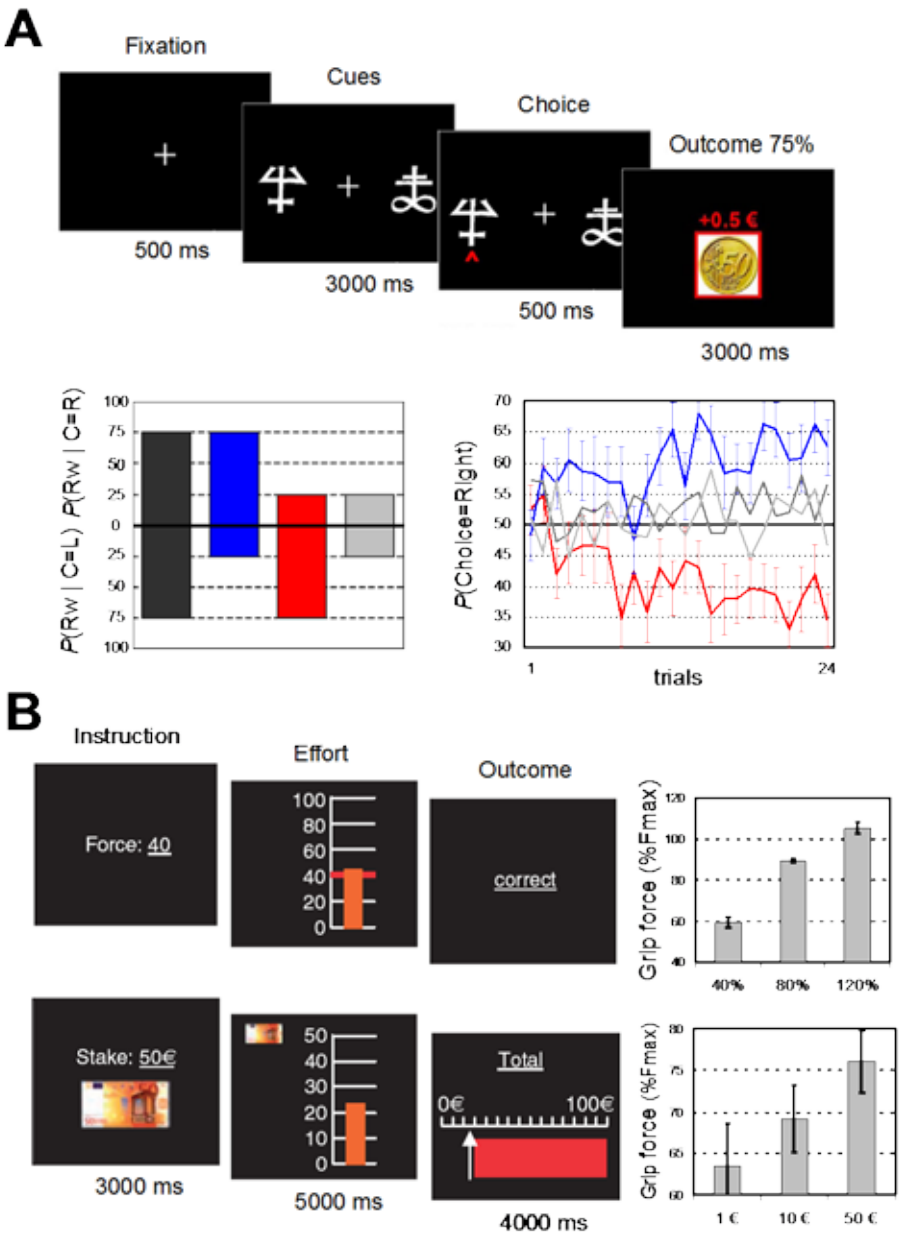

Figure 11: Experimental tests and typical behaviour

(A). Instrumental learning task. The successive screenshots displayed during one example trial are displayed from left to right. Subjects chose between left- and right-hand responses, based on the two corresponding abstract cues. They were first provided with a feedback on their choice (with a red pointer) and then with the monetary outcome (a 50c winning in this case). The left diagram indicates the reward (Rw) probability associated to each choice (C, left or right) for the different cue pairs (illustrated with different colors). Learning curves represent right choice rate averaged over the 24 participants of the study. Note that learning occurs only for pairs with unequal reward probability (blue and red). (B) Grip force tasks. In both tasks, subjects were first informed of the condition (instructed force or monetary incentive), then they squeezed a handgrip to move the orange cursor within a ladder scaled to twice their maximal force, and finally observed the outcome of their performance. In the instructed force task, subjects squeezed the grip so as to move the orange cursor up to the red line. The outcome was a feedback on whether they correctly produced the requested force. In the incentive force task (bottom), subjects squeeze the grip so as to win as much money as possible. The outcome was a cumulative total of monetary earnings, which were calculated for each trial as the percentage of the incentive corresponding to the height reached in the ladder. Bars indicate peak force (expressed as percentage of maximal force Fmax), averaged over the eight patients who performed the two tasks, for the different instructions and incentives (bottom). For both choices and forces, error bars represent inter-participant s.e.m.

3.2.2 Data set One: Pharmacological Manipulation of Motivational Processes

3.2.2.1 Description of Data and Models

We planned to employ these two tests to assess the effects of drugs affecting three main neuromodulatory systems (dopamine with L-Dopa, serotonin with Citalopram, noradrenalin with atomoxetine) and the opioid system (morphin and naloxone). Every drug is tested within subject (n=24) against a placebo. We envisage to provide a summary of behavioural results for each test and drug, together with a computational characterization using effort production and instrumental learning models.

3.2.2.2 How Data are Related to Specific Platform Requirements

Our task will provide a localiser for the brain structures involved in motivational processes.

3.2.2.3 Quantitative Indicators of Data Completeness

Behavioural data are currently being collected. We have completed the citalopram study (n=24). The opioid study has been started (n=8 so far).

3.2.2.4 Status of Data Delivery

Given that this task was only funded for the past six months, data delivery will occur in phase II.

3.2.2.5 List SP4 Collaboration Partners

None so far.

3.2.2.6 Data Provenance

All data were collected at the *Centre d'Investigation Clinique* at ICM.

3.2.2.7 Plan Until the End of the Ramp-Up Phase

We need to complete the opioid study. Dopamine and noradrenaline will be started in a few months. There is already fMRI data corresponding to these tests,[49,50] which could be provided at a later stage.

3.3 Dissecting the Brainstem Modulation of Cortical Decision Computations (T3.2.3)

3.3.1 Overview

Within T3.2.3 is led by Tobias DONNER, UVA and Andreas Karl ENGEL, *Universitätsklinikum Hamburg-Eppendorf* [UKE – P103]). Neuroimaging data from human participants were generated using fMRI at UVA, by one post-doc and one PhD student (Olympia COLIZOLI and Jan Willem DE GEE), and at UKE (using MEG) by Jan Willem DE GEE.

The goal is to make three data sets available by the end of the Ramp-Up Phase. These data sets target the question of how decision-making mechanisms in the cerebral cortex are shaped by ascending modulatory brainstem systems. The data sets are described below.

3.3.2 Data set One: Pupil-linked Brainstem Responses and the Computation of Yes vs. No Decisions (fMRI)

3.3.2.1 Description of Data and Models

The data set aims to characterise the coupling between pupil dilation and neuromodulatory brainstem nuclei. It also aims to to pinpoint how modulatory brainstem systems shape the computation of elementary decisions, focusing on a visual yes-no

decision (Figure 12). Participants performed a yes-no contrast detection task (Figure 12A) during concurrent whole-brain high-resolution fMRI (1.7mm x 1.7mm inplane). Pupil diameter was monitored. Dynamic noise was continuously present in a circular aperture around fixation. During the decision interval (onset cued by a tone), participants searched for a faint contrast grating target signal that was superimposed onto the noise on 50% of the trials. They indicated their yes or no choice by pressing a button with one of their index fingers. The signal contrast was adjusted individually, such that each subject was correct about 75% of the time.

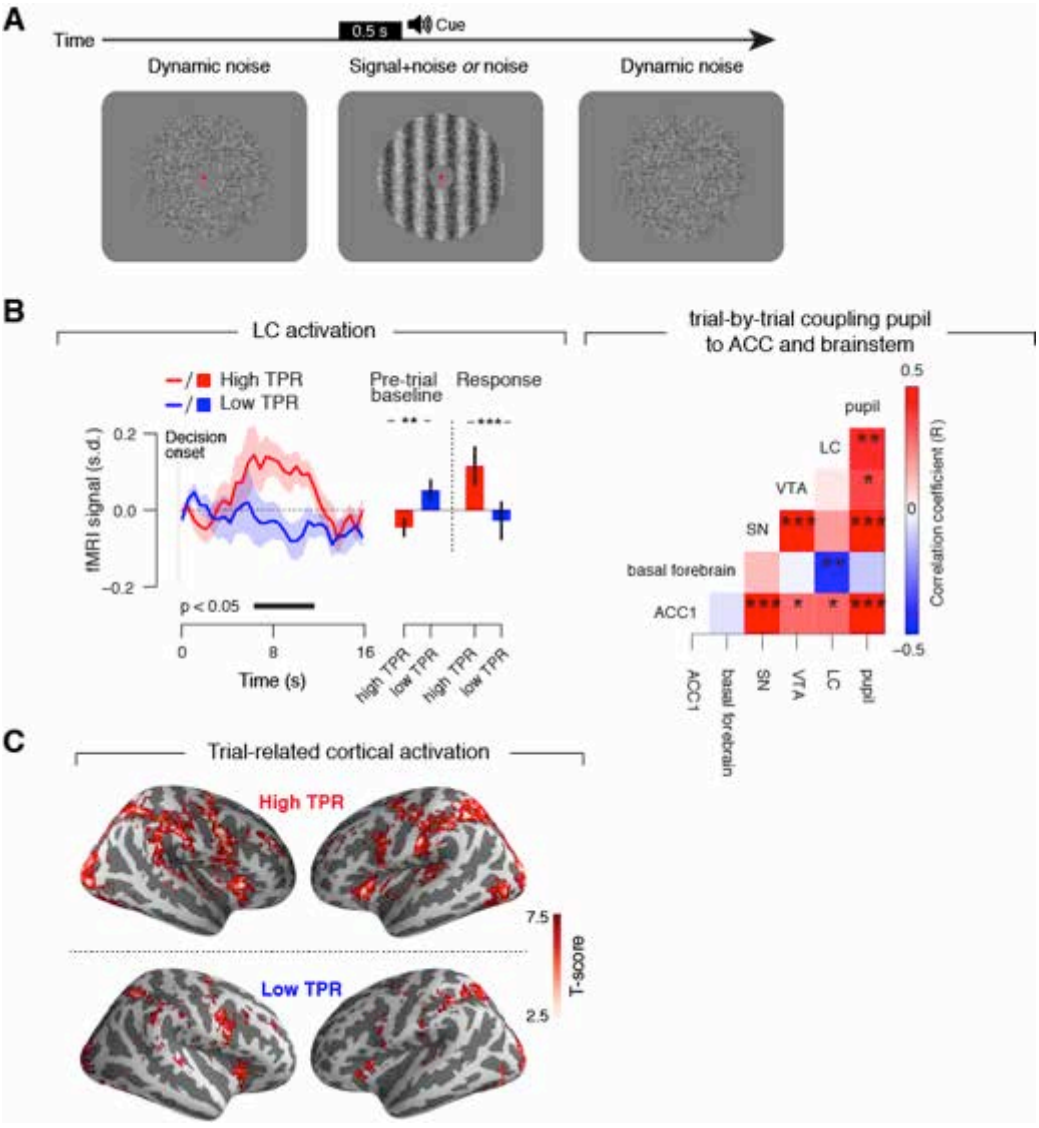

Figure 12: Pupil-linked Brainstem Responses During a Visual Yes vs. No Decision

(A) Sequence of events during a single trial. Dynamic noise is continuously present in a circular aperture around fixation. During the decision interval (onset cued by a tone), the subject searches for a low-contrast grating target signal superimposed onto the noise, and forms a yes vs. no decision about target presence. The final choice is indicated by one of two button presses. The signal is shown at high contrast for illustration purposes only, but titrated to the individual 75% correct detection threshold in the actual experiment. (B) Pupil-linked brainstem responses during decision-making. Left panel, trial-related LC responses and baseline LC signal levels for high vs. low TPR trials. Right panel, matrix of the correlation between trial-related responses in the pupil and several brainstem regions, as well as the ACC. (C) High TPR is also linked to stronger responses in cortical

decision networks. Abbreviations: TPR, trial-related pupil response. LC, locus coeruleus. VTA, ventral tegmental area. SN, substantia nigra. BF, basal forebrain. ACC, anterior cingulated cortex.

Trial-related pupil responses (TPR) were robustly coupled to task-related responses in the (individually delineated) noradrenergic locus coeruleus (LC) of the brainstem (Figure 12B, left). Significant coupling between pupil and brainstem responses was also observed for dopaminergic midbrain nuclei (SN and VTA), but not the cholinergic basal forebrain (Figure 12B, right). There was also a significant anti-correlation between decision-related responses in the LC and the cholinergic basal forebrain. Finally, there was significant coupling between trial-related responses in the anterior cingulate cortex that sends strong top-down projections to the brainstem.

Strong trial-related pupil responses are associated with boosted decision-related responses in the cortical decision network (Figure 12C). Computational modelling of subjects' behaviour indicates that strong, pupil-linked neuromodulation during the decision pushes the decision process towards making more yes-judgments (data not shown).

3.3.2.2 How Data are Related to Specific Platform Requirements

In the first phase, we plan to deliver data in the form of (i) dataframes (csv-files) with the trial-wise behaviour of each subject (choice, reaction time) suitable for decision-model fitting as well as (ii) the trial-related pupil and brainstem nuclei responses (suitable for event-related and correlation analyses as in Figure 12B), and (iii) whole brain statistical maps of the main contrasts of interest at the group level (nifti-files). The raw data could be made available at a later stage.

3.3.2.3 Quantitative Indicators of Data Completeness

The combined behavioural, pupil, and fMRI dataset is now fully acquired. The data set comprises N = 15 subjects, 2 sessions per subject in the main experiment and 1 retinotopic mapping session from 8 of the 15 subjects who were new in our data base and for whom retinotopic maps were not yet available. The analysis of all aspects of the data is on-going, but close to completion (Figure 12).

3.3.2.4 Status of Data Delivery

Raw data is available. Fully processed data will be delivered, upon publication of the data, during data-delivery phase II.

3.3.2.5 List of SP4 Collaboration Partners

Gustavo DECO, UPF.

3.3.2.6 Data Provenance

The fMRI dataset was collected by Jan Willem DE GEE (UKE) and Olympia COLIZOLI (UvA).

3.3.2.7 Plan Until the End of the Ramp-Up Phase

Finalise data analysis and publish the results.

3.3.3 Data set Two: Pupil-linked modulation of the cortical dynamics underlying yes vs. no decisions (MEG)

3.3.3.1 Description of Data and Models

The data set aims to identify how pupil-linked modulatory signals shape the dynamics of the cortical decision network during a visual yes vs. no decision.

Participants performed the same yes-no decision-making task as described in section 3.3.2, during concurrent whole-head MEG recordings and monitoring of pupil diameter. The task was described as above with the following exceptions:

- There were different noise levels in different blocks.
- An online staircase procedure ("Quest") kept each subject's performance at 75% correct answers.
- At the end of each trial, subjects reported how confident they were of their decision.

3.3.3.2 How Data are Related to Specific Platform Requirements

We plan to deliver the key statistical results of the MEG analysis in the form of statistical time-frequency maps. These will show power or coupling differences between experimental conditions at the group level (selected sensor groups/regions of interest and whole-brain). The MEG data will be analysed with Fieldtrip, thus the statistical results will be provided as Matlab .mat files. The raw data could be made available at a later stage.

3.3.3.3 Quantitative Indicators of Data Completeness

The combined behavioural, pupil, and MEG dataset (N = 25 subjects, 2 sessions per subject) is now fully acquired. The data analysis is still on-going. All MEG and pupil data is pre-processed, and the main analyses will start upon submission of the paper on the fMRI project described in section 3.3.2.

3.3.3.4 Status of Data Delivery

Raw data is available. Fully processed data will be delivered, upon publication of the data, during data-delivery phase II (end of the Ramp-Up Phase, March 2016).

3.3.3.5 List of SP4 Collaboration Partners

Gustavo DECO, UPF.

3.3.3.6 Data Provenance

The MEG dataset was collected by Jan Willem DE GEE (UKE) and Niels KLOOSTERMAN (UVA).

3.3.3.7 Plan Until the End of the Ramp-Up Phase

We aim to fully analyse the results of the MEG study and report them in a submitted publication.

3.4 Characterise Multiscale Brain Architecture of Decision-related Motivational States and Values (T3.2.4)

3.4.1 Overview

The goal of T3.2.4 (led by Talma HENDLER, Foundation for Medical Research Infrastructural Development & Health Services [TASMC – P98]) was to provide a comprehensive neuro-behavioural deconstruction of the human motivational domain into its elementary processes, states and accounts. It also aimed to further reveal the brain mechanisms supporting each process, and how they are regulated while engaged in naturalistic behaviour. To do this, multilevel data was collected from humans using the same paradigms during fMRI and intracranial recordings of LFP's and single-cells. This will ultimately provide a basis for computational modelling of motivational decision-making.

The main paradigm used in our study is aimed at capturing the spontaneous on-going motivational behavioural tendencies which occur in response to incentives and threats, with an important distinction between goal-conflict and no-conflict situations. Manipulating controllability (i.e. controlled vs. uncontrolled conditions) further allowed the extraction of the neural correlates of approach behaviour, as well as a neural

dissociation of the human motivation domain into the incentive and hedonic accounts, and the way they interact to regulate behavioural decision making.

Figure 13 shows a new ecological interactive computer game. This was constructed to manipulate approach and avoidance behaviours during an on-going dynamic goal-conflict, while enabling dissociation of incentive and hedonic accounts. The goal of the game is to earn money by catching coins and avoiding balls. There are two ways to gain or lose money. These are controlled (Con), where the player actively approaches coins and avoids balls (Figure 13, upper panel), and uncontrolled (NoC), where the player is hit by random coins and balls from an animated figure (Figure 13, lower panel). Each coin-catch resulted in a five-point gain, and each ball hit resulted in loss of five points, regardless of controllability. The game is played for four sessions of six minutes each (each session serves as a separate scan run). A fixation point is presented for one minute at the beginning of each session to establish a baseline condition. At the end of each session, subjects rate their feelings and attention towards each condition of the game (Con and NoC, winning and losing) on a nine-point Likert scale. Prior to each experimental session (fMRI or intracranial recordings), subjects were introduced to the game and played it for one minute, to ensure that the instructions were fully understood.

This paradigm has been running in our lab on healthy populations, providing convincing results which have been prepared for publication.

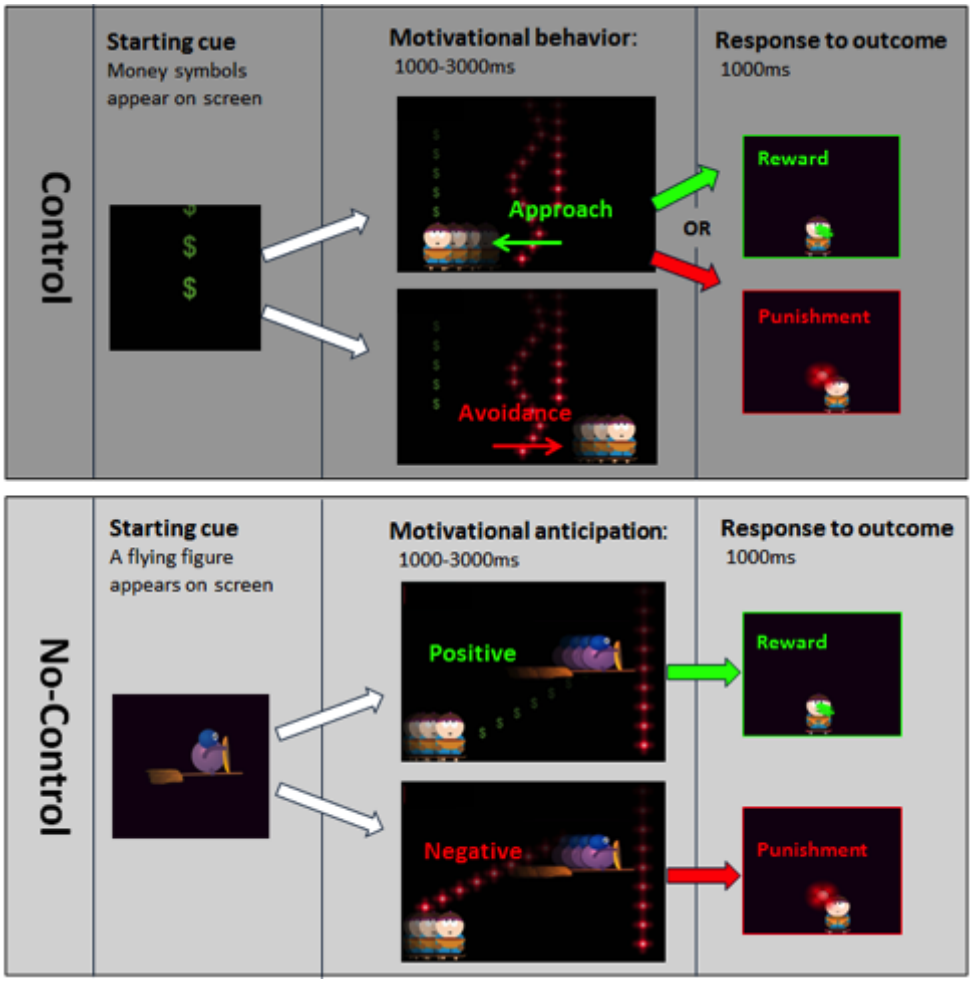

Figure 13: The Punishment, Reward and Incentive Motivation (PRIME) Game: Conditions of Interest

The goal of the game is to earn money by catching coins and avoiding balls. There are two ways to gain or lose money: controlled, where the player actively approaches coins and avoids balls (upper panel), and uncontrolled, where an animated figure throws random coins and balls that hit the player (lower panel). Subjects are told at the beginning of the game that these events are uncontrollable. For controlled conditions, each trial begins when a coin appears at the top of the screen (upper left panel). The subject chooses either to move towards the coin, or to move away from balls (incentive behaviour: upper centre panel, duration 1000-3000ms). The subject then succeeds in catching a coin, or gets hit by a ball (response to outcome: upper right panel, duration 1000ms). For No-Control conditions, each trial begins when a flying figure appears on the screen (lower left panel). The player then anticipates the coin/ball that falls and "chases" them (motivation anticipation: lower centre panel, duration 1000–3000ms), then the coin or ball hits them (response to outcome: lower right panel, duration 1000ms). Trials (behaviour and response) were separated by 0.5-5.5 seconds ISI.

The second paradigm used in our study is a well-established interactive risky-choice game developed in our lab[51-53].

Figure 14 shows a paradigm that allows us to separate the motivational decision, anticipation of reward/punishment states, and response to outcome. It is a two-player competitive domino game. The opponent's responses ware randomly generated by a computer in a predetermined pattern, to allow a balanced design. Players, however, were told that the opponent was the experimenter, and that their choices could increase their chances of winning. At the beginning of each game, 12 random domino chips were assigned to the player, and were shown at the bottom of the board. At the same time, one master domino chip, which remained constant throughout the game, appeared at the top left corner of the board. Players won the game if they were able to successfully dispose of all 12 chips within four minutes. Each assigned chip could either match the master chip (have one of the master chip's numbers), or not. In each round of the game, players had to choose one chip (decision making), place it face down adjacent to the master chip (execution), and then wait for the opponent's response (anticipation), to see whether the opponent challenged this choice by uncovering the chosen chip or not (outcome). Since the master chip remained constant throughout the game, it was only possible to win by choosing both matching and non-matching chips. In the game context, matching chips are considered 'safe' moves, since they are associated with rewards if uncovered and non-matching chips are considered 'risky' moves, since they are associated with punishments if uncovered. Specifically, based on the player's choice and opponent's response, there are four possible consequences per game round (i.e. 'outcome' possibilities):

1) Show of a non-match chip: the choice of a non-match chip is exposed, and the player is punished by receiving the selected chip back, plus two additional chips from the deck.
2) No show of a non-match chip: the choice of a non-match chip remains unexposed and only the selected chip is disposed of, so the player is not punished.
3) Show of match chip: the choice of a match chip is exposed and the player is rewarded by the disposal of the selected chip, and one additional random chip from the game board.
4) No show of a match chip: the choice of a match chip is not exposed, and only the selected match chip is disposed of, so the player is not rewarded.

Overall, player's choices and opponent's responses are interactively determined by the flow of the game round after round, creating a natural progression of the game situation. This lasts for four minutes, or until the player wins. Each player played consecutively for 14 min. For more details of the game, see Figure 14, and GONEN et al, 2012 [52].

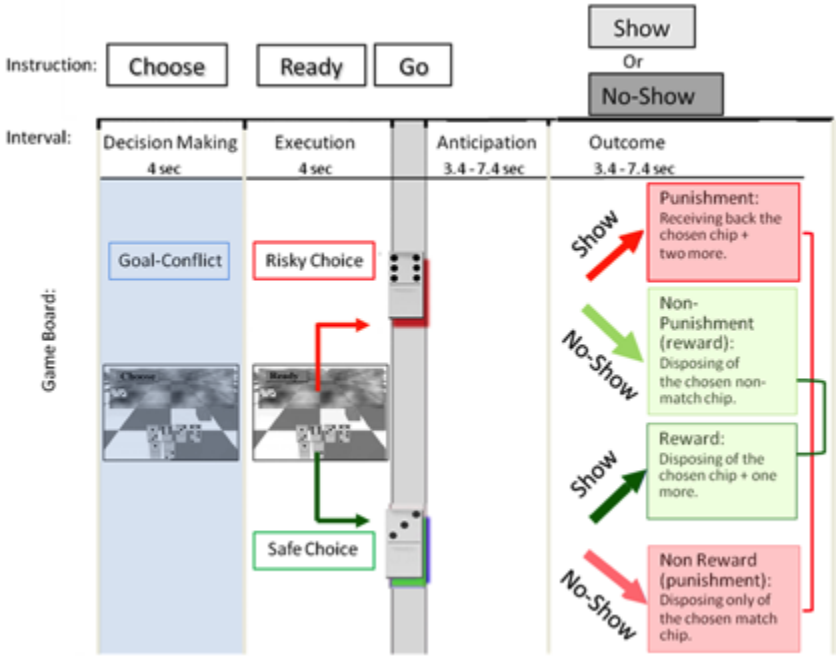

Figure 14: Risky Choice Domino Game Paradigm.

Each round of the game is composed of four intervals: the player chooses which chip to play next (first interval: "choose" 4 second), moves the cursor to the chosen chip and places it face down adjacent to the master chip (second interval: "ready" and "go". 4 second). The player then waits for the opponent's response (third interval: "anticipation"; jittered randomly to 3.4, 5.4 or 7.4 second), and sees whether the opponent challenges this choice by uncovering the chosen chip or not (fourth interval: "outcome"; jittered randomly to 3.4, 5.4 or 7.4 second). The player's choices and opponent's responses are interactively determined by the flow of the game round after round, creating a natural and unpredictable progression of a game situation, which lasts four min, or until the player wins. Each player played consecutively for 14 min.

3.4.2 Data set 1: Intracranial Single Cell and LFP Dataset

3.4.2.1 Description of Data and Models

The set of data collected within this task provides one of the few opportunities to observe local small-scale recordings of single neurons, and small neuronal populations within deep regions of the brain. The data of five patients will be provided in Phase I. Additional data will be provided by the end of the Ramp-Up Phase. Table 1 describes the overall location of electrodes available from these five patients.

The data delivered to the HBP platforms will include the following:

1) A summary table of electrode location in xyz Montreal Neurological Institute (MNI) coordinates, and their atlas labels using the neuromorphics atlas (http://www.oasis-brains.org/, http://Neuromorphometrics.com/ segmenting the human brain to 207 brain regions). This includes microwire locations, which can detect single cell recordings, and macro electrode locations recording local field potentials (LFP).
2) A table describing neuronal firing. This will show a significant increase or decrease in firing rate in response to, or in anticipation of, a paradigm induced event (e.g.: an account of neurons in different brain locations responding to control punishment in the PRIMO paradigm, or responding to the show match conditions in the risky-choice domino game).

3) Matlab matrices describing the LFP signal power at the different frequency bands and different spatial locations, responding to paradigm induced events.

area\patient	D1	D2	D3	D4	D5
Hipocampus	B	B	R	B	B
Para-hippocapus		R			
Entorhinal		R	R	B	B
Amygdala	B	B	R	B	B
Lateral temporal	B	B	R	B	
Basal temporal					
Dorsal Cingulate			R	B	B
Ventral cingulate	B	B	R	B	B
Lateral frontal	B	B	R	B	

Table 1: Overall Electrode Locations Per Patient.

L=Left, R=Right, B=Bilateral. More detailed coordinates will be provided in the data.

3.4.2.2 How Data are Related to Specific Platform Requirements

Atlas coordinates will be provided, along with Matlab structures and files.

3.4.2.3 Quantitative Indicators of Data Completeness

The data from five patients (as detailed in the above description of data) is complete. This includes the complete mapping of electrode locations, and neuronal responses to paradigm stimuli at the different locations. The remaining dataset of an additional six patients will be provided by the end of the Ramp-Up Phase. This data will be regarded as complete when it includes the final localisation of all channels (from 11 patients), and neural responses at the different scales.

3.4.2.4 Status of Data Delivery

In Phase I, the localised results of paradigm-induced reactions in single neuronal activity and LFP (as detailed in the above description of data) of five patients will be delivered.

3.4.2.5 List of SP4 Collaboration Partners

The micro scale and multiscale dataset provided by this work should be of great value for SP4 in general, and in particular WP4.1, dealing with “bridging scales” aiming to create models for intral and extral cellular recordings, LFP and EEG. Contact with SP4 partners for feeding models with real human neuronal data is planned.

3.4.2.6 Data Provenance

The data is owned by TASMC. The data were collected and analysed by a large group of collaborators, including neurosurgeons, neurologists, technicians and neuroscientists.

3.4.2.7 Plan Until the End of the Ramp-Up Phase

The dataset of an additional six patients will be provided by the end of the Ramp-Up Phase. Deeper analysis into system dynamics and correlation between regions and scales will be performed.

4. Learning and Memory (WP3.3)

4.1 Skills and Habits (T3.3.1)

4.1.1 Overview

The aim of the studies conducted in Avi KARNI's group, University of Haifa (UHAIFA – P72) is to address cortical dynamics (repetition suppression, repetition enhancement, functional connectivity) as brain signatures of accumulating experience, plasticity, and procedural memory consolidation in motor skill learning in typical young adults. A key strategic point is that we are following on from the work of KARNI et al, (1995), (1998) [54,55]. This means looking at short-term modulations of the evoked BOLD signals in motor cortex, and the motor system in general, as enduring signatures of previous experience. Importantly, we are also seeing these as signatures of overnight procedural memory consolidation. Thus, we are testing whether activity in a given brain area is modulated by task repetition in a differential manner, as a function of whether prior experience was afforded, i.e. reflecting local mnemonic processes, specifically procedural memory consolidation.

This focus on the temporal modulation of activity (as reflected in the metabolic BOLD signal) is complemented by tests for repetition-dependent modulations of the functional connectivity between areas engaged in the performance of the task. Our proposal is that M1 serves as a hub for a motor working memory system, wherein a temporarily stabilised network in the cortex and striatum promotes an integrated representation of the new movement sequence (i.e. the movement syntax). The M1-straitum co-activation is down regulated for a well-consolidated (automatic) movement sequence.

4.1.2 Data set One: Short-term Cortical Modulation by Task Repetition as Signatures of Procedural Memory Consolidation

4.1.2.1 Description of Data and Models

Strategic question: are mnemonic processes reflected in the modulation of neuronal responses to task repetition (how $T_i \neq T_{i+1}$)? We investigated how units/columns in the human motor cortex (M1) address repeated experience, i.e. tasks repeated across a brief (30 second) rest period. We show clear repetition dependent dynamics in signal intensity[56] and in connectivity[57]. With the data set, we aim to identify the brain signatures of the processes underlying overnight procedural memory consolidation of a trained movement sequence.

Behaviour data: Participants (n=36) were trained in performing a five-element finger opposition movement sequence (Figure 15A). Training consisted of 160 blocked, cued, repetitions of the assigned movement sequence (T-FOS). Performance was tested for speed of execution and accuracy in four blocks of 30 seconds each. The control was an identically constructed movement sequence, with movements arranged in the mirror-reversed sequence (U-FOS). Behavioural results are shown in Figure 15B. Training resulted in both within-session ("online") gains in performance, and in additional robust overnight (delayed, consolidation phase, "offline") gains in both speed and accuracy. Importantly, the gains in performance that occured overnight (delayed "offline" gains, DG), were specific to the trained movement sequence (T-FOS).

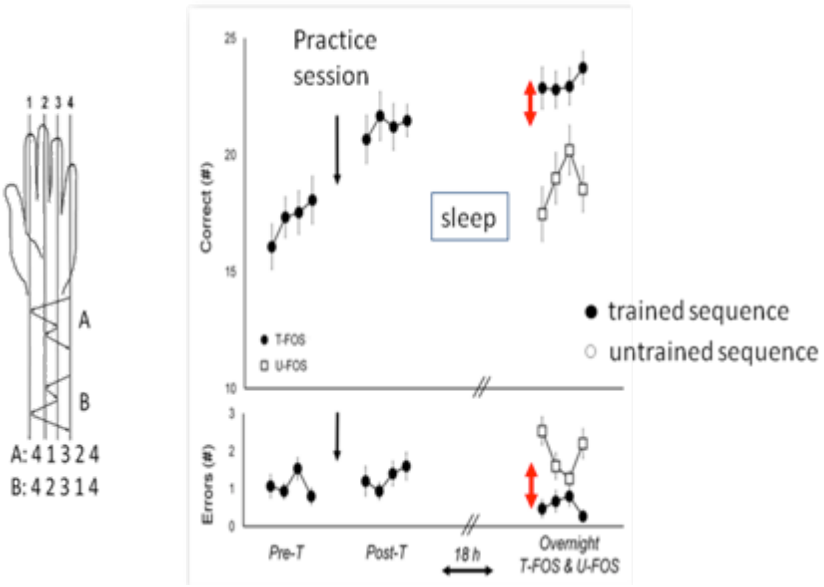

Figure 15: Task Design for T4.1.2 and Behavioural Results

Left panel: the two sequences. There were two five-element sequences of finger to thumb opposition movements.These were both composed of the same movements and performed at a fixed, paced, equal rate (in the scanner). However, the component movements were arranged in two different orders (syntax) that mirror imaged each other (sequence one: 4-1-3-2-4, sequence two: 4-2-3-1-4, each number is a finger, 1 = index, 4 = little finger). Only one sequence was trained and allowed to be consolidated overnight (=T-FOS). The other was introduced for the first time in the scanner (= U-FOS). Only one of the sequences was assigned for training (160 repetitions).

Right panel: behavioural results. Subjects were tested before, (Pre-T) and immediately after, the training session (Post-T), and were then re-tested immediately after the fMRI scanning session (Overnight). The overnight test assessed performance for both sequences. The results show that training resulted in both within-session ("online") gains in performance, and in additional robust overnight (delayed, consolidation phase, "offline") gains. The gains in performance that occur overnight (delayed "offline" gains, DG) are specific to the trained movement sequence (T-FOS).

Brain imaging: comparing movement representation changes across a brief rest period () occurring overnight

In the brain imaging study, we acquired fMRI data in 16 of the same participants. The data set was acquired using whole brain coverage at 1.5 isotropic resolution. The data were collected while participants performed the FOS task, either the trained (T-FOS) or the untrained, complementary sequence (U-FOS). The brain imaging data collection approach is shown in Figure 16.

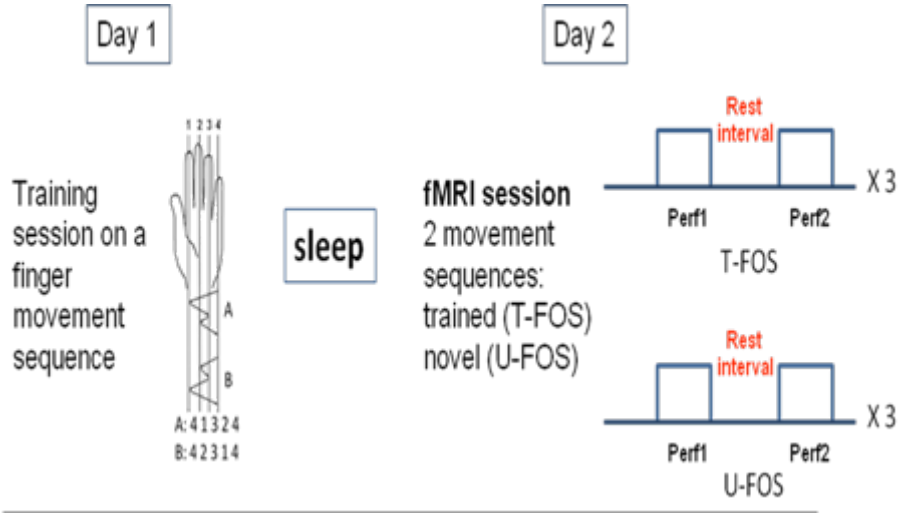

Figure 16: Task Performance Paradigm for T4.1.2 in fMRI Session

Left panel: task one of the sequences was assigned for training (160 repetitions). Right panel: overnight scanning session. There were two five-element sequences of finger (to thumb) opposition movements. These were both composed of the same movements, and performed at a fixed, paced, equal rate (in the scanner). Only the component movements were arranged in two different orders (syntax), as they mirror imaged each other. One sequence was trained the day before and was consolidated overnight (T-FOS). The other was introduced for the first time in the scanner (U-FOS). Each sequence was performed in two intervals. Perf1 was performed for 30 seconds (continuously and in a paced manner), followed by a rest interval (30 seconds), and then Perf2 (30 seconds). The evoked signals in Perf1 and 2 were compared.

Importantly, there is no difference in the average evoked activity in the cortex, or in sub-cortical structures, which differentiates between two such movement sequences when both are performed at the same rate. So, we looked at task repetition effects (signal and connectivity modulations). The logic behind this is that consolidation processes generate local changes within the column. This may be reflected in inhibition-excitation balance, and thus in signal modulation, during task repetition, rather than in averages across task repetitions. The results of the different analysis approaches are in the press[56,57]. We demonstrate clear repetition dependent dynamics in 1) signal intensity (Figure 17) and 2) connectivity (Figure 18).

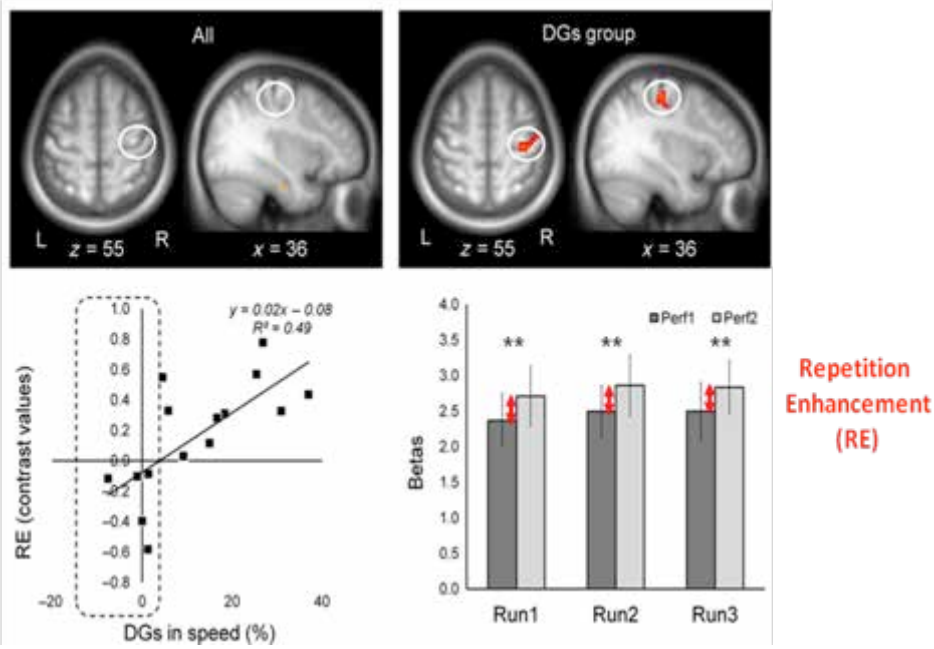

Figure 17: Brief but Robust Modulation of M1 Signals by Task Repetition.

The top panels show the motor cortex (M1) contralateral to the left hand performing the sequences (i.e. in the right hemisphere). This was the only brain area showing significant repetition enhancement (RE) effects, but this was only for the trained, consolidated movement sequence, when tested overnight. Repeating the U-FOS resulted in repetition suppression (RS). The result is not shown, as it is a well-known phenomenon of motor novelty (KARNI et al, [1995], [1998]). The bottom left-hand panel shows the correlation between the behavioural measure of consolidation; the expression of overnight Delayed Gains in speed (DG, x axis) and the RE in M1 (in terms of the BOLD signal differences, deltas, y axis) upon task repetition. Each data point shows a single subject's behaviour (overnight, delayed, performance gains, DG's) and the corresponding signal modulation in M1.

1) There is repetition suppression (RS) for repeating new movement sequences, and repetition enhancement (RE) effects for repeating well-consolidated sequences. Importantly, the enhancement effect is well correlated with the behavioural effect of consolidation, i.e. overnight, offline movement speed gains (Figure 17).

2) Connectivity between M1 and the basal ganglia (BG) increases when a new movement sequence is repeated after the short rest. The connectivity between M1 and the BG tends to decrease after the brief rest for a well-consolidated sequence (Figure 18). We think that this reflects the setting up of a short-lived motor working memory for the untrained sequence (U-FOS), but the representation of the trained sequence (T-FOS) is BG independent.

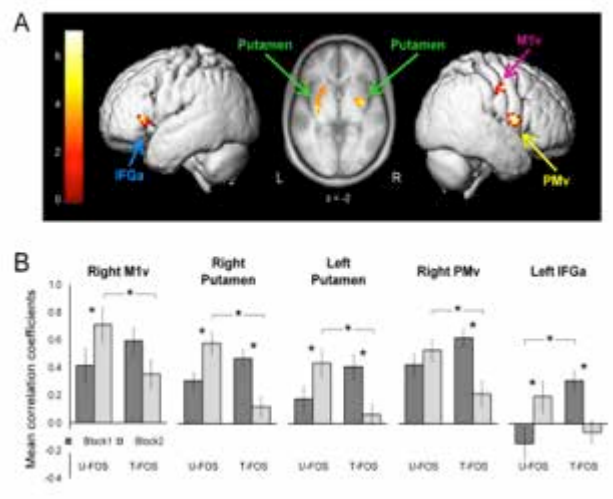

Figure 18: Brief Dynamic Modulations of Neural Activity and Connectivity, During Task Repetition, May Constitute Robust Signatures for Mnemonic Processes in the Cortex.

A) Images showing five brain areas/structures (from left to right in A: Inferior frontal gyrus [IFG], the putamen (part of the BG), shown bilaterally, the ventral pre-motor area [PMv], and the ventral M1 — a part of M1 representing the trained hand (other than the "seed" voxels of the right M1). All of these brain structures showed functional connectivity changes with an M1 seed upon task repetition. These are brain structures in which activity significantly correlates with the M1 seed; the right (contraleteral to the performing hand) M1's signal during task performance.

B) This shows differential modulations of M1's connectivity with the five brain structures upon task repetition (before [Perf1] and after [Perf2] a 20 second rest interval). It is clear that modulation is different for the two sequences tested: the trained consolidated sequence (T-FOS) shows a consistent pattern of decreased connectivity upon repetition. However, when the untrained, novel sequence of movements is repeated, the correlation between all five brain areas, and importantly, between the pre-motor areas, the BG (bilaterally) and the right M1 increases (y axis = mean correlation coefficients, measure of functional connectivity).

A small number of voxels in M1, contralateral to the task performing hand, were used as a "seed" (standard term designating the source of the time-course data, to which parts of the rest of the brain time-correlate). What parts of the brain act in sync (positively or in reverse phase) to the "seed" area. We discovered that for a novel movement sequence, connectivity increases between the motor cortex and the BG, pre-motor (sequence planning) areas, and even other parts of the M1 itself (more of it is recruited for repeated task performance than for initial performance). The connectivity is down-modulated by repeating a well-consolidated movement sequence.

4.1.2.2 How Data are Related to Specific Platform Requirements

In addition to publishing the key findings and analysis results, we plan to deliver the key statistical results of behaviour, and the fMRI analysis in the form of contrasts at group level. The fMRI data is being analysed with Statistical Parametric Mapping software (SPM toolbox, Matlab), and the statistical results will be provided as SPM.mat files. The raw data could be made available in a later phase.

4.1.2.3 Quantitative Indicators of Data Completeness

The behavioural and brain imaging datasets have now been fully acquired. The behavioural data set has been fully analysed and published[56,57]. The fMRI data analysis results have also been published in part, but additional fMRI data analyses are underway. A third paper addressing transfer (remote) effects to the other hemisphere is under review (GABITOV, MANOR and KARNI).

4.1.2.4 Status of Data Delivery

Raw data is available. Fully processed data will be delivered during data-delivery phase II.

4.1.2.5 List of SP4 Collaboration Partners

None, but this is currently being explored.

Our behavioural and brain imaging results provide an important challenge for models and simulations at the multi-column level. The results should be considered as providing important tests and insights into simulations. This is because they suggest the dynamics in repeated cortical networks are not “noise”, but rather reflect patterned dynamic modulations of neural activity and functional connectivity during task repetition. They therefore constitute robust signatures for novelty, repeated experience and long-term mnemonic processes.

4.1.2.6 Data Provenance

The behavioural data was acquired in the KARNI Lab at UHAIFA. The fMRI data were collected by members of the KARNI Lab (supervised by Ella GABITOV and Rinatia MAARAVI-HESSEG) At the Sheba Medical Center, Tel Hashomer, and at the Rambam Medical Center, Haifa, Israel.

4.1.2.7 Plan Until the End of the Ramp-Up Phase

We aim to continue publishing the results of the brain imaging study. We also aim to continue investigating the mnemonic processes initiated by action observation, rather than actual physical performance, using the novel paradigm (including additional fMRI data collection — see below). This is related to cross WP collaboration with partners from WP3.6. and WP2.3.

A behavioural study (completed) and an fMRI brain imaging study (on-going), are in progress. These aim to address motor cortex plasticity driven by visual input (action observation). The behavioural data suggest that executing and observing movements improves task performance and triggers skill consolidation processes. However, consolidation could be blocked by ensuing action but not by observation, indicating that skills acquired in doing or observing do not overlap in the brain. A paper is being prepared (MAARAVI-HESSEG, GAL, KARNI).

4.2 Memory for Facts and Events (T3.3.2)

4.2.1 Overview

Yadin DUDAI’s group has generated a human memory protocol combining behaviour and fMRI. This allowed us to identify behavioural and brain mechanisms that trigger episodic memory consolidation under real-life conditions. It also allowed us to tease apart the contribution of encoding and retrieval in a single experience. We have specifically focused on the role of the hippocampus in these processes. We have integrated this into a flowchart brain-inspired functional model of the initiation of episodic memory consolidation that guides and constrains the modelling of acquisition storage and use of declarative memory in the human medial temporal lobe.

4.2.2 Data Set 1: Cognitive Architecture of Episodic Memory Consolidation

4.2.2.1 Description of Data and Models

4.2.2.1.1 Goal

The goal is to identify circuits that help to trigger the consolidation of realistic episodic memory.

4.2.2.1.2 Hypothesis

Our hypothesis is that realistic episodes undergo binding in a temporary episodic buffer as soon as they make sense, cued by event boundaries.

4.2.2.1.3 Boundary Conditions

In on-going episodes, the activation of brain circuits that encode events on the fly confounds the identification of representations of posited closure cues.

4.2.2.1.4 Strategy

The strategy is to present brief episodes encoded (4—20 seconds) in the form of audiovisual clips, with intercalated 'rest' (no stimulus) periods. The protocol is then pursued to identify brain activation that is time-locked to the offset the episode, and predict subsequent memory. As a second stage, participants are presented with the same set of episodes multiple times, to separately assess the effect of familiarity on brain activation at event onset vs. event offset.

4.2.2.1.5 Protocol

Stage One:

Each experiment consists of a “study” phase in the fMRI scanner and a subsequent “test” phase outside the scanner[58,59]. The procedure aims to identify brain regions exhibiting delayed encoding-related activation (i.e. a higher BOLD response to subsequently remembered vs. forgotten clips, initiated at clip offset). It uses eight second audiovisual clips that the participants had not seen before. A total of 180 clips are used, of which 160 were narrative movie clips (Movie) and 20 were visually scrambled clips (Scrambled), accompanied by non-distinctive background noises. The intercalated rest period involved 4—12 (jittered) blank screens. The fMRI data acquired during the presentation of Movie clips were subsequently divided into Remembered and Forgotten events. Similarly, fMRI data acquired during the presentation of blank screens following the clips were divided into R-Blank, F-Blank and S-Blank periods (blank screens following Remembered, Forgotten and Scrambled clips, respectively). The conjunction contrast of R-blank>F-blank and F-Blank>baseline yielded several brain regions (combined $p<0.000025$, uncorrected, minimal cluster size of five contiguous functional voxels). These included the right hippocampal body, bilateral hippocampus head (extending to the amygdala-hippocampal junction), right optic radiations (directly posterior to the hippocampus), bilateral dorsal caudate nucleus, and bilateral posterior cerebellum. The results were replicated in several studies in our laboratory and included in several publications. The identified circuit is currently predictive at group level, and we are attempting to modify the protocol to achieve predictability at individual subject level.

Stage Two

Similarly to stage one, the experiment is divided into a study phase, which takes place in an fMRI scanner, and a test phase outside the scanner. Participants are presented with 80 narrative movie clips, 40 of which are repeated six times (Repeated) and 40 of which are presented once (Single-Pres). Performing an ROI-analysis on the hippocampus, which was identified in Stage one, we assessed the effect of increased familiarity (across

presentations) at event onset vs. offset. We found that the offset response decreases with familiarity, in line with an encoding signal, while an onset response emerges only for familiar events, in line with a retrieval signal. This enabled us, for the first time, to tease apart encoding and retrieval signals in response to the same event[60].

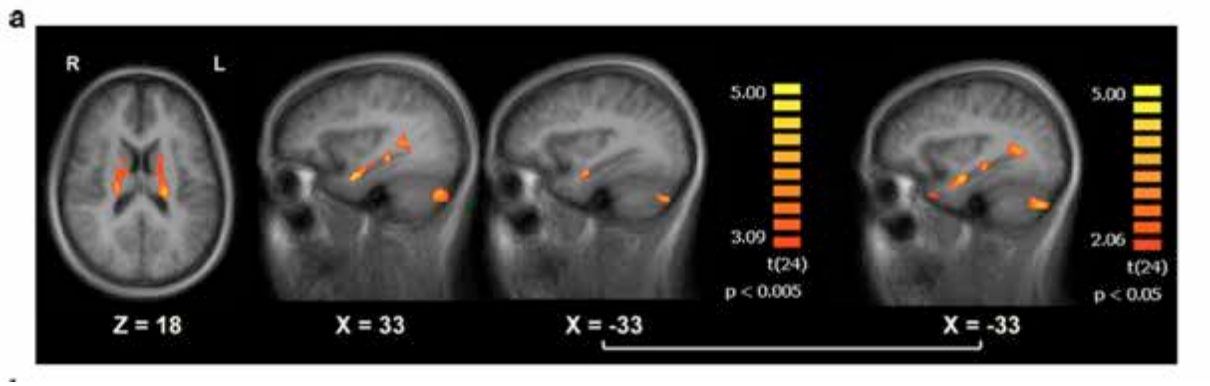

Figure 19: Brain Regions Predicting Stimulus-offset-locked Memory Predicting Activity

Striatal, hippocampal and cerebellar activations are identified. From Ben-Yakov and Dudai 2011[58].

4.2.2.2 How Data are Related to Specific Platform Requirements

The protocols allow us to identify the role of hippocampal formation and other brain circuits in specific steps in the initiation and retention of episodic memory. This therefore clarifies the cognitive architecture of a major unique function of the human brain. The data obtained feeds into a flowchart model of the initiation of memory consolidation, and is integrated into available information on the human medial temporal lobe and neocortex.

4.2.2.3 Quantitative Indicators of Data Completeness

We have so far acquired about 80% of the data required, and performed about 50% of the analyses that we expect to perform on these data.

4.2.2.4 Status of Data Delivery

We can supply fMRI and behavioural data that identify the role of the hippocampus in triggering human episodic memory consolidation immediately at the offset of short episodic segments in realistic conditions (see cognitive architecture document enclosed), and in switching between encoding and retrieval mode in a single episodic experience[59,60]. The data collected is currently in Brainvoyager proprietary format. We can supply the individual timecourses for each functional run of each participant, extracted from anatomically-defined regions of interest, as well as design files that indicate the timings of different events in each functional scan. Both of these can be supplied as matlab variables in a .mat file. If required, the anatomical scans, currently in Brainvoyager format, can be converted into nifti format.

4.2.2.5 List of SP4 Collaboration Partners

We have no targeted collaboration on this project with SP4, but have had several focused exchanges so far with Dr. Misha TSODYKS on potential memory models. We predict that once our data become available to SP4 principle investigators, some of them will integrate it into their work.

4.2.2.6 Data Provenance

The fMRI and behavioural data were collected and analysed by Aya BEN-YAKOV, Neetay ESHEL, Micah RUBINSON and Meytar ZEMER. The data were also analysed by Noga COHEN, at the WIS.

4.2.2.7 Plan Until the End of the Ramp-Up Phase

We expect to complete the acquisition of additional complementary data related to the role of event boundaries in initiation of consolidation (as predicted by our functional and neuroanatomical model). We plan to use the same data sets to analyse pre-stimulus predictors of subsequent memory, and the effect of the passage of time in modifying the contribution of medial temporal role in memory representation and transformation. We expect to provide improved functional localisers and functional models of episodic memory consolidation, to feed into SP4 as required.

4.2.3 Model One: Neural mass models of the sleeping brain

4.2.3.1 Description of Data and Models

4.2.3.1.1 Goal

The overarching project aim is to model the transformation of hippocampus-dependent memory during sleep-dependent system consolidation. To this end, as a first stage we aimed to model sleep using neural mass models. This would allow us to predict the outcome of experimental setups investigating the influence of sleep on memory consolidation. In modelling sleep, we put special emphasis on the interaction between the neocortex, the thalamus and the hippocampus as the key structures contributing to active system consolidation of hippocampus-dependent memory. To validate our models, we used parallel studies in rats. We recorded local field potentials and single unit activity concurrently, from the key structures of interest, during sleep and wakefulness, and in the context of specific memory tasks.

4.2.3.1.1 Hypothesis

Neural mass models provide a direct link between mesoscopic measurements, such as EEG, and local field potential oscillations and the underlying neural network dynamics, as explored in our *in-vivo* experiments in rats. Incorporating different experimental settings enables us to validate our model directly, and predict the dynamic between activity patterns thought to be particularly relevant for memory processing during sleep, i.e. the hippocampal sharp wave-ripples, the thalamic spindles and the neocortical slow oscillations.

4.2.3.1.2 Strategy

Changes in brain dynamics are driven by neuromodulators that are highly specific to the respective brain structure. Furthermore, it has been shown that there is a strong temporal relationship between the structures of interest here, i.e. a grouping of neocortical slow oscillations, thalamic spindles and hippocampal sharp wave-ripples. Consequently, we focus on developing independent models of the relevant brain structures (cortex, thalamus, and hippocampus), which are then incorporated into a unified framework. This approach enables us to investigate the interplay between the different brain structures, and validate our models by comparison with the experimental studies in rats that specifically target the different brain structures.

4.2.3.1.3 Progress

Stage One:

We developed a model of the sleeping cortex within the neural mass framework, allowing for a cost efficient modelling of a sleep EEG. Based upon our findings, we were able to describe the emergence of K-complexes and slow oscillations during NonREM sleep, and how the cortex transitions from wakefulness to deep sleep[61].

Stage Two:

Based upon our findings in stage one, we developed a model of the sleeping thalamus[62]. We were able to show that our simple approach was sufficient to generate realistic spindle activity in the thalamic model. Additionally, we combined both models from stages one and two, and investigated the thalamo-cortical interaction. The combined model was able to reproduce the EEG from sleep stages N2 and N3 to a high degree, including cortical K-complexes, slow wave activity and thalamic spindles. Furthermore, we could show that our model is able to reproduce the temporal relationship between cortical slow oscillations/K-complexes and thalamic spindles, which is thought to be crucial for memory consolidation.

In our studies in rats, we have so far concurrently recorded spontaneous local field potentials and single unit activity from cortical and hippocampal regions during wakefulness and sleep. The data will be used to test and optimise our model.

4.2.3.2 How models are Related to Specific Platform Requirements

Currently our models focus on the generation of realistic EEG signals, and their link to network spiking activity. However, there is also a direct link between the activity of neural masses and the BOLD signal measured in fMRI, which would enable us to additionally validate our model against fMRI data.

4.2.3.3 Quantitative Indicators of Data Completeness

We have validated our different models against multiple pre-existing experimental data. Validation shall be extended to data that will be obtained from recordings of the rat thalamus. Once we expand our model to include a hippocampal component, we will also add tests with hippocampal data.

4.2.3.4 Status of Data Delivery

We have developed simulation routines with interfaces to commonly used analysis software e.g. Spike2 and MATLAB. If there is demand for other software interfaces, we should be able to add them easily. Additionally, full model descriptions are available through our publications and can be easily implemented individually.

4.2.3.5 List of SP4 Collaboration Partners

Our theory should be particularly relevant to theorists in SP4 aiming at reproducing global brain signals associated with vigilance, e.g. Alain DESTEXHE, Gustavo DECO.

4.2.3.6 Data Provenance

Full model description and implementation details of our model are provided in our publications. They are sufficient to completely reproduce our findings.

4.2.3.7 Plan Until the End of the Ramp-Up Phase

We are currently working on a neural mass model of the hippocampus, which is able to generate sharp wave-ripples. Once we have validated our results with our experimental rat data, we plan to integrate it into our existing neural mass framework, to investigate hippocampal - thalamocortical interactions in depth. We will put special emphasis on the temporal relationship between sharp wave-ripples and slow oscillations/thalamic spindles, i.e. the generation of spindle-ripple events, which we see in our recordings from rats.

4.3 Working Memory (T3.3.3)

4.3.1 Overview

Working memory (WM) maintains information over brief periods of time. This feature is required for goal-directed behaviour, and allows us to act beyond the confines of the here and now. WM can thus be conceptualised as providing an interface between perception, long-term memory, and action. As such, WM is taxed by numerous laboratory and everyday cognitive challenges. The delayed match-to-sample (DMS) task captures the essence of WM: maintenance of information during a delay period, when there is no sensory input/external support. Various versions of the DMS task have been used in many past human and primate studies, demonstrating that a network of brain regions implements WM. However, the specific contribution of each network component remains unclear. Also, a long-standing assumption of the relation between WM and consciousness has recently been questioned, and should be further investigated. Here we describe a dataset that will consist of fMRI data from participants performing a DMS task, under conditions of conscious and non-conscious perception of the sample stimuli.

4.3.2 Data set One: Short-term Maintenance of Conscious and Non-conscious Information.

4.3.2.1 Description of Data

During fMRI scanning, participants perform a delayed match-to-sample task, where sample stimuli are shown either consciously or non-consciously. This is followed by a delay period, and then a probe stimulus (always conscious) that either does or does not match the sample. Trials with no sample stimulus are used as a reference condition (subjectively identical to non-conscious trials). A critical aspect of the experiment is to dissociate brain activity related to the different trial components (sample presentation, delay period, response), and to compare sample-absent and non-conscious trials, and conscious and non-conscious trials, in relation to brain activity that is specifically associated with the delay period.

Data collection is made on a GE 3 Tesla Discovery MR750 scanner. T2*-weighted images are obtained with a single-shot GE-EPI sequence with the following parameters: field of view: 25 cm, matrix size: 96 x 96, slice thickness: 2.9 mm, 37 slices (interleaved, no inter-slice interval), echo time: 30 ms, repetition time: 2.0 s, flip angle: 90 degrees.

4.3.2.2 How Data are Related to Specific Platform Requirements

FMRI data will be analysed with SPM. We plan to deliver the key statistical results of the fMRI analysis in the form of contrasts (volumes of t/F-statistics), and also to provide the statistical models used to generate the contrasts (SPM.mat files). The raw data could be made available in a second phase.

4.3.2.3 Quantitative Indicators of Data Completeness

An initial dataset has been collected (n=27), but additional data collection is required to allow conclusive results.

4.3.2.4 Status of Data Delivery

Raw data is partially available (initial dataset). Fully processed data will be delivered during data-delivery phase II (end of the Ramp-Up Phase, March 2016).

4.3.2.5 List of SP4 Collaboration Partners

None

4.3.2.6 Data Provenance

The data has been, and will be, collected by Fredrik BERGSTRÖM at Umeå Center for Functional Brain Imaging (UFBI), Umeå University, Sweden.

4.3.2.7 Plan Until the End of the Ramp-Up Phase

We plan to complete the data collection, and analyse and report the results in a publication.

5. Space, Time and Numbers (WP3.4)

Only the Space part of the WP, "identifying circuits for spatial navigation and spatial memory", is funded during the HBP Ramp-Up Phase, and is therefore the object of the present report. The Time and Numbers parts were scheduled to start in the second phase.

5.1 Identifying and Analysing the Multi-modal Circuits for Spatial Navigation and Spatial Memory (T3.4.1)

5.1.1 Overview

Within T3.4.1, Neil BURGESS' group (UCL) has identified the critical data for constraining models of navigation from the existing literature on experiments in rodents. In addition to published reports of the firing patterns of place cells, grid cells, head direction cells and boundary cells, we have focused on the behavioural/lesion findings of PACKARD and MCGAUGH, 1996; and PEARCE et al., 1998 [63,64]. The PEARCE et al. study describes the behaviour of rats in a modified version of the Morris Water Maze: providing a local landmark at a fixed distance and direction from the submerged platform (see Figure 20). More specifically, it quantifies the time necessary for rats to reach the platform as a function of experience for animals with and without hippocampal lesions. The PACKARD and MCGAUGH study measures the number of animals that exhibit place vs response learning as a function of number of training days on a plus maze, and how this is affected by inactivation of the hippocampus or striatum.

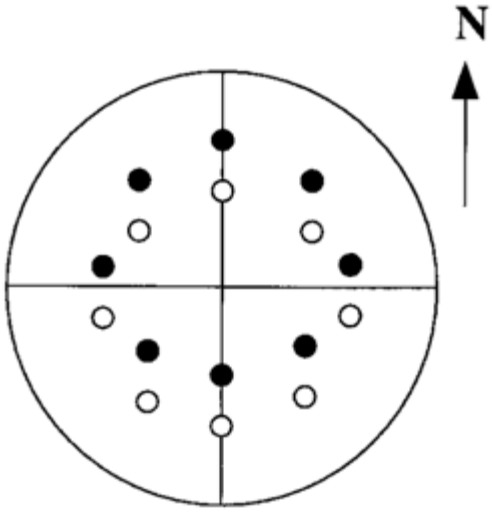

Figure 20: Water Maze with Submerged Platform Positions (empty circles) and Landmark (black circles)

5.1.2 Data Sets One and Two: Performance of Lesioned and Control Rats

The first dataset[64] aims to show the performance (in seconds) of rats trying to find a submerged platform in the Morris Water Maze. The rats used in the experiments were either normal controls, or rats with ibotenic-acid-induced lesions of the hippocampus.

The second dataset[63] aims to show the number of rats in each treatment group (caudate nucleus or hippocampal injection) that exhibited place or response learning on both the Day Eight and Day 16 test trials.

5.1.2.1 Description of Data and Models

The neuronal-level model under development aims to reproduce the behaviour and the performance of control as well as rats with a damaged hippocampus, by reproducing the functioning of the areas involved in spatial navigation and decision-making, namely the hippocampus and the striatum.

5.1.2.2 How Data are Related to Specific Platform Requirements

We plan to deliver the key statistical results of the simulation in the form of reaction times, provided as an Excel file. The raw output of simulations could be made available in a second phase.

5.1.2.3 Quantitative Indicators of Data Completeness

The simulations of the behaviour of the neuronal-level models (30 animals) are now fully acquired and analysed. The code is being uploaded as part of our collaboration with SP4. The results are being submitted for publication.

5.1.2.4 Status of Data Delivery

Experimental data have already been published. Fully processed simulation data will be delivered during the data-delivery phase II.

5.1.2.5 List of Collaboration Partners

At the beginning, we will use the neuronal population density simulator developed by P110 (Marc DE KAMPS, University of Leeds [ULEEDS]) to run faster versions of our rodent navigation simulations. We will also collaborate with P1 (Marc Oliver GEWALTIG, EPFL) to run our software exploiting high performance computing architectures in closed loop configurations. We will receive a Spinnaker Board from P73 (David LESTER, University of Manchester - UMAN) to run accelerated spiking neuron versions of our simulations. On this board, we will implement neuron models developed by P7 (Alain DESTEXHE, CNRS). Once the task is running correctly in our own developed simulator, we will collaborate with P53 (*Technische Universität München* [TUM]) to implement it in their newly developed physics engine, and later on the real robot.

5.1.2.6 Data Provenance

The behavioural data concerned were obtained in summary form from the literature - collected by Mark PACKARD and James MCGAUGH (Department of Psychology, University of New Orleans; Department of Psychobiology, University of California, Irvine), and by John PEARCE, Amanda ROBERTS and Mark GOOD (School of Psychology, Cardiff University). The simulation data were generated within the HBP by our own lab (BURGESS lab, UCL).

5.1.2.7 Plan Until the End of the Ramp-Up Phase

We aim to publish the results of the simulation studies (publication in preparation), and to publish the cognitive constraints on neural mechanisms of spatial navigation that we identified (special issue of Neuron organised by Stanislas DEHAENE is in preparation).

6. From Sensory Processing to Multimodal Perception (WP3.5)

6.1 Neural Correlates of Unimodal Perception and Self-organisation of Internal Knowledge in Mammalian Primary Cortical Areas (T3.5.1)

6.1.1 Overview

This report section describes the database of recordings from cat V1, obtained by Yves FRÉGNAC's lab. It also describes some of the results from analysing these data, which are used to constrain the computational models developed with the help of the CNRS, the EC FET Integrated Project BrainScaleS, and the Flagship HBP. The technical underpinnings of the database can be obtained from author Andrew DAVISON (HBP SP5 and SP9 task leader) at CNRS-UNIC. Here we provide information on accessing the database, present some screenshots of the web-interface, and give some examples of using the Python client interface. Since the data were not obtained primarily through HBP funding, the Database access is on request only for the read-out part. Access to raw data will be given on the conditions that authorisation is granted by the data owner (Yves FRÉGNAC, CNRS-UNIC Unit of Neuroscience, Information and Complexity) and a collaboration has been established with the experimenters allowing a full understanding of the metadata.

6.1.2 Data set One

6.1.2.1 Description of Data and Models

6.1.2.1.1 Introduction

Collaborative science requires the sharing of data, associated metadata, and the results and methods of data analysis. The metadata provides the experimental context — the stimulus used, the model specification, the biological preparation, the hardware setup, etc. — without which analysis of the data is impossible. Traditionally, especially for *in vivo* experiments, the metadata have been recorded by hand in paper lab notebooks, while data analysis results are scattered over multiple folders on multiple computers, and shared by e-mail or removable disks. One of the goals of the BrainScaleS database was to augment/replace the paper notebook with a structured (meta)database. This database should contain the context of biological experiments, numerical and analogue simulations, and analyses that need to be shared with potential users, together with links to the actual data files.

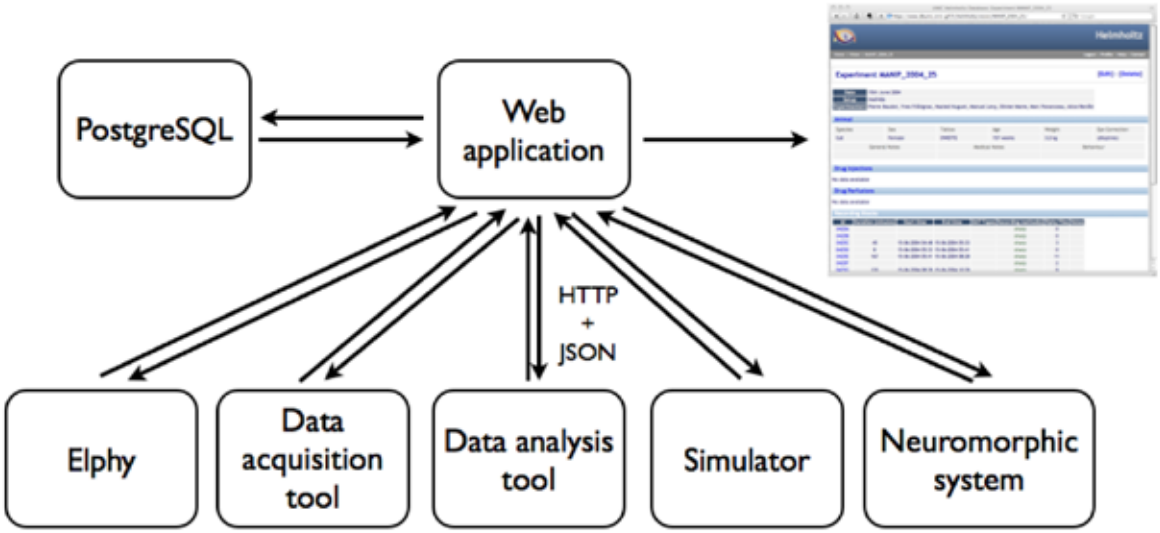

Figure 21: Architecture of the Helmholtz Framework Underlying the V1 database

The figure shows multiple clients accessing the database through a web-services API, with a relational database backend.

Updates and improvements have been implemented, notably:

- Support for XML-based web services has been added to the Elphy data acquisition and analysis software developed by Gérard SADOC at CNRS-UNIC, and has already been used by several international research groups.
- A high-level Python client library, building on top of the low-level "requests" module, has been added.
- The web interface has been re-implemented using a modern CSS/Javascript framework (Bootstrap 3).

All data and metadata in the database are under access control. Read-only access is available on request. The BrainScaleS V1 database is available at: https://brainscales.unic.cnrs-gif.fr/

6.1.2.1.2 The Web Interface

The web interface provides four main views of the database:

- By publication – Figure 22,
- By experiment (where one experiment is a recording session lasting two to four days) – Figure 23,
- By cell (typically several cells are recorded during each experiment, and several stimulation protocols are run on each cell) – Figure 24.
- By data analysis or visualisation result – Figure 25 and Figure 26

- 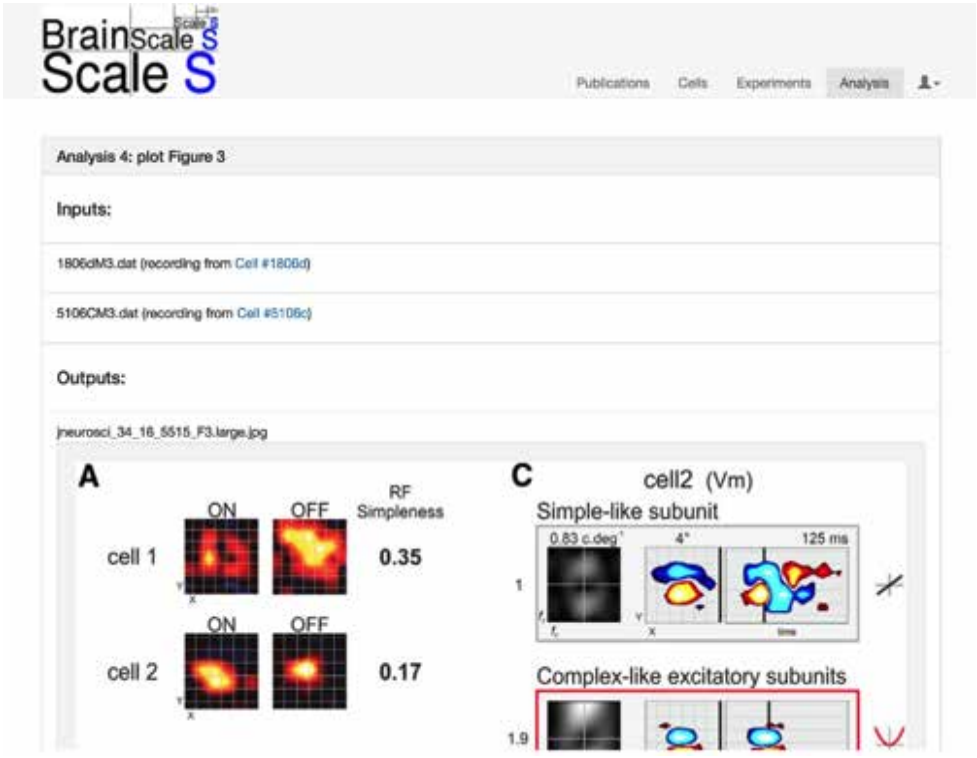
BrainScaleS
Publications
Cells
Experiments
Analysis
Analysis 4: plot Figure 3
Inputs:
1806dM3.dat (recording from Cell #1806d)
5106CM3.dat (recording from Cell #5106c)
Outputs:
jneurosci_34_16_5515_F3.large.jpg
A
ON
OFF
RF Simpleness
cell 1
0.35
cell 2
0.17
C
cell2 (Vm)
Simple-like subunit
0.83 c.deg⁻¹
4°
125 ms
Complex-like excitatory subunits

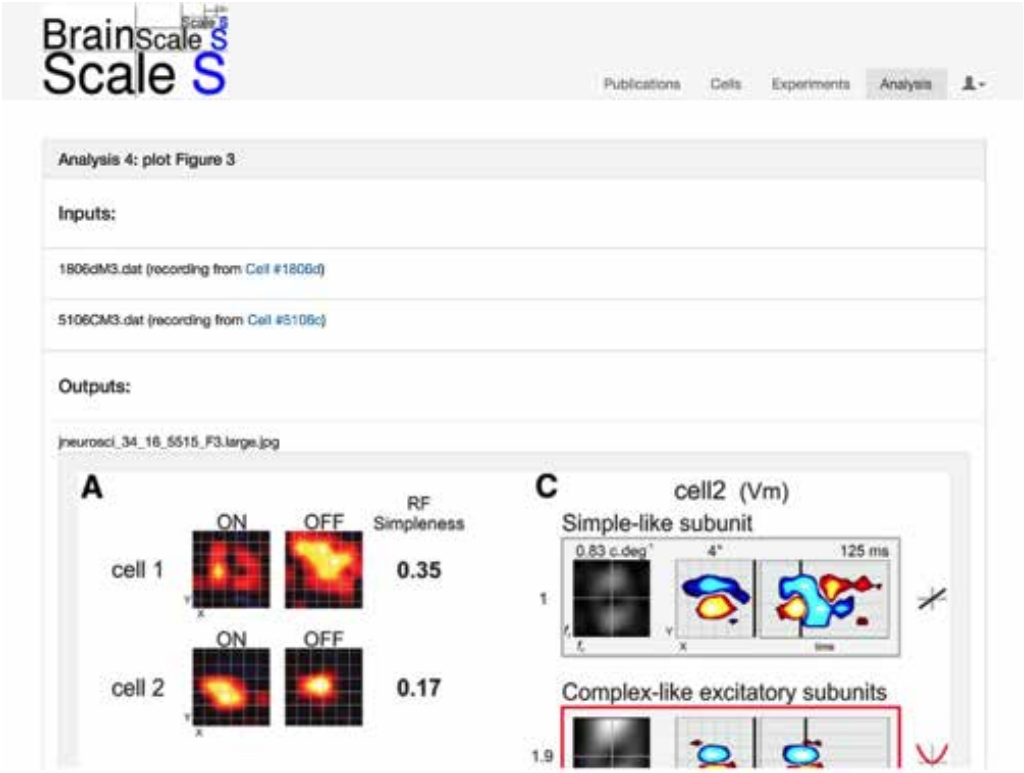
BrainScaleS
Publications
Cells
Experiments
Analysis
Analysis 4: plot Figure 3
Inputs:
1806dM3.dat (recording from Cell #1806d)
5106CM3.dat (recording from Cell #5106c)
Outputs:
jneurosci_34_16_5515_F3.large.jpg
A
ON
OFF
RF Simpleness
cell 1
0.35
cell 2
0.17
C
cell2 (Vm)
Simple-like subunit
0.83 c.deg⁻¹
4°
125 ms
Complex-like excitatory subunits

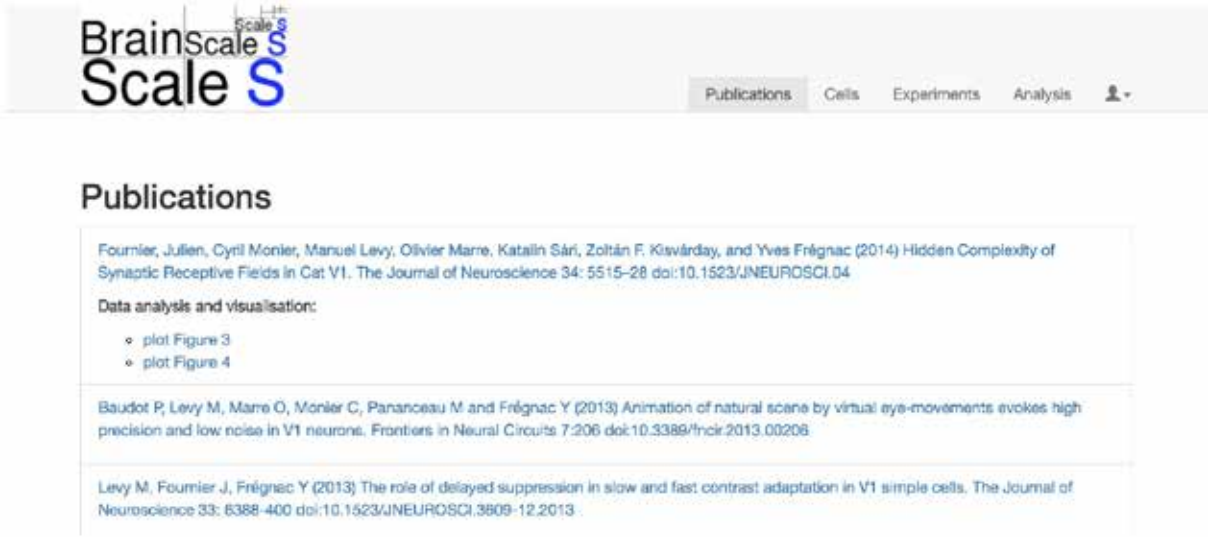

Figure 22: A Screenshot of the Publications View, Linking Published Articles to the Underlying Raw Data and Data Analysis

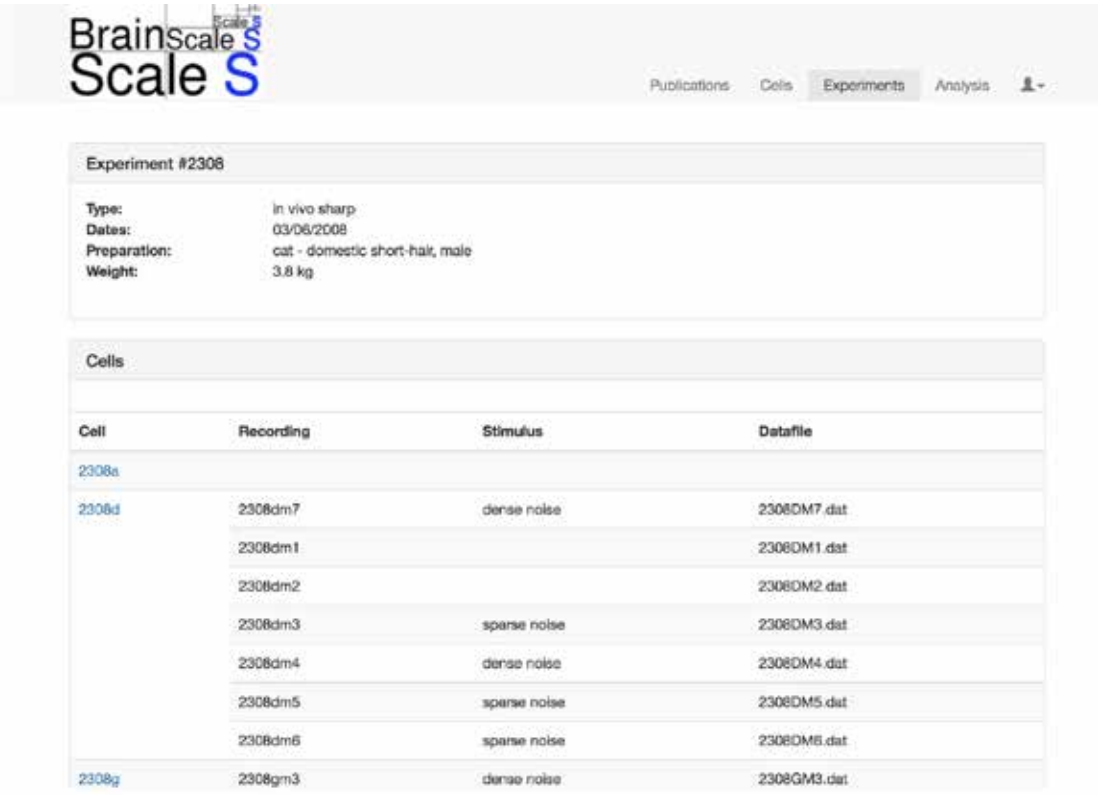

Figure 23: A View of One Specific Recording Session

The figure includes metadata about the preparation and links to all of the neurons recorded during that session

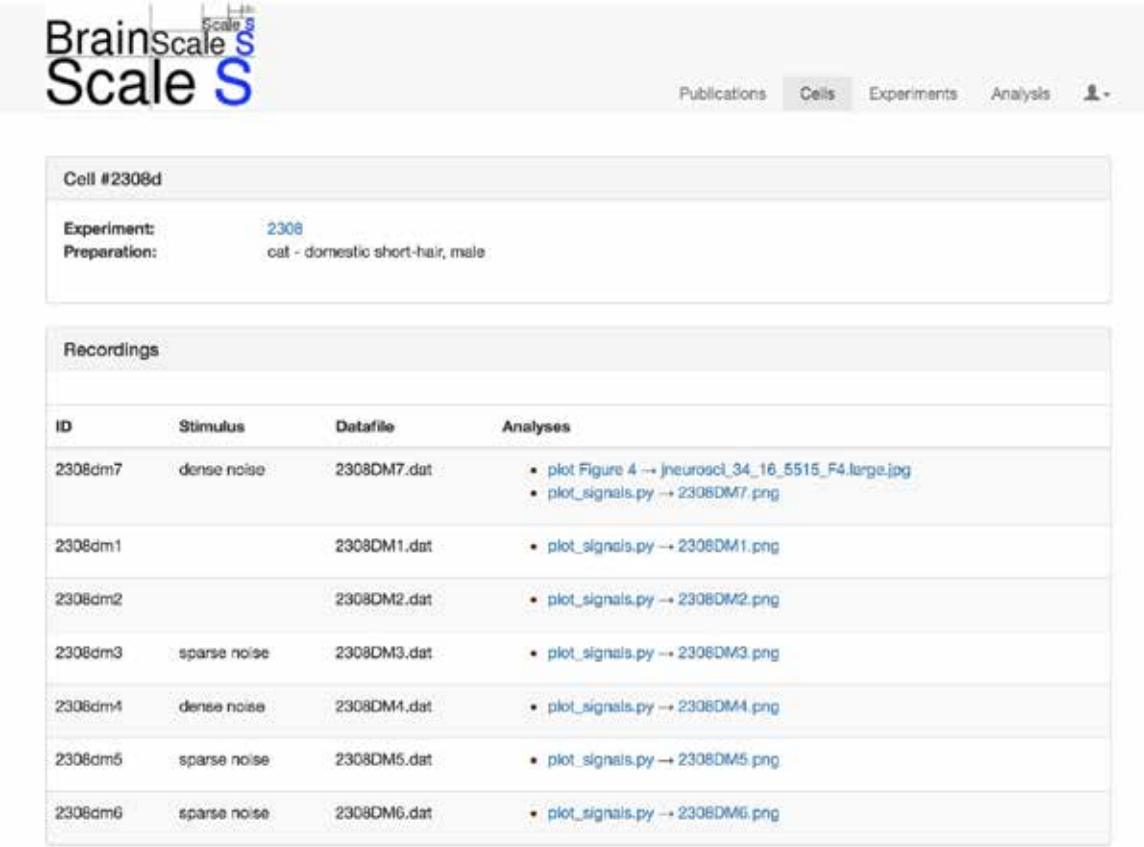

Figure 24: A View of Intracellular Recordings from an Individual Neuron, and Associated Data Analysis

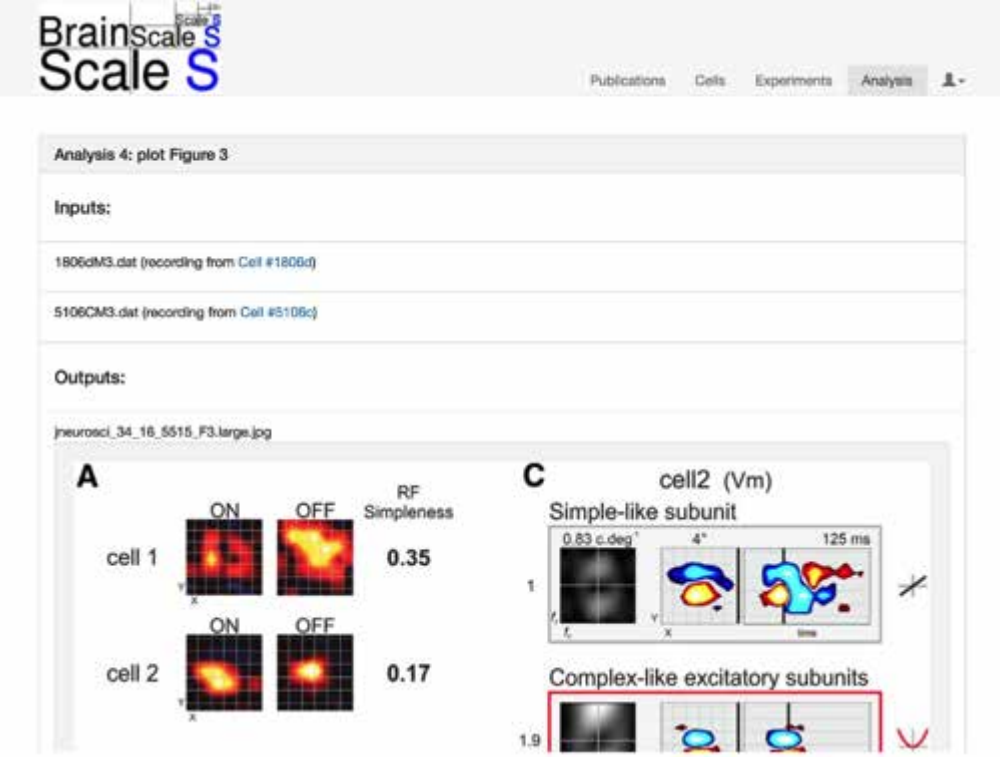

Figure 25: A High-level View of a Data Analysis Originally Performed Before the Introduction of the Database

This provides links from a published figure to the underlying raw data.

A more fine-grained view of the data analysis pipeline, showing each of the intermediate steps, is possible for new data analyses, and will be applied retrospectively to key earlier results.

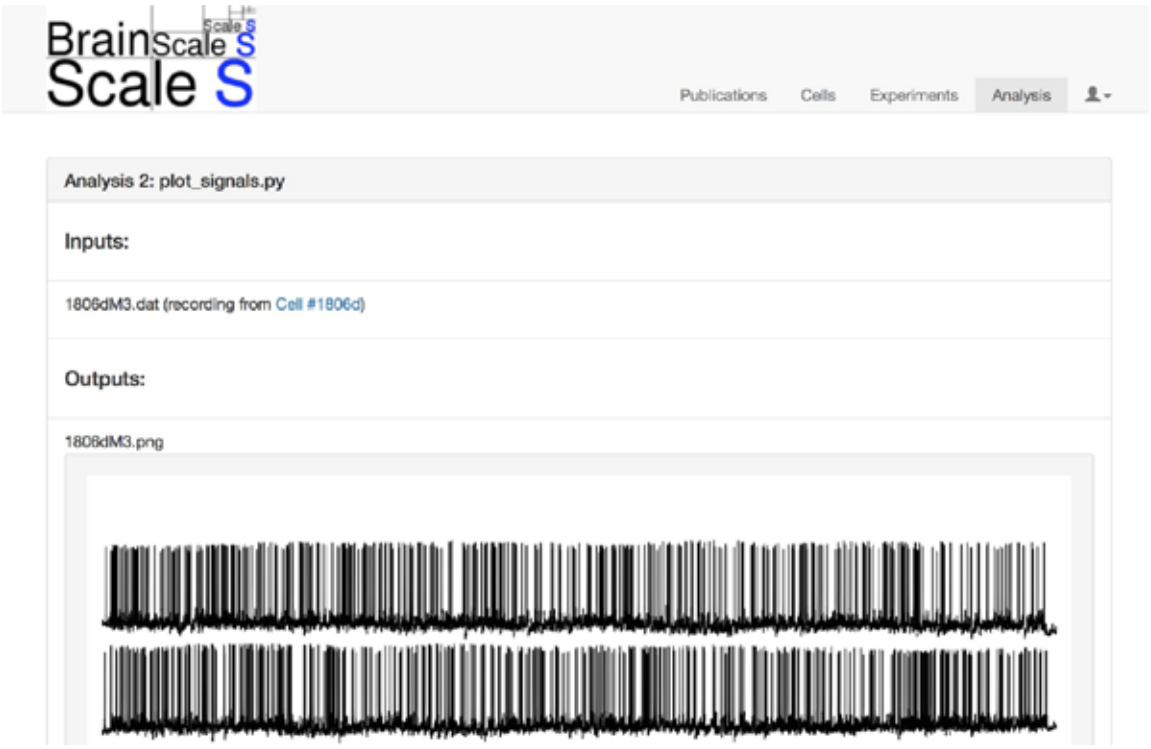

Figure 26: A Visualization of a Single Recording.

6.1.2.1.3 The Python Client

Here are some examples of accessing the web services API through Python, using the *requests* library, for example:

```
$ import requests
$ r = requests.get('http://127.0.0.1:8000/neuralstructures/brainregion/',
    auth=("username", "password"))
$ r.json()
{'meta': {'limit': 1000,
  'next': None,
  'offset': 0,
  'previous': None,
  'total_count': 1},
 'objects': [{'abbreviation': 'V1',
  'name': 'Primary visual cortex',
  'parent': None,
  'resource_uri': '/neuralstructures/brainregion/nlx_143552',
  'species': ['/species/species/1'],
  'url': 'http://neurolex.org/wiki/Category:Visual_cortex_primary'}]}
```

This method of accessing the database is still available, but we have additionally begun to develop a more user-friendly, object-orientated Python client aimed at scientists with a basic knowledge of Python, but not requiring advanced programming skills. The new client is currently available in the Github repository for the Helmholtz framework (https://github.com/apdavison/helmholtz).

Some examples of using the client:

Connect to the database:

```
$ from helmholtz.client.ooclient import Client
$ c = Client(username="username", password="password",
        entrypoint="https://brainscales.unic.cnrs-gif.fr", verify_certificates=False)
```

List recording blocks (for intracellular recordings, one recording block corresponds to one cell):

```
$ cells = c.list_blocks(cascade=True)
$ cells[:10]
[Block('1806a', uri='/recordings/block/1'),
 Block('1806b', uri='/recordings/block/2'),
 Block('1806c', uri='/recordings/block/3'),
 Block('1806d', uri='/recordings/block/4'),
 Block('1806e', uri='/recordings/block/5'),
 Block('1806f', uri='/recordings/block/6'),
 Block('1806g', uri='/recordings/block/7'),
 Block('5106a', uri='/recordings/block/8'),
 Block('5106b', uri='/recordings/block/9'),
 Block('5106c', uri='/recordings/block/10')]
```

Display metadata about the experimental preparation for one cell:

```
$ cells[18].experiment.preparation.type
'IN-VIVO-SHARP'
$ cells[18].experiment.preparation.animal.species
'cat'
$ cells[18].experiment.preparation.animal.strain
'domestic short-hair'
$ cells[18].experiment.preparation.animal.sex
'M'
```

List the recordings obtained from the cell:

```
$ cells[18].recordings
[Recording('2308dm7', uri='/recordings/recording/3'),
 Recording('2308dm1', uri='/recordings/recording/5'),
 Recording('2308dm2', uri='/recordings/recording/6'),
 Recording('2308dm3', uri='/recordings/recording/7'),
 Recording('2308dm4', uri='/recordings/recording/8'),
 Recording('2308dm5', uri='/recordings/recording/9'),
 Recording('2308dm6', uri='/recordings/recording/10')]
```

Display information about the stimulus and data file for a given recording:

```
$ cells[18].recordings[0].stimulus
Stimulus(type='dense noise', uri='/stimulations/stimulus/2')
$ cells[18].recordings[0].file
File('/data/2308DM7.dat', mimetype='application/vnd.cnrs.unic.elphy')
```

6.1.2.2 How Data are Related to Specific Platform Requirements

The present data are not related to specific platform requirements. However, Andrew DAVISON (CNRS-UNIC) in SP5, who is in charge of the management of the BrainScaleS database, will consider in the second phase of HBP, if funding is available, the necessary steps required for the implementation of the V1 model (still under construction) for neuromorphic computation.

6.1.2.3 Quantitative Indicators of Data Completeness

The functional database of BrainScaleS is based on 200 cells recorded intracellularly with sharp electrodes and patch electrodes in the anesthetised cat V1. The complete entry of metadata requires, however, additional human resources for which we have not received funding. This is why we chose to populate a front-end database with published and summary data.

6.1.2.4 Status of Data Delivery

Summary data for dependency on input statistics are available. Fully processed data concerning long-distance integration through horizontal axons (involved in "self-organisation of internal knowledge") will be delivered during data-delivery phase II.

6.1.2.5 List of Collaboration Partners

We participate actively to EITN conferences in Paris and the CNRS-UNIC lab is responsible for the administration of the infrastructure of the European Institute of Theoretical Neuroscience (Scientific Director: Alain DESTEXHE), with the help of the Foundation "*Voir et Entendre*". We are in the process of organising an international symposium on V1 with the CNRS, HBP and the Idex Paris-Saclay (ICode), which will be held at the EITN in Spring 2016. We collaborate closely with Andrew DAVISON (task leader in SP5 and SP9), with whom we co-supervise PhD students and Postdoctoral fellows (Jan ANTOLIK). We collaborate closely with Alain DESTEXHE (Director of SP4) and Olivier MARRE (SP4) on power-law analysis and correlation studies in asynchronous irregular networks. We

collaborate with Olivier FAUGERAS (SP4) to promote links between Neuroscience and Mathematics through the organization of interdisciplinary conferences.

6.1.2.6 Data Provenance

The data were acquired by Yves FRÉGNAC's team at CNRS-UNIC, in Gif sur Yvette, in cats bred by the CNRS animal care facilities.

6.1.2.7 Plan Until the End of the Ramp-Up Phase

At the time of writing, the database contains a subset of the data acquired and/or analysed associated with peer-reviewed publications. We intend to include further acquired data associated with future publications. Note that, since the HBP does not contribute to the build-up of these databases, and seems to have excluded future support to animal experiments apart from mouse and humans from the next FPCA, the funding for continued database operation and maintenance in cat V1 will be provided by the CNRS, while future technical developments will be supported by external grants.

6.2 Neural Correlates of Unimodal and Multi-modal Perception in Mammalian Primary Sensory Areas (T3.5.2)

6.2.1 Overview

Everyday perception is multisensory, and the brain combines cues from different sensory modalities to interpret the environment. There is increasing evidence that these cross modal interactions can occur as early as in primary sensory cortical areas. To precisely model this type of interactions, strategic data are necessary. In the framework of the HBP, we have developed the methodology, performed experiments and analysed the data to provide a precise example of multisensory interactions in the mouse visual cortex during perception in the awake state. Using two-photon calcium imaging, we have generated a large dataset of V1 neuron responses during stimulation, with time-varying images and amplitude or frequency modulated sounds. This data shows clear evidence of strong "ON"-type auditory responses in V1. In addition, while most of the neurons sum additively auditory and visual responses, we also observed a substantial fraction of neurons displaying non-additive multimodal responses and signalling the specific coincidence of certain auditory and visual stimuli. We are currently acquiring and analysing a symmetric dataset for the mouse primary auditory cortex (A1) that we will deliver with the V1 dataset.

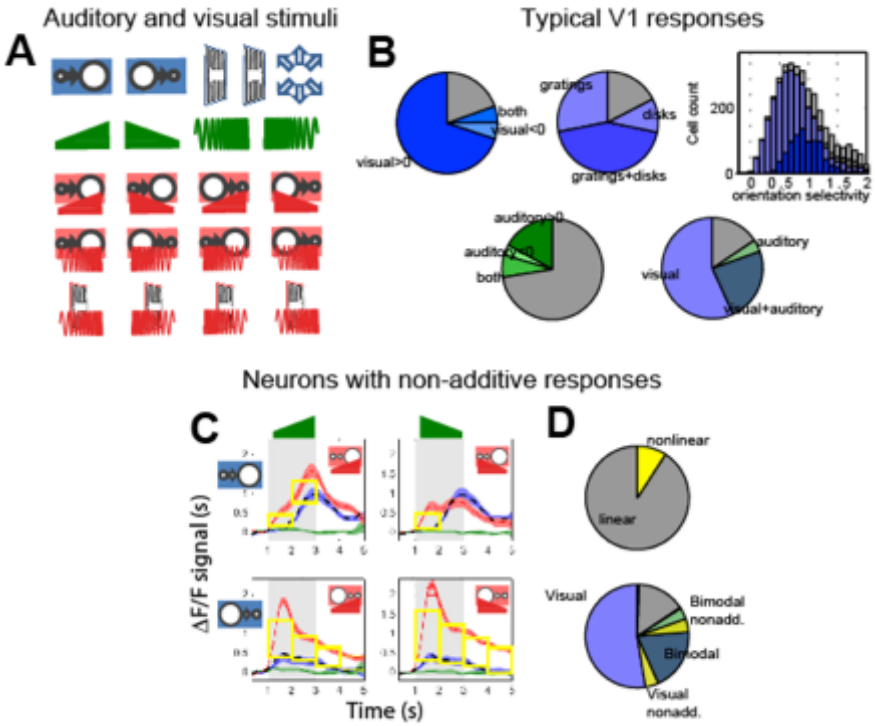

Figure 27: Summary of Auditory and Visual Responses in V1 Neurons.

A. Visual (blue), auditory (green), auditory-visual stimuli. These include looming receding disks and gratings of different orientations, combined with amplitude and frequency modulated sounds. B. Analysis of uni- and multi-sensory responses in V1. From top left to bottom right: fraction of visually responsive cells. Fraction of cells responding exclusively to gratings, disks or to both types of stimuli. Fraction of V1 cells responding to sounds. Fractions of cell responding to auditory and/or visual stimuli. C. Averaged calcium signals for one neuron responding in a non-linear manner to combined auditory and visual stimuli.

6.2.2 Data set One: Two-photon Calcium Imaging of Mouse V1 and A1 Response During Time-varying Auditory Visual Stimulation

6.2.2.1 Description of Data and Models

The data consists of 12 already acquired two-photon calcium imaging sessions in the mouse primary visual cortex (V1), and a planned total of 12 sessions in the mouse primary auditory cortex A1. The V1 dataset includes the activity of approximately 3500 neurons during the presentation of auditory and visual stimuli to awake mice. The data consists of raw or deconvolved calcium signals, giving an estimate of the variations in the neurons' firing rates around and during stimuli presentation. The data include four auditory stimuli (two amplitude modulated white noise, and two frequency modulated sine waves), 10 visual stimuli (one receding and one looming disk, 10 drifting grating with different orientations), and 12 combinations of auditory and visual stimuli. Each stimulus is presented 20 times to the animals, which are passively attending to them.

The statistical analysis for the detection of neurons responding to visual (resp. auditory) stimuli is performed using the general linear model method (GLM). Non-additive bimodal neurons are also identified with a GLM, comparing the following hypotheses:

- Null hypothesis (additivity): responses to bimodal stimulations are fully predicted by responses to unimodal stimulations.

- Full hypothesis (no-additivity): responses to bimodal stimulations are modelled separately.

6.2.2.2 How Data are Related to Specific Platform Requirements

We plan to deliver the key statistical results of the two-photon calcium imaging analysis in the form of the fraction of cells responsive to each of the stimulus conditions, and the fraction of cells responding in a non-additive fashion to multimodal stimuli. The statistical results will be provided as Matlab structures in a .mat file, similar to the fMRI data provided by some SP3 Partners. The raw data will be made available in a second phase, hopefully when the results are published.

6.2.2.3 Quantitative Indicators of Data Completeness

The mouse V1 cortex imaging dataset is now fully acquired and analysed (five mice for a total of 3500 identified neurons recorded in 12 sessions). The mouse A1 cortex imaging dataset is being acquired and analysed (five mice for a total of 2017 identified neurons already acquired in eight sessions).

6.2.2.4 Status of Data Delivery

Raw data is available. Fully processed data will be delivered during data-delivery phase II.

6.2.2.5 List of Collaboration Partners

We participate in EITN conferences in Paris. We collaborate with Wolfgang MAASS (SP4) to analyse the two-photon calcium imaging data in the mouse auditory cortex, that was acquired by Brice BATHELLIER.

6.2.2.6 Data Provenance

The data were acquired by Brice BATHELLIER's team at CNRS-UNIC in 2014. The data is taken from awake Bl6C57-J mice.

6.2.2.7 Plan Until the End of the Ramp-Up Phase

Until the end of the Ramp-Up Phase, we will:

- Use a light flash count discrimination paradigm to test whether the auditory response in mouse V1 correlates with perceptual effects similar to the double flash illusion observed in humans. This point is key for showing the relevance of our mouse-based recordings to human cognitive architecture.
- Finish recording and analyse the dataset for mouse A1. The imaging has already started.
- Publish the results, if possible, together with behavioural data.

7. Capabilities Characteristics of the Human Brain (WP3.6)

7.1 Symbols and their Manipulation (T3.6.1)

Task T3.6.1 aims to understand the cortical mechanisms that support our ability to recognise and manipulate letters and numbers. The task is investigated by Thomas HANNAGAN (CEA), under the supervision of Stanislas DEHAENE (CEA). Research on T3.6.1 only started when Thomas HANNAGAN entered the project in mid-December 2014. Consequently, the task has not yet produced deliverable data. The means of investigation for T3.6.1 being computational in nature, the task will in time produce data in the form of computational models (code, simulated experiments, and analyses). Our position in this task is not to run new experiments, but to try and make sense of the colossal knowledge that has been acquired experimentally in recent years, especially regarding the maturation of letter and number form areas in the brain. Three projects are under way:

1) An invited opinion paper for "Trends In Cognitive Science", on the origins of symbol form areas in the ventral occipitotemporal cortex. In addition to Stanislas DEHAENE, this involves three collaborators outside the HBP: Amir AMEDI (Hebrew University of Jerusalem), Laurent COHEN (INSERM/ICM), Ghislaine DEHAENE-LAMBERTZ (from SP2; CNRS). This opinion paper has been submitted.
2) A computational model on mirror invariance for visual symbols, before and after the acquisition of literacy, using deep convolutional networks. One paper is currently in revision, with co-authors outside the HBP: Arash YAZDAMBAKSH and Jasmin LÉVEILLÉ (Boston University), Felipe PEGADO (Leuven University) and Jonathan GRAINGER (CNRS). Another computational investigation of the detailed mechanism underlying mirror invariance is on-going, with Clément MOUTARD (CEA, HBP).
3) A neural field computational model on the emergence of form areas in the ventral occipitotemporal cortex, which operates at the level of cortical columns, and where the hypotheses laid out in the opinion paper (1) are being tested. The simulations are in progress and the paper in preparation.

7.2 Linguistic and Non-Linguistic Nested Structures (T3.6.2)

7.2.1 Overview

In task T3.6.2, data from human participants are generated in NeuroSpin. This task, led by Christophe PALLIER (CEA) aims to shed light on the problem of how the human brain encodes tree structures — a neural code whose mechanisms are currently unknown, and which has been hypothesised as perhaps unique to humans as opposed to non-human primates. To clarify which areas are involved and how they operate, we rely on three studies which are only partially funded by HBP.

Experiment one uses fMRI to examine how humans extract the regularities of linguistic nested-structures (Christophe PALLIER and Murielle FABRE). Experiments two and three examine how humans extract the regularities of non-linguistic structure. Experiment two (Florent MEYNIEL, Maxime MAHEU) examines this capability with MEG data, using sequences structured by the transition probabilities between the stimuli. Experiment three (Liping WANG, Marie AMALRIC) investigates this capability with behavioural and fMRI data, using sequences structured by chunks and nested rules.

7.2.2 Data set One: Encoding of Syntactic Structures

According to linguistic analyses, sentences possess syntactic structures that can be described formally as trees whose leaves — that is, the terminal nodes — typically correspond to words. These structures capture the notion of constituency, and some of the dependencies between words, as attested by example of structural ambiguity: compare ((black taxi) driver) vs. (black (taxi driver)). PALLIER, DEVAUCHELLE and DEHAENE (2011)[65] used fMRI to identify cortical areas where activation increased with the size of syntactic trees, defined as the number of words forming a constituent. This provided quantitative data that models of human sentence processing must match. The current experiment builds on this result, and seeks the neural correlates of more abstract syntactic properties: the empty positions created by syntactic movement.

The final word order in a sentence reflects the outcome of merging and moving operations that apply to words and phrases, building and transforming the tree. For example, in French, one way to form an interrogative is to invert the verb and the subject (e.g. “Vient-il?” Is he coming?). The verb movement is assumed to leave an empty, non-pronounceable element, also known as a trace, in the tree structure (see Figure 28).

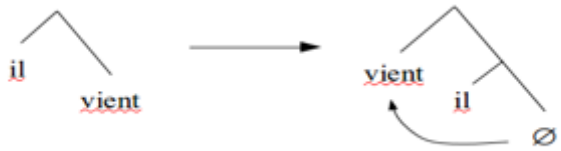

Figure 28: Example of Verb Movement in French

For the present experiment, we generated a set of short sentences (from two to four overt words and two to seven syntactic positions when including empty traces), applying different types of movements (Wh-movement, verb movement, clitic movement and NP-movement).

The experimental conditions, obtained by crossing all meaningful combinations of movement types, are described in the following tables.

1 Argument Unacc	Example
c01_Unacc_Decl_NP_1Ag	Il maigrit.
c02_Unacc_ynQ_NP_1Ag	Tu déchantes?
c03_Unacc_Qinv_NP_V_1Ag	Brille-t-elle?

1 Argument Unerg	Example
c04_Unerg_Decl_1Ag	Tu bailles.
c05_Unerg_ynQ_1Ag	Tu défiles?
c06_Unerg_Qinv_V_1Ag	Dort-elle?

2 Arguments loc	Example
c07_Unacc_Decl_NP_2Ag_loc	Il hiberne là.
c08_Unacc_ynQ_NP_2Ag_loc	Tu vis là?
c09_Unacc_Qinv_NP_V_Wh_2Ag_loc	Où réside-t-elle?
c10_Unacc_Qinv_NP_V_2Ag_loc	Siège-t-il là?
c11_Unacc_Decl_NP_Cl1_2Ag_loc	Tu y survis.
c12_Unacc_ynQ_NP_Cl1_2Ag_loc	Elle y figure?
c13_Unacc_Qinv_NP_V_Cl1_2Ag_loc	Y déteint-t-il?
c14_Unacc_Q_NP_Wh_2Ag_loc	Où elle revient?

3 Arguments obj loc	Example
c23_transy_Decl_3Ag_loc	Il abandonne ça là.
c24_transy_ynQ_3Ag_loc	On adosse ça ici?
c25_transy_Qinv_V_3Ag_loc	Assigne-t-on ça ici?
c26_transy_WhQinv_V_Wh_3Ag_loc	Où colles-tu ça?
c27_transy_Decl_Cl1ob_3Ag_loc	Tu l'enlèves là.
c28_transy_ynQ_Cl1ob_3Ag_loc	On l'adresse là?
c29_transy_Qinv_V_Cl1ob_3Ag_loc	Le retire-t-elle là?
c30_transy_WhQ_Wh_3Ag_loc	Où elle envoie ça?

2 Arguments obj	Example
c15_Trans_Decl_2Ag_obj	Tu détruis ça.
c16_Trans_ynQ_2Ag_obj	Il méprise ça?
c17_Trans_Qinv_V_2Ag_obj	Critique-t-il ça?
c18_Trans_whQinv_V_Wh_2Ag_obj	Qui méprise-t-il?
c19_Trans_Decl_Cl1_2Ag_obj	Tu l'esquives.
c20_Trans_ynQ_Cl1_2Ag_obj	Elle l'imite?
c21_Trans_Qinv_V_Cl1_2Ag_obj	L'adopte-t-il?
c22_Trans_whQ_Wh_2Ag_obj	Qui elle écoute?

3 Arguments obj dat clitic	Example
c31_transy_WhQ_Wh_Cl_3Ag_dat	Qui on lui présente?
c32_transy_WhQ_Wh_Cl_V_3Ag_dat	Qui lui soumet-elle?

3_Arguments_2Clitics obj loc	Example
c33_Decl_2Clobjloc_3Ag_4W_2EC	On l'y joint.
c34_ynQ_2Clobjloc_3Ag_4W_2EC	Tu l'y appliques?
c35_Qinv_V_2Clobjloc_3Ag_4w_3EC	L'y associes-tu?

Table 2: The 35 Experimental Conditions Obtained by Combining Several Types of Syntactic Movements.

7.2.2.1 Description of Data and Models

High-resolution fMRI data sets (isotropic 1.5 mm voxels) were acquired from 24 native French speakers, who read the short sentences that were flashed for 200 ms on the centre of the screen (four participants were rejected because of movements that were too large, or technical failure during the acquisition. The group analysis was performed on the remaining 20 participants). Data were pre-processed in the classic manner: slice timing, movement correction, and spatial normalisation to the MNI template and smoothing at 5 mm. The model at individual level includes one regressor per condition, and covariates of non-interest (movements detected by the realignment step, as well a covariate representing the expected HRF modulated by text size). At group level, a repeated measurement Analysis of Variance model is used, with 35 maps per participant, corresponding to each of the conditions.

7.2.2.2 How Data are Related to Specific Platform Requirements

The results will be provided as effect-size maps and t-values maps for the main contrasts of the group analysis, stored using nifti format. In addition, we will provide the response profiles — that is, effect sizes plots showing responses to the 35 conditions — for a set of regions of interests from the literature on sentence processing.

7.2.2.3 Quantitative Indicators of Data Completeness

Data acquisition is complete. The main statistical models have been designed and estimated. The whole brain analyses have been performed. We are currently performing regions of interest analyses.

7.2.2.4 Status of Data Delivery

Not yet initiated.

7.2.2.5 List of SP4 Collaboration Partners

Our data are optimally suited to all SP4 partners interested in the neuronal implementation of nested or recursive sequences.

7.2.2.6 Data Provenance

The data were collected at NeuroSpin by Christophe PALLIER and Murielle FABRE.

7.2.2.7 Plan Until the End of the Ramp-Up Phase

We will complete the regions of interest analyses to provide summary response profiles for various linguistic questions (the response profile across the 35 conditions have already been computed).

7.2.3 Data Set Two: Bayesian Modelling of Expectation Effects in Sequences

7.2.3.1 Description of Data and Models

When exposed to any type of sequences, even random ones, humans search for regularities, such as streaks and alternations. In line with this idea, new observations may reinforce the current characteristic inferred from the sequence, or alternatively, be at odds with this estimate. When expectations are violated, surprise signals are detected in the brain, e.g. as the amplitude of the P300 in EEG recordings[66], or with fMRI[67] and in the behavioural measures such as reaction times[68].

The aim of this dataset is to use the high-temporal resolution of MEG to characterise the temporal dynamic of the computations that underpin the extraction of the characteristics of a sequence of stimuli. Our hypothesis is that this extraction is made by probabilistic inference. We operationalised this notion by focusing on basic characteristics: the frequency of stimuli in the sequence, and the transition probabilities between stimuli. These minimal characteristics are the simplest way to start the investigation of probabilistic learning. This simplicity nonetheless offers the foundation of a minimal hierarchical system the identification of transition probabilities requires the estimation of frequencies, but specifically on a context (the previous stimulus).

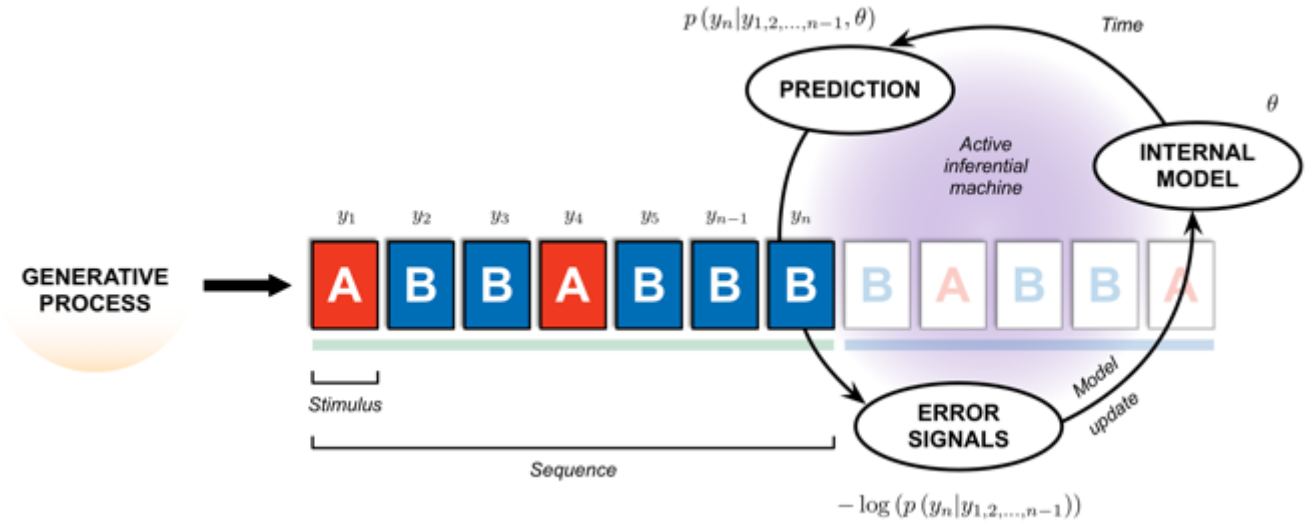

Figure 29: Active Bayesian Inference Based on a Sequence of Stimuli

Subjects were exposed to sequences of binary stimuli (say, A and B), generated as particular transition probabilities. In most trials, participants were passively listening to the stimuli, and in some catch trials they were asked to report the stimulus that should come next as quickly as possible. Our working hypothesis is that

the brain is constantly inferring the probabilistic characteristics of the sequence (an internal model) to predict future observations. Deviations between the actual observation and the prediction, which is formally quantified by the notion of surprise, may be used to update this internal model.

To characterise the computation of frequencies and transition probabilities in the brain, we exposed participants to random sequences of binary stimuli (see Figure 29) and we used different transition probabilities to generate the sequences:

- p(A|A)=p(A|B)=p(B|A)=p(B|B)=0.5: unbiased frequencies, unbiased transitions,
- p(A|A)=p(A|B)=1/3 and p(B|A)=p(B|B)=2/3: biased frequencies, unbiased transition,
- p(A|B)=p(A|B)=1/3 and p(B|B)=p(A|A)=2/3: unbiased frequencies, transitions biased toward repetitions,
- p(A|B)=p(A|B)=2/3 and p(B|B)=p(A|A)=1/3: unbiased frequencies, transitions biased toward alternations.

We also developed several Ideal Observer models to formalise and quantify what can be learned from a specific sequence of stimuli. These Observer models differ in several aspects of the inference:

- Their temporal horizon: whether they integrate observations only locally in time, or on protracted periods.
- The flexibility of this temporal horizon: whether it is adaptive chunking or a simple fixed memory limitation.
- The type of characteristics they infer: context-independent characteristics such as the frequency of stimuli, or context-dependent characteristics such as the transition probabilities between stimuli.
- The prior expectations on these inferred characteristics, whether there is no particular expectation (flat prior), or for instance biases favouring the perception of alternations, or of repetitions in the sequence of stimuli.

These different aspects can be combined so that the resulting Ideal Observer models formalise specific characteristics of the probabilistic inference. The information-theoretic variables derived from these models (prediction, surprise, update, etc.) can then serve as probes to disentangle brain signals that potentially overlap in space and time, based on the computational characteristics they reflect.

The MEG data were collected on an Elekta device, (300 MEG sensors and 64 EEG sensors) at 1024 Hz.

7.2.3.2 How Data are Related to Specific Platform Requirements

We plan to deliver the key statistical results of the MEG analysis in the form data matrices (space x time) that summarise the topography and time course of the computational signature identified at the group level. The data will be provided as .mat files, containing a data structure with the FieldTrip format (FieldTrip toolbox, Matlab). This format is commonly used in the field. The raw data could be made available in a second phase.

7.2.3.3 Quantitative Indicators of Data Completeness

The MEG dataset is still in the process of being acquired and analysed. Two subjects have been acquired so far.

7.2.3.4 Status of Data Delivery

Raw data from two pilot subjects is available. Fully processed data will be delivered during data-delivery phase II.

7.2.3.5 List of SP4 Collaboration Partners

We plan to present these data during an international workshop, to be held in September 2015 in Paris, entitled "Probabilistic inference and the Brain". This workshop will gather prominent scientists from the theoretical and experimental fields. It is a collaboration between SP3 and SP4. Stanislas DEHAENE (SP3), Alain DESTEXHE (SP4), Florent MEYNIEL (SP3) and Wolgang MAASS (SP4) are co-organising this workshop.

7.2.3.6 Data Provenance

The MEG data were collected by Florent MEYNIEL at NeuroSpin.

7.2.3.7 Plan Until the End of the Ramp-Up Phase

We aim to complete the data acquisition before June 2015.

7.2.4 Data Set Three: Encoding of Geometrical Structures in Human and Non-Human Primates

Is the ability to embed symbols into recursive structures a uniquely human ability? To examine this question, we invented a task which can be performed by both humans and non-human primates. Sequences of dots are displayed at the vertices of an octagon, following more or less complex rules (see Figure 30 below). Then, recordings of anticipatory eye movements can be used to assess the internal, mental representation of the sequence. At brain level, we use fMRI to search for activations that correlate with the level of complexity, and particularly the number of embeddings, and for new responses when rules are violated. This test, which is entirely non-linguistic in nature, allows us to experimentally test the HAUSER, CHOMSKY and FITCH (2002)[69] proposal that recursive embedding is a unique ability of the human brain.

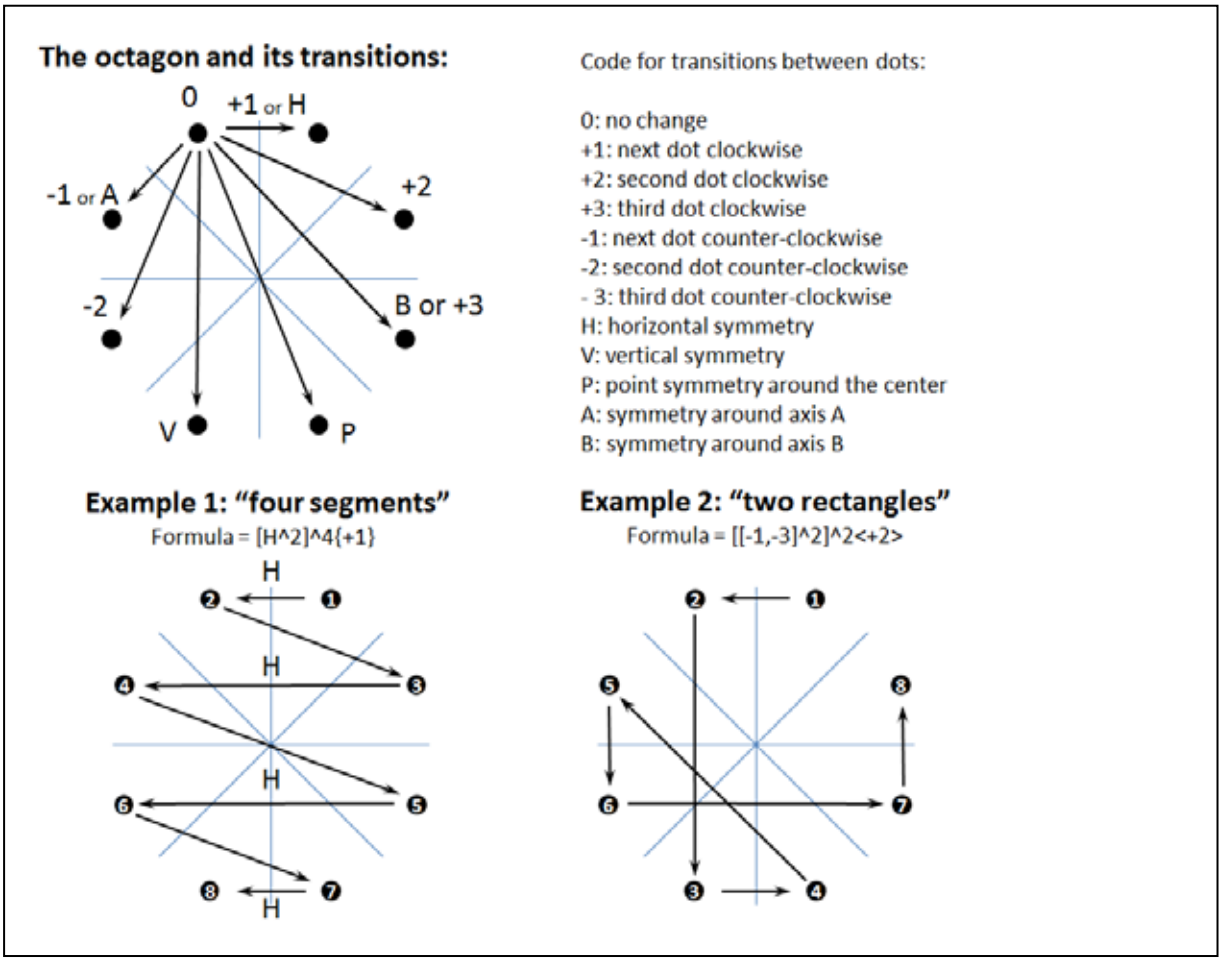

Figure 30: Protocol Testing for Recursion in the Mental Representation of Visual Sequences

For each trial, subjects are presented with a single instance of a sequence where eight dots are successively flashed. Pilot experiments indicate that even young children immediately identify structures when they are present, e.g. they detect the repetition of horizontal segments (example 1) or the presence of two rotated rectangles. Sequences containing such structures are more easily memorised, suggesting that the human brain "compresses" the sequence into an algebraic formula, similar to those shown.

7.2.4.1 Description of Data and Models

FMRI data are being collected, together with eye tracking data. In addition, similar data in macaque monkeys will be collected, using non-HBP funds.

Eye-tracking raw data has been converted into measures of accuracy, inversely related to the inverse of the distance of eye position to the expected target dot. Data corresponding to the figure below will be provided.

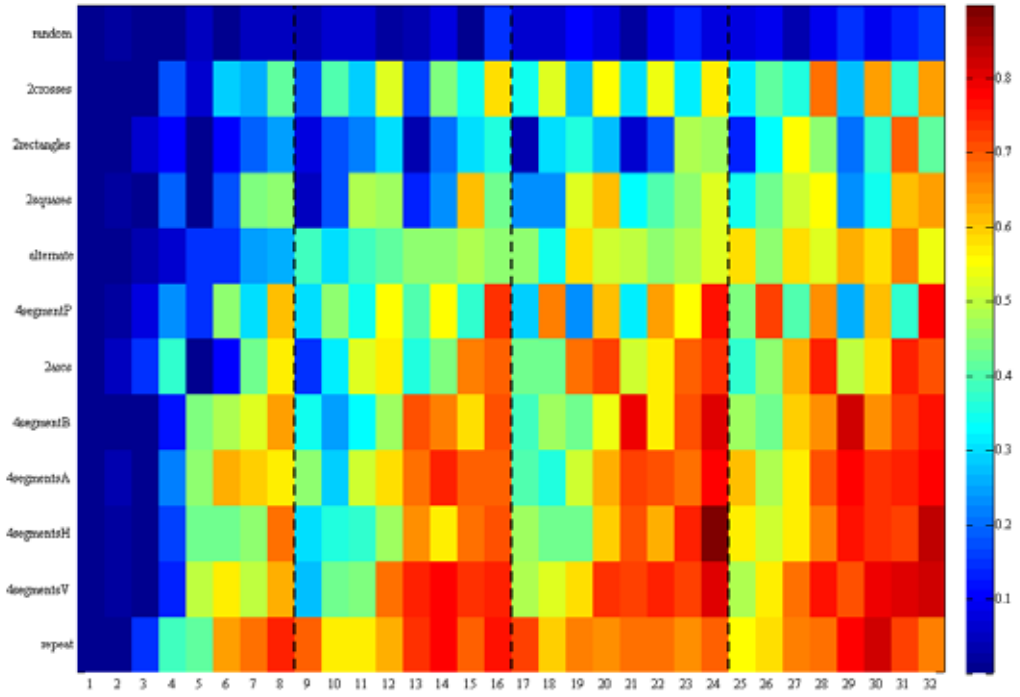

Figure 31: Accuracy of Anticipatory Eye Movements as a Function of Sequence Type

The fMRI data will consist of effect-size and statistical (T-values) maps for each of the different types of sequences relative to baseline, at group level.

7.2.4.2 How Data are Related to Specific Platform Requirements

We plan to deliver the stimulus set and the key results from the analysis of the fMRI data, in both humans and non-human primates. The data are being analysed with Statistical Parametric Mapping software (SPM toolbox, Matlab, http://www.fil.ion.ucl.ac.uk/spm/). The results will be delivered in the form of statistical parametric maps and contrast images. The raw data can also be delivered on request.

7.2.4.3 Quantitative Indicators of Data Completeness

The acquisition of eye tracking data has been completed. The data analysis pipeline is implemented and data analyses are in progress. Concerning fMRI, 14 out of 20 human participants have been scanned.

7.2.4.4 Status of Data Delivery

Not started yet, planned for Phase II.

7.2.4.5 List of SP4 Collaboration Partners

Our data are optimally suited to all SP4 partners interested in theorising the representation of nested or recursive sequences, and the evolutionary events that may have led to a uniquely human competence in this domain.

7.2.4.6 Data Provenance

The data were acquired at NeuroSpin by Liping WANG and Marie AMALRIC.

7.2.4.7 Plan Until the End of the Ramp-Up Phase

We will complete fMRI data acquisition. We will then analyse the data to search for brain areas where activation increases with rule complexity, and in particular the number of embeddings. We also plan to implement a computational model for the interpretation of current sequential learning tasks.

7.3 The Social Brain – Representing the Self in Relation to Others (T3.6.3)

7.3.1 Data set One: Social Localiser

7.3.1.1 Description of Data and Models

Riitta HARI's group (*Aalto-korkeakoulusäätiö* [AALTO – P2]) is building a localiser fMRI experiment to identify brain regions associated with social cognition. Our comprehensive set of social stimuli aims to target functional subregions supporting face and body perception, action understanding, and theory-of-mind capabilities. The localiser includes the following stimulus categories with appropriate control conditions (not listed here): biological movement, goal-directed action perception, self vs. other perception, perception of persons in social interaction, theory-of-mind ability (moving geometrical shapes), joint attention, face perception and body perception. For preliminary results, please see Figure 32.

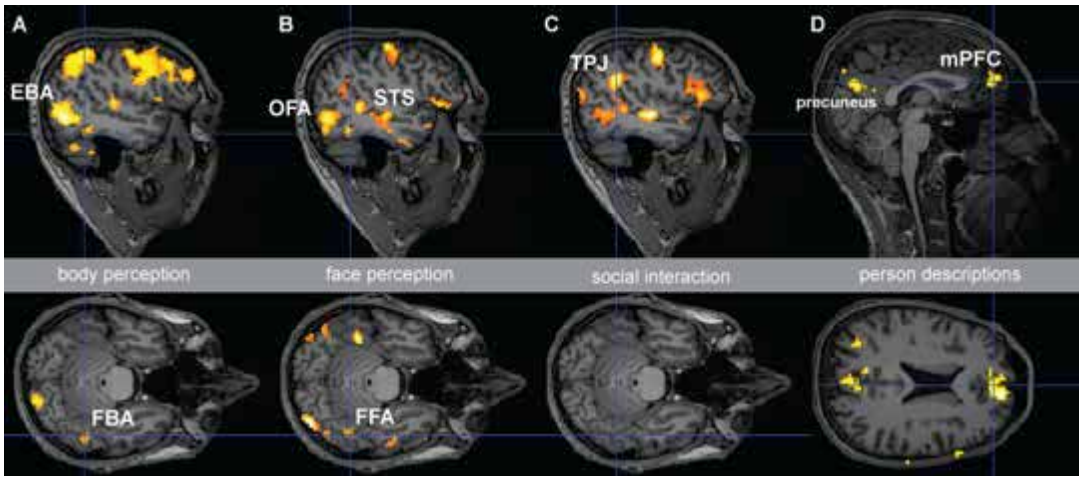

Figure 32: Preliminary Results on Social Localiser Experiment (pilot subject four).

A) Brain regions activated more strongly by pictures of body parts than of objects (puncorr<0.001, cth = 5 voxels); the areas include the extrastriate body area (EBA) and fusiform body area (FBA). B) Brain regions involved in face perception were identified by comparing activations elicited whilst viewing videos of faces vs. videos of natural scenes. These stimuli activated several brain regions, including the occipital face area (OFA), fusiform face area (FFA) and regions along the superior temporal sulcus (STS). C) Viewing of animated geometrical shapes depicted in social interaction activated regions along STS and temporoparietal junction (TPJ). D) Medial prefrontal cortex (mPFC) and precuneus showed stronger activation when the subject was making judgements on people rather than on objects.

7.3.1.2 How Data are Related to Specific Platform Requirements

We plan to deliver the stimulus set, and the key results from the analysis of the fMRI data. The data are being analysed with SPM software (SPM toolbox, Matlab, http://www.fil.ion.ucl.ac.uk/spm/). The data analysis comprises standard pre-processing

steps (slice-timing correction, movement correction, smoothing) and statistical analysis (general linear modelling). The results on key brain regions can be delivered, for example, in the form of statistical parametric maps and contrast images. The raw data can also be delivered on request.

7.3.1.3 Quantitative Indicators of Data Completeness

We have acquired pilot data, and have been optimising the localiser based on the pilot results. The plan is to acquire a comprehensive data set by October 2015.

7.3.1.4 Status of Data Delivery

Pilot data can be delivered on request. Fully processed data will be delivered during data-delivery phase II.

7.3.1.5 List of SP4 Collaboration Partners

No active SP4 collaboration has been established yet.

7.3.1.6 Data Provenance

Data were collected using a 3-T whole-body MRI scanner (Magnetom Skyra, Siemens) at the Advanced Magnetic Imaging Centre (http://ani.aalto.fi/en/ami_centre/) at *Aalto-korkeakoulusäätiö*, in Finland. The pilot fMRI data were collected by Timo NURMI and Linda HENRIKSSON between October 2014 and March 2015 at the Department of Neuroscience and Biomedical Engineering, *Aalto-korkeakoulusäätiö*.

7.3.1.7 Plan Until the End of the Ramp-Up Phase

By the end of the Ramp-Up Phase, we aim to provide a working localiser experiment, key results on brain regions involved in different social tasks, and, on request, the pre-processed raw fMRI data from a complete set of subjects.

Annex A: References

1. Harmelech, T. and Malach, R. Neurocognitive biases and the patterns of spontaneous correlations in the human cortex. *Trends Cogn. Sci.* **17,** 606–615 (2013).

2. Harmelech, T., Friedman, D. and Malach, R. Differential Magnetic Resonance Neurofeedback Modulations across Extrinsic (Visual) and Intrinsic (Default-Mode) Nodes of the Human Cortex. *J. Neurosci.* **35,** 2588–2595 (2015).

3. Yellin, D., Berkovich-Ohana, A. and Malach, R. Coupling between pupil fluctuations and resting-state fMRI uncovers a slow build-up of antagonistic responses in the human cortex. *NeuroImage* **106,** 414–427 (2015).

4. Hahamy, A., Behrmann, M. and Malach, R. The idiosyncratic brain: distortion of spontaneous connectivity patterns in autism spectrum disorder. *Nat. Neurosci.* **18,** 302–309 (2015).

5. Hahamy, A. *et al.* Normalisation of brain connectivity through compensatory behaviour, despite congenital hand absence. *eLife* **4,** (2015).

6. Tarr, M. J. and Bülthoff, H. H. Is human object recognition better described by geon structural descriptions or by multiple views? Comment on Biederman and Gerhardstein (1993). *J. Exp. Psychol. Hum. Percept. Perform.* **21,** 1494–1505 (1995).

7. Li, N. and DiCarlo, J. J. Unsupervised natural experience rapidly alters invariant object representation in visual cortex. *Science* **321,** 1502–1507 (2008).

8. Hirabayashi, T., Takeuchi, D., Tamura, K. and Miyashita, Y. Microcircuits for hierarchical elaboration of object coding across primate temporal areas. *Science* **341,** 191–195 (2013).

9. Michotte, A. *La perception de la causalité*. (Editions de l'Institut Supérieur de Philosophie, 1946).

10. Fleischer, F., Christensen, A., Caggiano, V., Thier, P. and Giese, M. A. Neural theory for the perception of causal actions. *Psychol. Res.* **76,** 476–493 (2012).

11. Caggiano, V. *et al.* View-based encoding of actions in mirror neurons of area f5 in macaque premotor cortex. *Curr. Biol. CB* **21,** 144–148 (2011).

12. Caggiano, V. *et al.* Mirror neurons encode the subjective value of an observed action. *Proc. Natl. Acad. Sci.* **109,** 11848–11853 (2012).

13. Caggiano, V. *et al.* Mirror neurons in monkey area F5 do not adapt to the observation of repeated actions. *Nat. Commun.* **4,** 1433 (2013).

14. Caggiano, V., Giese, M., Thier, P. and Casile, A. Encoding of point of view during action observation in the local field potentials of macaque area F5. *Eur. J. Neurosci.* **41,** 466–476 (2015).

15. Fleischer, F., Caggiano, V., Thier, P. and Giese, M. A. Physiologically inspired model for the visual recognition of transitive hand actions. *J. Neurosci. Off. J. Soc. Neurosci.* **33,** 6563–6580 (2013).

16. Giese, M. A. Mirror representations innate versus determined by experience: a viewpoint from learning theory. *Behav. Brain Sci.* **37,** 201–202 (2014).

17. Barraclough, N. E., Keith, R. H., Xiao, D., Oram, M. W. and Perrett, D. I. Visual adaptation to goal-directed hand actions. *J. Cogn. Neurosci.* **21,** 1806–1820 (2009).

18. Nelissen, K., Luppino, G., Vanduffel, W., Rizzolatti, G. and Orban, G. A. Observing Others: Multiple Action Representation in the Frontal Lobe. *Science* **310,** 332–336 (2005).

19. Ionta, S. *et al.* Multisensory mechanisms in temporo-parietal cortex support self-location and first-person perspective. *Neuron* **70,** 363–374 (2011).

20. Ionta, S., Martuzzi, R., Salomon, R. and Blanke, O. The brain network reflecting bodily self-consciousness: a functional connectivity study. *Soc. Cogn. Affect. Neurosci.* (2014). doi:10.1093/scan/nst185

21. Lenggenhager, B., Mouthon, M. and Blanke, O. Spatial aspects of bodily self-consciousness. *Conscious. Cogn.* **18,** 110–117 (2009).

22. Hadjipapas, A., Lowet, E., Roberts, M. J., Peter, A. and De Weerd, P. Parametric variation of gamma frequency and power with luminance contrast: A comparative study of human MEG and monkey LFP and spike responses. *NeuroImage* (2015). doi:10.1016/j.neuroimage.2015.02.062

23. Zachariou, M., Roberts, M., Lowet, E., De Weerd, P. and Hadjipapas, A. Contrast-dependent Modulation of Gamma Rhythm in V1: a Network Model. in *24th Annual Computational Neuroscience Meeting* (2015).

24. Arnulfo, G., Narizzano, M., Cardinale, F., Fato, M. M. and Palva, J. M. Automatic segmentation of deep intracerebral electrodes in computed tomography scans. *BMC Bioinformatics* **16,** 99 (2015).

25. Arnulfo, G., Hirvonen, J., Nobili, L., Palva, S. and Palva, J. M. Phase and amplitude correlations in resting-state activity in human stereotactical EEG recordings. *NeuroImage* **112,** 114–127 (2015).

26. Sporns, O., Tononi, G. and Kötter, R. The Human Connectome: A Structural Description of the Human Brain. *PLoS Comput Biol* **1,** e42 (2005).

27. Breakspear, M., Heitmann, S. and Daffertshofer, A. Generative models of cortical oscillations: neurobiological implications of the kuramoto model. *Front. Hum. Neurosci.* **4,** 190 (2010).

28. Ott, E. and Antonsen, T. M. Low dimensional behaviour of large systems of globally coupled oscillators. *Chaos Interdiscip. J. Nonlinear Sci.* **18,** 037113 (2008).

29. Kiani, R. and Shadlen, M. N. Representation of confidence associated with a decision by neurons in the parietal cortex. *Science* **324,** 759–764 (2009).

30. Zylberberg, A., Barttfeld, P. and Sigman, M. The construction of confidence in a perceptual decision. *Front. Integr. Neurosci.* **6,** 79 (2012).

31. Gold, J. I. and Shadlen, M. N. The neural basis of decision making. *Annu. Rev. Neurosci.* **30,** 535–574 (2007).

32. Yeung, N. and Summerfield, C. Metacognition in human decision-making: confidence and error monitoring. *Philos. Trans. R. Soc. Lond. B. Biol. Sci.* **367,** 1310–1321 (2012).

33. Ratcliff, R. Continuous versus discrete information processing modeling accumulation of partial information. *Psychol. Rev.* **95,** 238–255 (1988).

34. Kiani, R. and Shadlen, M. N. Representation of confidence associated with a decision by neurons in the parietal cortex. *Science* **324,** 759–764 (2009).

35. Mainen, Z. F. and Kepecs, A. Neural representation of behavioural outcomes in the orbitofrontal cortex. *Curr. Opin. Neurobiol.* **19,** 84–91 (2009).

36. Hebart, M. N., Schriever, Y., Donner, T. H. and Haynes, J.-D. The Relationship between Perceptual Decision Variables and Confidence in the Human Brain. *Cereb. Cortex* bhu181 (2014). doi:10.1093/cercor/bhu181

37. Pessiglione, M. *et al*. How the brain translates money into force: a neuroimaging study of subliminal motivation. *Science* **316,** 904–906 (2007).

38. Schmidt, L., Lebreton, M., Cléry-Melin, M.-L., Daunizeau, J. and Pessiglione, M. Neural mechanisms underlying motivation of mental versus physical effort. *PLoS Biol.* **10,** e1001266 (2012).

39. Tachibana, Y. and Hikosaka, O. The primate ventral pallidum encodes expected reward value and regulates motor action. *Neuron* **76,** 826–837 (2012).

40. Schmidt, L. *et al*. Disconnecting force from money: effects of basal ganglia damage on incentive motivation. *Brain J. Neurol.* **131,** 1303–1310 (2008).

41. Cléry-Melin, M.-L. *et al*. Why don't you try harder? An investigation of effort production in major depression. *PloS One* **6,** e23178 (2011).

42. Palminteri, S. *et al*. Critical Roles for Anterior Insula and Dorsal Striatum in Punishment-Based Avoidance Learning. *Neuron* **76,** 998–1009 (2012).

43. O'Doherty, J. *et al*. Dissociable roles of ventral and dorsal striatum in instrumental conditioning. *Science* **304,** 452–454 (2004).

44. Pessiglione, M., Seymour, B., Flandin, G., Dolan, R. J. and Frith, C. D. Dopamine-dependent prediction errors underpin reward-seeking behaviour in humans. *Nature* **442,** 1042–1045 (2006).

45. Palminteri, S. *et al*. Pharmacological modulation of subliminal learning in Parkinson's and Tourette's syndromes. *Proc. Natl. Acad. Sci. U. S. A.* **106,** 19179–19184 (2009).

46. Frank, M. J., Seeberger, L. C. and O'Reilly, R. C. By Carrot or by Stick: Cognitive Reinforcement Learning in Parkinsonism. *Science* **306,** 1940–1943 (2004).

47. Rutledge, R. B., Dean, M., Caplin, A. and Glimcher, P. W. Testing the reward prediction error hypothesis with an axiomatic model. *J. Neurosci. Off. J. Soc. Neurosci.* **30,** 13525–13536 (2010).

48. Worbe, Y. *et al*. Reinforcement learning and Gilles de la Tourette syndrome: dissociation of clinical phenotypes and pharmacological treatments. *Arch. Gen. Psychiatry* **68,** 1257–1266 (2011).

49. Palminteri, S., Boraud, T., Lafargue, G., Dubois, B. and Pessiglione, M. Brain Hemispheres Selectively Track the Expected Value of Contralateral Options. *J. Neurosci.* **29,** 13465–13472 (2009).

50. Schmidt, L. *et al*. Get aroused and be stronger: emotional facilitation of physical effort in the human brain. *J. Neurosci. Off. J. Soc. Neurosci.* **29,** 9450–9457 (2009).

51. Assaf, M. *et al*. Brain activity dissociates mentalization from motivation during an interpersonal competitive game. *Brain Imaging Behav.* **3,** 24–37 (2009).

52. Gonen, T., Admon, R., Podlipsky, I. and Hendler, T. From animal model to human brain networking: dynamic causal modeling of motivational systems. *J. Neurosci.* **32,** 7218–7224 (2012).

53. Kahn, I. *et al*. The role of the amygdala in signaling prospective outcome of choice. *Neuron* **33,** 983–994 (2002).

54. Karni, A. *et al*. Functional MRI evidence for adult motor cortex plasticity during motor skill learning. *Nature* **377,** 155–158 (1995).

55. Karni, A. *et al*. The acquisition of skilled motor performance: fast and slow experience-driven changes in primary motor cortex. *Proc. Natl. Acad. Sci. U. S. A.* **95,** 861–868 (1998).

56. Gabitov, E., Manor, D. and Karni, A. Done that: short-term repetition related modulations of motor cortex activity as a stable signature for overnight motor memory consolidation. *J. Cogn. Neurosci.* **26,** 2716–2734 (2014).

57. Gabitov, E., Manor, D. and Karni, A. Patterns of modulation in the activity and connectivity of motor cortex during the repeated generation of movement sequences. *J. Cogn. Neurosci.* **27,** 736–751 (2015).

58. Ben-Yakov, A. and Dudai, Y. Constructing Realistic Engrams: Poststimulus Activity of Hippocampus and Dorsal Striatum Predicts Subsequent Episodic Memory. *J. Neurosci.* **31,** 9032–9042 (2011).

59. Ben-Yakov, A., Eshel, N. and Dudai, Y. Hippocampal immediate poststimulus activity in the encoding of consecutive naturalistic episodes. *J. Exp. Psychol. Gen.* **142,** 1255–1263 (2013).

60. Ben-Yakov, A., Rubinson, M. and Dudai, Y. Shifting Gears in Hippocampus: Temporal Dissociation between Familiarity and Novelty Signatures in a Single Event. *J. Neurosci.* **34,** 12973–12981 (2014).

61. Weigenand, A., Schellenberger Costa, M., Ngo, H.-V. V., Claussen, J. C. and Martinetz, T. Characterization of k-complexes and slow wave activity in a neural mass model. *PLoS Comput. Biol.* **10,** e1003923 (2014).

62. Schellenberger Costa, M. *et al*. A thalamocortical neural mass model of the EEG during NREM sleep and its response to auditory stimulation. *Submitt. NeuroImage*

63. Packard, M. G. and McGaugh, J. L. Inactivation of Hippocampus or Caudate Nucleus with Lidocaine Differentially Affects Expression of Place and Response Learning. *Neurobiol. Learn. Mem.* **65,** 65–72 (1996).

64. Pearce, J. M., Roberts, A. D. L. and Good, M. Hippocampal lesions disrupt navigation based on cognitive maps but not heading vectors. *Nature* **396,** 75–77 (1998).

65. Pallier, C., Devauchelle, A.-D. and Dehaene, S. Cortical representation of the constituent structure of sentences. *Proc. Natl. Acad. Sci. U. S. A.* **108,** 2522–2527 (2011).

66. Squires, K. C., Wickens, C., Squires, N. K. and Donchin, E. The effect of stimulus sequence on the waveform of the cortical event-related potential. *Science* **193,** 1142–1146 (1976).

67. Huettel, S. A., Mack, P. B. and McCarthy, G. Perceiving patterns in random series: dynamic processing of sequence in prefrontal cortex. *Nat. Neurosci.* **5,** 485–490 (2002).

68. Schvaneveldt, R. W. and Chase, W. G. Sequential effects in choice reaction time. *J. Exp. Psychol.* **80,** 1–8 (1969).

69. Hauser, M. D., Chomsky, N. and Fitch, W. T. The Faculty of Language: What Is It, Who Has It, and How Did It Evolve? *Science* **298,** 1569–1579 (2002).